

U1 x U2 x U3: QuantumVisions

Stefan Heusler[†], Gregor Schwellenbach, Michael Tewiele

[†]Institut für Didaktik der Physik, Wilhelm-Klemm-Str. 10, 48149 Münster, Germany

Abstract. The project QuantumVisions (<https://www.quantumvisions.net/en/>) provides a visual approach to quantum physics. In a period of 15 years (2008-2023), more than 100 short animation movies have been produced. Based on well-established mathematical and experimental results, a visual *language* is introduced for quantum states, entanglement, the measurement process and the topology of the Hilbert space (denoted *quantum dimension* in this project). In this documentation, we provide the full text and weblinks of the animations. Moreover, we comment on the structure of the project, its mathematical foundation, and on the accompanying movie *Shadow Worlds*, where *Alice* and *Bob* try to enter the quantum dimension, searching for the entangled state *Omega*. The part U1: Quantum Dimensions of the project U1xU2xU3 Quantum Visions has been published as DVD in 2010 from [SCIENCeMOTION](#).

Contents

1	U1: Quantum Dimensions	8
1.1	Pyramid of probabilities (U1-01)	8
1.1.1	Binomial water pyramid	8
1.1.2	Particles and paths	8
1.1.3	Paths and Probabilities	8
1.1.4	Probabilities and Measurements	9
1.1.5	Two stepped pyramids	9
1.1.6	Conclusions	10
1.2	Sound interference (U1-02)	10
1.2.1	Sound beats	10
1.2.2	Tuning fork	11
1.2.3	Spinning wheel	11
1.2.4	Modeling a single tuning forks with a spinning wheel	11
1.2.5	Two tuning forks	12

1.2.6	Interference	12
1.2.7	Sound intensity	13
1.2.8	Beat	13
1.3	Reflection probability - photons at the beam splitter (U1-03) . .	14
1.3.1	Reflection and transmission	14
1.3.2	A laser beam hitting the beam splitter	14
1.3.3	Single photons at the beam splitter	14
1.3.4	Reflection and transmission probability	15
1.4	Light Interference – Wave property of light on a soap film (U1-04)	16
1.4.1	Dazzling colors (U1-04-01)	16
1.4.2	Interference patterns on a soap film	16
1.4.3	Wave Theory of Light	16
1.4.4	The Thales circle – interference at thin layers	16
1.5	The double slit experiment - a milestone in the history of physics (U1-05)	17
1.5.1	Light at the beginning of the 19th century	17
1.5.2	Single-slit experiment	17
1.5.3	Diffraction pattern at single and double slit	17
1.5.4	Single photons at single- and double slit	18
1.6	The Heart of Quantum Mechanics - the spinning wheel (U1-06)	18
1.6.1	Interference and Probability	18
1.6.2	Single and double slit with classical light	18
1.6.3	Vectors sums describing interference	19
1.6.4	Single and double slit with single photons	20
1.6.5	Probability distribution	20
1.6.6	Wave Interference and Particle Probability	20
1.7	Paths into the quantum dimension - the path integral (U1-07) .	21
1.7.1	Turning the wheel	21
1.7.2	The laser beam in the empty space	21
1.7.3	Paths and probabilities in the quantum dimension	22
1.7.4	The Cornu spiral	22
1.7.5	The Michelson interferometer	23
1.8	Polarisation of light - an interplay of vibration nodes and antinodes (U1-08)	23
1.8.1	The polarisation	23
1.8.2	Experiment with a single polarisation filter	24
1.8.3	Polarisation filters and polarisation rotators	24
1.8.4	Polarisation of single photons	25
1.8.5	Probability distribution	25
1.8.6	Probability and interference	25
1.8.7	Polarization of a single photon in the quantum dimension	26
1.8.8	Summary	26

1.9	Correlation function - searching for order in randomness (U1-09)	26
1.9.1	Tow random patterns	26
1.9.2	Two coins, one coin	26
1.9.3	Correlation function	27
1.9.4	Theory and experiment	27
1.10	Combined measurement of polarisaton - The two-doors metaphor (U1-10)	28
1.10.1	Two-doors metaphor	28
1.10.2	The detectors "Alice" and "Bob"	28
1.10.3	Correlation function	29
1.11	Entangled photons - before and after measurement(U1-11)	29
1.11.1	Birefringence	29
1.11.2	"Non-local or local chess": Omega's shadow on the wall	29
1.11.3	Experiments with entangled photons	30
1.11.4	The entangled quantum state Omega	30
1.11.5	Rotating coin	30
1.11.6	The "Omega Donut" in the quantum dimension	31
1.11.7	Visualization of the measurement process	32
1.11.8	Quantum mechanical calculation of the correlation function	32
1.11.9	Alices and Bobs series of measurements	33
1.11.10	Experimental determination of the correlation function	33
1.11.11	Shadow world and quantum dimension	34
1.12	Bell's inequality (U1-12)	34
1.12.1	"Maybe he was murdered"	34
1.12.2	Experimental determination of the correlation function	34
1.12.3	The "spooky" quantum dimension under close scrutiny	35
1.12.4	Hidden variables	36
1.12.5	Bell's inequality	36
1.12.6	Comparing theory and experiment	37
1.12.7	The truth is... interpretations of quantum physics	37
1.13	On the high pass of quantum mechanics (U1-13)	37
1.14	Quantum computation (U1-14)	38
1.14.1	Checkerboard patterns	38
1.14.2	Classical computing	38
1.14.3	Space of probabilities	38
1.14.4	Quantum dimension of a single qubit	39
1.14.5	Two qubits	39
1.14.6	The four Bell states in the "Seventh Dimension"	40
1.14.7	Local and non-local dimensions	41
1.14.8	The metaphor of the "non-local grains of rice"	41
1.14.9	The future of quantum physics	43

2	U2: Quantum Reflections	45
2.1	Visualizatons of sound waves (U2-1)	45
2.1.1	Spinning wheels	45
2.1.2	Sound wave and sound intensity	46
2.1.3	Phase of a sound wave	47
2.2	Sound interference (U2-2)	47
2.3	Overtones (U2-3)	47
2.3.1	From wave to source	47
2.3.2	Fourier transformation	48
2.4	Good vibrations (U2-4)	49
2.4.1	Vibrating guitar string	49
2.4.2	Spectrum of the guitar string	49
2.4.3	Standing waves	49
2.5	Spherical Vibrations (U2-5)	51
2.5.1	Water waves	51
2.5.2	Cladni sound figures	51
2.5.3	Vibrating cup	52
2.5.4	Vibrating soap bubble	54
2.5.5	Spherical Harmonics	54
2.6	Plancks constant as key to the quantum dimension (U2-6)	55
2.6.1	Candle and Mirror	55
2.6.2	Rotation operator	55
2.6.3	The spectrum of the rotation operator	56
2.6.4	Quantum Mirror	57
2.7	The middle mirror (U2-7)	58
2.7.1	Haunted Mirror	58
2.7.2	Spin	59
2.7.3	Stern-Gerlach experiment	59
2.8	From Bohr to the quantum dimension (U2-8)	61
2.8.1	Stair steps	61
2.8.2	Atomic spectra	61
2.8.3	Balmer-formula	61
2.8.4	Rutherford-scattering	62
2.8.5	Bohrs atomic model	64
2.8.6	States, operations and the hydrogen atom	65
2.8.7	Atomic orbitals	67
2.8.8	Table of elements	67
2.9	Quantum organ - dancing electrons (U2-9)	70
2.9.1	Quantum organ	70
2.9.2	Helium-Neon-Laser	70
2.9.3	Quantum nodes	72
2.9.4	Pauli exclusion principle	73

- 2.9.5 Guitar reflections 74
- 3 U3: Quantum Symmetries 76**
- 3.1 Permutations and transformations (U3-1) 76
 - 3.1.1 Shadow worlds 76
 - 3.1.2 Sound permutations (U3-1-02) 77
 - 3.1.3 Music operations 78
 - 3.1.4 Qubit operations 78
- 3.2 Quantum cryptography (U3-2) 80
 - 3.2.1 Alice Chessboard-Code 80
 - 3.2.2 One-time pad 80
 - 3.2.3 Quantum cryptography 80
- 3.3 Topology of the quantum dimension (U3-3) 81
 - 3.3.1 Omegas’ Secret Lab 81
 - 3.3.2 Complex rotation 81
 - 3.3.3 Complexified function 82
 - 3.3.4 Complex Quantum Dimension 83
 - 3.3.5 Spin and polarization 84
 - 3.3.6 Topology and quanten nodes 85
 - 3.3.7 Twists 86
 - 3.3.8 Alice and Omega 87
- 4 Mathematical comment 89**
- 4.1 Visualization of the measurement process in U1-12 90
- 4.2 The topology of spin-j states 92
- 4.3 Making distinctions: From *nothing* to the speed of light c 94
- 4.4 The 4π -realm and the 2π -realm: $SL(2, \mathbb{C})$ as double cover of the Lorentz group $SO(3, 1)$ 96
- 4.5 Twist-operations in the quantum dimension at the price of Planck’s constant h 97
- 4.6 Selection rules 98
- 4.7 Quantum dimensions and Shadow World: stroboscopic 2π -realm views in Planck-times τ_{Pl} slices 101
- 5 Acknowledgements 103**

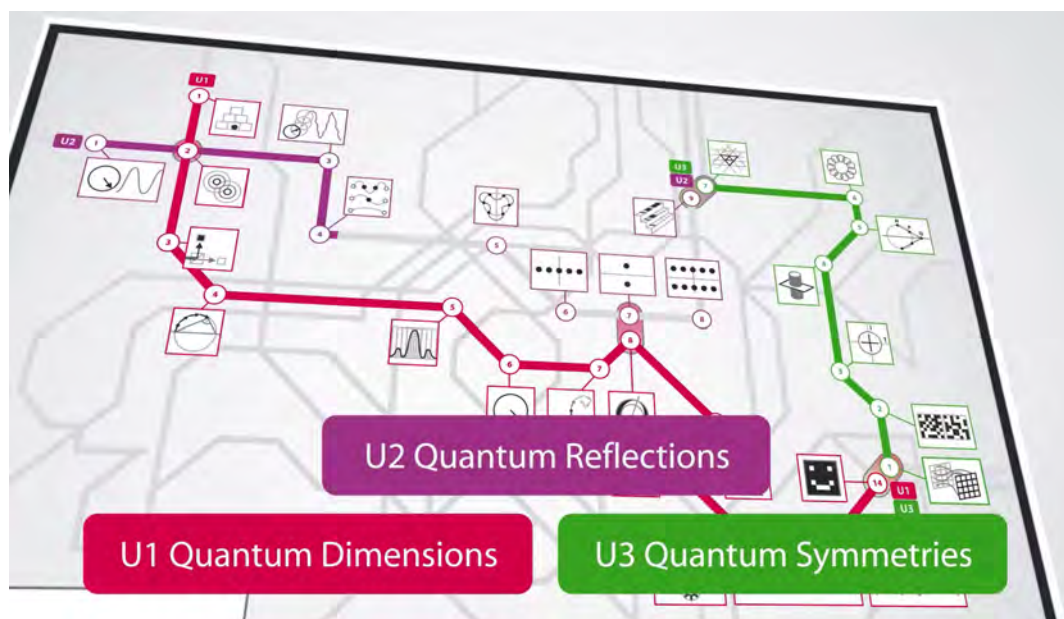


Figure 1. Screenshot showing the three subway lines $U(1) \times U(2) \times U(3)$ of Omega City

U1 x U2 x U3: QuantumVisions

Based on well-established mathematical and experimental results, the project [QuantumVisions](#) introduces a visual *language* for quantum states, entanglement, the measurement process and the topology of the Hilbert space (denoted *quantum dimension* in this project). Essential is the distinction between four levels of representations: First, we distinguish theory and experiment. In experiment, we distinguish those with single quanta from those with very many quanta. In theory, we distinguish observable probabilities from unobservable amplitudes in Hilbert space (the *quantum dimension*), see Fig. 2 for the example of photons: Experiments with many photons (e.g., thermal light or laser light) lead to intensities, experiments with single photons to probabilities. In theory, probabilities can be calculated from the unobservable amplitudes in the *quantum dimension*. All animations are arranged in the three subway-lines $U(1) \times U(2) \times U(3)$:

- U1: *Quantum Dimensionens* - double slit, entanglement, quantum computing.
- U2: *Quantum Reflections* - standing waves, atomic models, table of elements.
- U3: *Quantum Symmetries* - quantum cryptography, topological properties of bosons and fermions in the quantum dimension.

The individual stations of the subway lines cross Omega City, which is still unknown in many aspects and whose outlines have only gradually emerged since the advent of quantum physics in the 1920s. "Omega" is a metaphor for all entangled states in

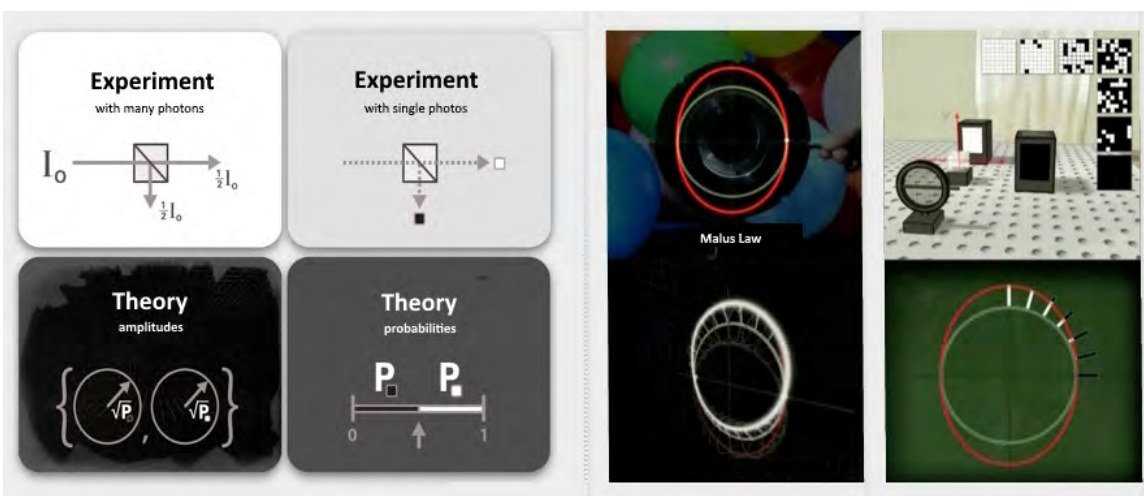


Figure 2. Left: Scheme of four quadrants, Right: representation of the polarisation of photons within the four quadrants-scheme (U1-08)

Hilbert space. In particular, the Bell-state $|\Omega\rangle = \frac{1}{\sqrt{2}}(|00\rangle + |11\rangle)$, plays a crucial role in the subway line U1: Quantum Dimension.

At the same time, Omega is also the supervisor Alice and Bob are looking for in the feature film [Shadow Worlds](#). In the feature film, Alice and Bob embark on a journey into the quantum dimensions of light. The journey begins with the search for the mysterious Omega, who is supposed to have disappeared because of his quantum research. Alice and Bob meet Omega's janitor - played by [Harald Lesch](#). Unbeknownst to them, the janitor leads the two into an invisible network of another dimension - the subdimension.

The subtle interplay between observable and unobservable quantities is one of the causes for the fascination that emerges from quantum physics. The detectors Alice and Bob cannot observe the full entangled quantum state $|\Omega\rangle$ directly, as local measurements cannot give complete access to non-local quantum states in the quantum dimension.

In much the same way, simply watching the feature film *Shadow Worlds* cannot give complete access to the actual action behind the plot. The key story is not directly observable and defies any causal or chronological relationships. In the subway lines $U1 \times U2 \times U3$, the hidden image clues are reassembled like puzzle pieces and form the entry into the subdimension, where the actual journey goes. In the final chapter of this documentation, we provide a mathematical comment concerning the visualizations used in the project.

The animations of the subdimension have been realized in several production phases between the years 2008-2023. The subway line U1: *quantum dimensions* was first published in 2010 as DVD. Alma Lares has been co-author of the the subway line U1. In cooperation with the [Quantum Visions production team](#), all other subway lines have been realized. All animations as well as further publications are available in German and English language via the website www.quantumvisions.net/ (CC BY-NC-ND license).



Figure 3. The janitor leading Alice through the *Shadow Worlds*. During the movie, hints to the stations of the subdimension are given (here: station $U1 - 09$). The two chessboard at the right and left play a crucial role for the communication of Alice and Bob with $|\Omega\rangle$. The one-time-pad to be decrypted in $U3-2$ can be seen on the top.

1. $U1$: Quantum Dimensions

1.1. Pyramid of probabilities ($U1-01$)

How can be describe the behaviour of classical particles? What is the influence of observation upton probabilities? Does observation have an influence on the state of the classical particle?

1.1.1. Binomial water pyramid [Link to U1-1-01](#)

Alice and Bob are facing one of the most important examples of classic probability calculus – the binomial distribution. Key ideas for quantum mechanics - to which we will revert as we go along - can be derived from this “water pyramid”.

1.1.2. Particles and paths [Link to U1-1-02](#)

Bob is replacing water molecules with balls in the model. With this stepped pyramid, we can trace the various paths of the balls through it. With each additional level, the paths are split further. The more paths lead into a box, the more balls land in it. If, however, we only observe a single ball, can we then, prior to the ball passing along the route, make a prediction about the possible path of the ball?

1.1.3. Paths and Probabilities [Link to U1-1-03](#)

The particle reaches the first level via two possible paths - “White” and “Black”.

For each of the two possible paths on the first level, we can specify only a probability. Four possible paths lead from the ground level to the second level. The balls from the “White - Black” and “Black - White” paths land in the same box. The particle travels from the ground level to the third level via eight possible path combinations. The probability of the particle staying in any of the four boxes always arises from the number of possible paths into the box concerned, which is divided by the total number of path combinations, that is, eight path combinations on the third level.

1.1.4. Probabilities and Measurements [Link to U1-1-04](#)

Next, we drop a particle on an invisible path down to Level 3. In which of the four boxes is the ball now? Prior to measuring the location, we only know the eight possible paths.

The sum of probabilities into all possible boxes is $1/8 + 3/8 + 3/8 + 1/8 = 1 = 100$ percent. Next, we open a box and thus perform a measurement – the ball has been located. The probability for that box becomes 100 percent. For all other boxes, the probabilities immediately drop to zero, independent of spacial distances. Again, we open a box and thus perform a measurement – the box is empty. This measurement causes again all other probabilities to change immediately, since the probabilities needs to be normalized 100 percent. Prior to measuring, the probability for this box was equal to $3/8$; after measuring, it is zero, and, for the other boxes, accordingly $1/5$ or $3/5$. Thus, the probability of each individual path is now $1/5$. Wherever there are causal connections between probabilities, each measurement alters all the other probabilities, without any delay, irrespective of how far a box is away from the measurement. Thus, any given measurement brings about a non-local change in all probability distributions. However, the ball already dropped prior to taking the measurement. This means that the measurement does not affect the possible measurement results. It is only our awareness of the possible location of the ball that changes through the measurement.

1.1.5. Two stepped pyramids [Link to U1-1-05](#)

Next, we compare two stepped pyramids. In the case of the right-hand pyramid, we open a box on Level 3, blocking the route to this box before the balls drop. The probabilities in the right-hand pyramid only change compared to the left-hand pyramid in the direct vicinity of the box opened in the following way: N is the large number of balls dropping through the pyramid. If p is the probability for an individual ball to reach this box, N times p balls will land in each box. For Level 2, the ball distribution is still the same for both pyramids, namely $N/4$, $N/2$, $N/4$. For Level 3, it is $N/8$, $3N/8$, $3N/8$, $N/8$ for the left-hand pyramid. For the right-hand pyramid, however, the distribution is $N/8$, $5N/8$, 0 and $2N/8$. The value for the box on the far left remains the same for both pyramids, that is, $N/8$. In the right-hand pyramid, the opening and blocking of the box already prior to taking the measurement has led to a local change in the probabilities. Only the probabilities of the directly adjacent boxes are affected.

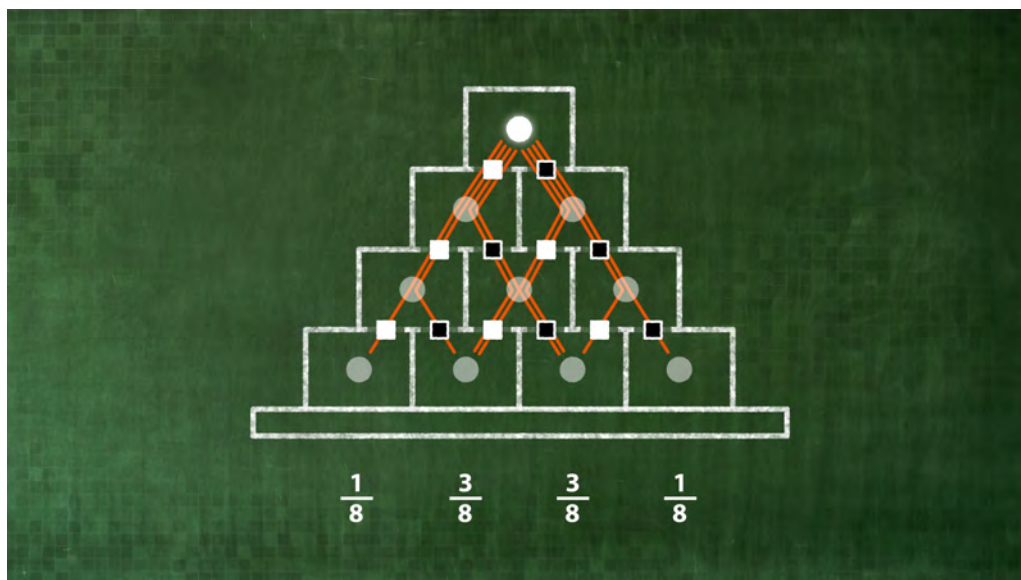


Figure 4. U1-1: Possible paths through the stepped pyramid.

A local change in the probabilities is independent of the measurement. A non-local change in the probabilities only occurs through a measurement.

1.1.6. Conclusions [Link to U1-1-06](#)

Let us summarise what we have found out about paths and probable locations of an individual particle in a stepped pyramid, and, for that purpose, look at the path of a particle from A to B.

1. The probability P (“A to B”) of the particle to reach Box B is determined by the sum of the individual probabilities P_k of all possible paths $k = 1, 2, 3$ to that box.

2. The measurement in a box affects the probability of the balls being located in any other causally connected boxes, irrespective of how far away from the measuring point these boxes are. For the transition from the pyramid of probability to quantum physics, a further conceptual step is necessary, which is dealt with at the Station U1-06, “The Heart of Quantum Physics”.

1.2. Sound interference (U1-02)

How will classical waves propagate through real space? What is the role of the observer? What happens if waves superpose on different possible paths?

1.2.1. Sound beats [Link to U1-2-01](#)

We can hear Omega’s doorbell against the background music. The bell resounds with cyclic changes in volume, the so-called beats. How do they come about?

1.2.2. *Tuning fork* [Link to U1-2-02](#)

In this slide, we shall discuss the amplitude and frequency of sound waves using an example of different tuning forks. At concert pitch A, the tuning fork vibrates back and forth 440 times per second. Its frequency is therefore 440 hertz.

If the vibrations are weaker, the wave crests and troughs become smaller. In other words, the maximum deflection, or the so-called amplitude, decreases. The sound becomes lower. The wavelength, which is represented with λ , remains the same. If the vibrations are stronger, the wave crests and troughs increase, and the amplitude increases with them. The sound becomes louder. The wavelength λ does not change. If the tuning fork is heavier, it vibrates slower. That means its frequency decreases, and the pitch becomes deeper. The wavelength λ increases. If the tuning fork is lighter, it vibrates quicker. That means its frequency increases, and the pitch becomes higher. The wavelength λ decreases. The sound wave propagation speed c remains constant at about 340 metres per second. It is equal to λ times f .

1.2.3. *Spinning wheel* [Link to U1-2-03](#)

The Spinning wheel, which is used to represent frequency, amplitude, and phase of a vibration, is also called phasor diagram in the literature. It is extremely useful for the calculation and visualization of vibrations. A phasor is rotating inside the spinning wheel. The length of the phasor corresponds to the radius of the wheel. The number of circular revolutions per second represents the frequency of the sound wave. The radius corresponds to the amplitude of the sound wave. The wavelength λ is calculated from the ratio of the wave propagation rate c and the frequency f .

Let us consider the red dot on the wave, and let us think of the best way to clearly describe its position, or, more precisely, the phase of the wave. One option is to use the dot's distance δ to the next zero crossing of the wave. The distance δ can be used in the following formula: phase shift ϕ equals two pi times δ divided by λ . That is precisely the phase of the sound wave we have already seen in the previous station. This slide shows the mathematical definition of this phase.

1.2.4. *Modeling a single tuning forks with a spinning wheel* [Link to U1-2-04](#)

Let us now explain the relationship between the wheel and the tuning fork in more detail. The maximum tine displacement determines the high and low-pressure areas that the tuning fork generates in the surrounding air. The resulting amplitude, or radius of the wheel, is used to describe these pressure fluctuations.

If the tuning fork vibrations are weaker, the fluctuations in pressure and density decrease. The sound becomes lower. The amplitude is reduced, while the wavelength does not change. If the vibrations are stronger, the fluctuations in pressure and density rise. The sound becomes louder. The amplitude increases, while the wavelength does not change. If the tuning fork vibrates slower, the rotation frequency of the phasor

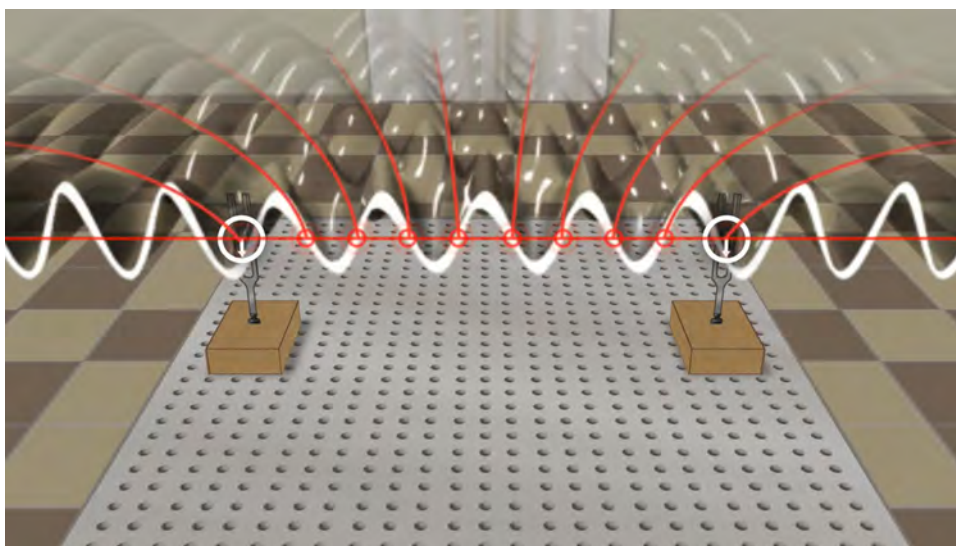


Figure 5. U1-2: Interference of two sound waves.

decreases. The sound becomes deeper, and the wavelength increases. If the tuning fork vibrates faster, the rotation frequency of the phasor increases. The sound becomes higher, and the wavelength decreases.

1.2.5. *Two tuning forks* [Link to U1-2-05](#)

Two identical tuning forks are struck one after the other. The sound waves produced by both tuning forks interfere with each other as they travel through space.

When the crest of one wave overlaps with the crest of the other wave, or the troughs of two waves meet, the two waves reinforce one another, and the sound becomes louder. If a crest of one wave meets a trough of another wave, the waves cancel each other out, and the sound in this section ebbs away. Let us now consider a specific phenomenon that occurs on an imaginary line connecting two tuning forks. Two sound waves travelling in opposite directions interfere with each other, creating a so-called "standing wave". The points where the two sound waves always cancel each other out are called nodes, and they are one-half wavelength apart. Antinodes, where both sound waves reach maximum amplitude, form midway between the nodes. These nodes are starting points of nodal lines on the plane shown here, and of nodal surfaces in space. The sound waves cancel each other out on every nodal surface in space.

1.2.6. *Interference* [Link to U1-2-06](#)

We can see the antinodes and the nodal lines better from a bird's eye view. How do we apply frequency, amplitude, and phase to describe this "new" wave structure, a product of interfering sound waves that originate from two tuning forks, at a particular point in space?

To this end, let us assign a spinning wheel to each sound wave. We now have two sound waves that interfere at point B. Let us represent that interference by a combination of two wheels. Mathematically, the interference is defined as a sum of the two sound waves. This is the same as adding the vectors of the two phasors. At point B, both phasors point in the same direction. The phase difference is zero degrees. When we add the two radii, the amplitude doubles. The two sound waves produce maximum reinforcement, and the constructive interference can be heard due to the increase in volume. The point B moves further, which means that the path difference Δ is one-half wavelength. Both phasors now point in the opposite directions. The phase difference is 180 degrees. When we add together the two phasors, the result is zero, which means that the amplitude of the resultant wave is likewise zero. The destructive interference at this point is perceived as silence. Point B moves one more time by one-half wavelength, so that both phasors point again in the same direction. The acoustic effect which follows is, again, a doubling of the amplitude. The phase difference is 360 degrees. It corresponds to the path difference of precisely one wavelength. Δ equals λ .

1.2.7. *Sound intensity* [Link to U1-2-07](#)

Let us now consider the intensity of the resultant sound wave. We cannot hear sound waves directly; we can only perceive their intensity. What is the main difference between the amplitude of the sound wave and the sound intensity? Absolute silence cannot be negative. This means in mathematical terms that the sound intensity must be greater than or equal to zero. The sound intensity I is proportional to the square of the amplitude of the sound wave. As a result of squaring, the intensity is always greater than or equal to zero. The radius of the spinning wheel, or the amplitude, thus corresponds to the root of the sound intensity. Our brains perceive the rapid fluctuations in pressure and density, that have been generated by the tuning fork and arrive at our ears, not individually, but as a time-averaged pitch. Hence, calculating the sound intensity involves additional temporal averaging.

1.2.8. *Beat* [Link to U1-2-08](#)

We have now struck two tuning forks that vibrate at minimally different frequencies. What we hear are so-called beats. In other words, we perceive fluctuations in the volume of the resulting sound wave along the time axis.

What has happened due to the sound waves of the two tuning forks interfering? Initially, the first and the second sound wave had different frequencies, but their amplitudes and phases were equal. When we combine the two spinning wheels, it becomes apparent that the different rotation frequencies of the wheels result in an increasing phase difference over time. This causes the periodic volume fluctuations, or beats. That's exactly the effect we have observed at Omega's doorbell: when tones with

very similar frequencies are superimposed, the result is a beat. It is clearly audible as a variation in volume of the echoing sound.

1.3. Reflection probability - photons at the beam splitter (U1-03)

What happens to a photon hitting a beam splitter?

1.3.1. Reflection and transmission [Link to U1-3-01](#)

We see in the window both the face of the janitor and a weaker reflection of Alice. That means that light is partly reflected by the pane of glass, and partly transmitted through it. As light consists of many individual photons, we may ask ourselves how the individual photon on the window pane behaves. Based on the following experiment on the beam splitter, we will explain that it can't be predicted whether an individual photon is reflected or transmitted. If we were able to perceive individual photons, we could then recognise the strongly fluctuating random pattern of transmitted (white square, □) and reflected (black square, ■) photons. Only through the overwhelming number of photons, quantum randomness averages out, becoming invisible to the naked eye.

1.3.2. A laser beam hitting the beam splitter [Link to U1-3-02](#)

A continuous laser beam throws a red point on the wall. In the laser beam, we place a beam splitter. As a result, we obtain a second red point on the wall. With the helium neon laser used - wavelength equal to 632 nanometres - with the output being one milliwatt, 0.3×10^{16} individual photons per second hit the beam splitter cube. Of these N photons, 50 percent are reflected and 50 percent transmitted. That means that the reflection and transmission intensity are both proportional to $N/2$. To understand quantum randomness in transmission and reflection, we need to use a specific light source that is able to generate individual photons in a controlled manner.

1.3.3. Single photons at the beam splitter [Link to U1-3-03](#)

A notable characteristic of the beam splitter is that it divides the photon wave into exactly two equal amplitudes, describing a reflected component and a transmitted component. However, only one of the detectors displays a signal that can be observed, because the energy of a photon can only be measured at one location. When measuring a photon wave, either only the "white" detector or only the "black" detector displays a signal. In the quantum optics laboratory, the fundamental randomness in the transmission and reflection of individual photons can thus be proven experimentally using that method. If this measurement is repeated several times consecutively, a black-and-white random pattern emerges. Precisely this experimental set-up is used to generate random numbers that are entirely independent from one another.

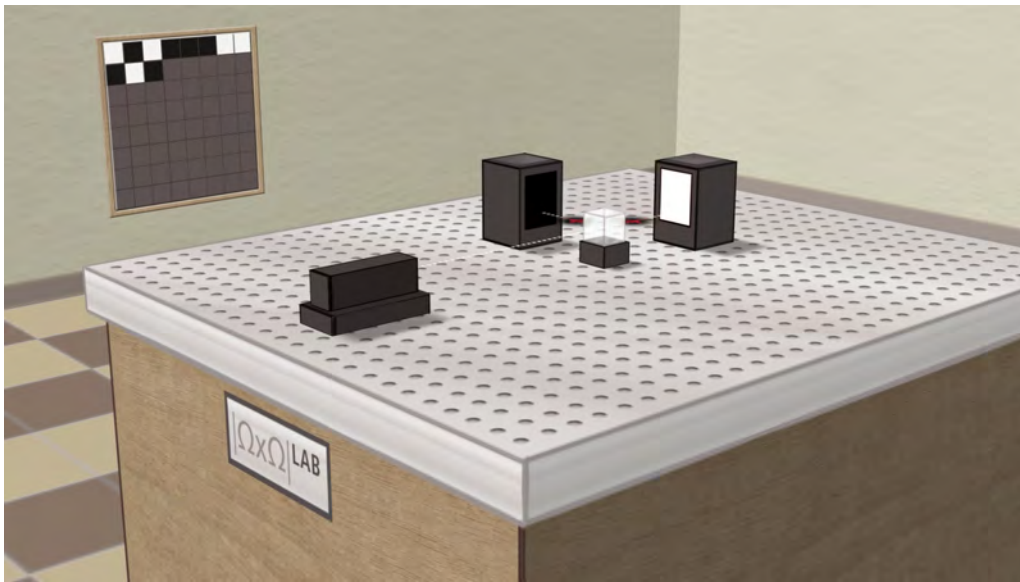


Figure 6. U1-3: Before the interaction with the detectors, a superposition of the amplitudes for transmission and reflection emerges. But only one of the two detectors will register the signal of the photon: transmission (□) or reflection (■).

Randomness cannot be calculated. Consequently, no computer can generate genuine random numbers. This experiment is crucial as it is an inexhaustible source of random numbers.

1.3.4. Reflection and transmission probability [Link to U1-3-04](#)

We cannot accurately predict the measurement result when looking at an individual measurement. We can only specify a probability, namely 50 percent for White (□), and 50 percent for Black (■). We see, in the image, 64 measurement results for 64 photons on the beam splitter. If we assume a 50:50 percentage probability, can we also conclude from this that we have 32 black fields and 32 white fields? Let us count up the fields. Doing so gives $N(\blacksquare)$ equal to 31 black fields and $N(\square)$ equal to 33 white fields. Theoretically, we expect the value P equal to 50 percent for either black or white. However, this value is not arrived at exactly in the experiment. Random fluctuations occur, which fluctuate around the theoretical value. The size of the fluctuations depends upon the total number N of measurements. The more measurements are conducted, the smaller the fluctuations around the anticipated value of 50 percent. This follows from the central limit theorem. $P(\text{experimental})$ approximates $P(\text{theoretical})$ as N approaches infinity.

For our observations in everyday life, that means that we see too many photons simultaneously. As a result, the intensity fluctuations and thus quantum randomness become invisible. Only in the quantum optics laboratory, this fundamental quantum randomness can be proven with single-photon experiments.

1.4. Light Interference – Wave property of light on a soap film (U1-04)

What happens is light hits a thin soap film? How can we explain the observation?

1.4.1. Dazzling colors (U1-04-01) [Link to U1-4-01](#)

Just as with the window, the incident light falling on the soap film is both reflected and transmitted. In contrast, however, a soap film is only a few thousandths of a millimetre thick, and thus only a little bit greater than the wavelength of the visible light. If the soap film changes its form by being blown, our viewing angle changes, too. There thus appears to be a dependence of the iridescent colours upon the thickness of the soap film, the viewing angle and the wavelength of the light.

1.4.2. Interference patterns on a soap film [Link to U1-4-02](#)

We illuminate a soap film with white light. White light is a mixture of various wavelengths or colours. On the soap film, we observe a pattern consisting of various coloured stripes, with the periodic sequence of the stripes becoming increasingly narrow towards the bottom. We can assume that, due to gravity, the soap film increases in thickness towards the bottom. It consequently looks as though the pattern depends upon the thickness of the soap film. If we consider that the light that hits the soap film was originally perceived by us as white light, it appears that red and green stripes occur wherever a wavelength disappears from the mixture. Thus, if a wavelength, in other words a colour, is removed from the incident white light, the complementary colour becomes visible on the soap film. We moreover observe that the colour appears to vary in intensity within the coloured stripes. How can colour pattern be explained? Just as with the acoustic waves, the observations lead us to the phenomenon of interference.

1.4.3. Wave Theory of Light [Link to U1-4-03](#)

A soap film becomes gradually thicker towards the bottom. We are continuing to represent the light as an electromagnetic wave. For the sake of simplicity, we will only take into consideration the electric field component. Let us recall the representation of an acoustic wave. In a similar way, we can also describe a given wavelength λ from the light spectrum. In order to do so, we need a frequency, an amplitude and a phase. For the colour red with the wavelength $\lambda = 650nm$, the rotation frequency amounts to approximately 4.6×10^{14} revolutions per second. We determine the amplitude which corresponds to the radius R of the rotating wheel from the square root of the incident light intensity I_0 . Is it possible to determine the increase in the thickness of the soap film from one red stripe to the next?

1.4.4. The Thales circle – interference at thin layers [Link to U1-4-04](#)

A small part of the red light is reflected in each layer. As the layer thicknesses δ are of equal size, the amplitudes that is, the lengths of the arrows are always of the same size. The frequencies of the rotating wheels representing the reflected partial waves are also identical. Just as with the two acoustic waves from Station 2, we recognise that only the resulting angle that arises between the first vertical arrow and the second arrow changes as the wave propagates a little through the soap film. The two reflected partial waves add up, in vector addition, to the resulting reflected light wave $\sqrt{I_R}$ at this point. As the thickness d of the soap wall increases, the number of layers with thickness δ also grows. We see that the incident light is reflected in all layers. Based on the phase shift between the individual layers, the individual amplitudes of the light wave move along the circumference of a circle. We can thus describe the reflection and transmission of a given light wave on a soap film using a Thales circle. The resulting reflection and transmission amplitudes are always perpendicular to one another. With the increasing thickness of the soap film towards the bottom, the Thales circle is traversed several times. This corresponds to the periodic sequence of minima and maxima of reflection or transmission of red light.

1.5. The double slit experiment - a milestone in the history of physics (U1-05)

We compare the interpretation of the single- and double slit experiment with classical light and with single photons.

1.5.1. Light at the beginning of the 19th century [Link to U1-5-01](#)

At the beginning of the 19th century, the English physicist Thomas Young conducted a simple, yet groundbreaking, experiment with light. Light from a coherent light source falls through an aperture that has two narrow slits, finally hitting a viewing screen. Due to this interference pattern, Young could prove that light behaves like a wave. At the fifth station, we compare the interference pattern emerging from a single slit with that from a double slit.

1.5.2. Single-slit experiment [Link to U1-5-02](#)

A laser beam hits the single slit. What happens if we gradually decrease the size of the opening of the slit? We observe that the red dot dissolves, and additional light and dark stripes emerge in the vicinity. Behind the slit, light thus not only hit the screen following a straight path, but takes all kinds of directions, with fluctuating degrees of intensity, so that we see the stripes at various points on the screen.

1.5.3. Diffraction pattern at single and double slit [Link to U1-5-03](#)

In the case of a very narrow slit, which corresponds roughly to the size of the

wavelength of the laser beam, we see in the middle of the screen a main peak, and at the edge the first secondary peak. What pattern can we expect when a second narrow slit is opened? A doubling of the pattern of the single slit? In the case of the double slit, an intensely luminous main peak appears in the middle of the screen, which is, however, narrower in comparison to the single slit. We moreover observe that the distances between the various peaks are shorter than in the case of the single slit. Based on the clearly recognisable interference pattern, Thomas Young proved the wave nature of light.

1.5.4. Single photons at single- and double slit [Link to U1-5-04](#)

Today, we can conduct experiments with individual photons in the quantum optics laboratory. In case of the single slit, the random photon distribution gradually converges to the intensity distribution of continuous laser light, and thus to the bending pattern on the single slit with increasing number of single photons hitting the screen. Once again, the question arises what pattern will be seen if a second slit is opened. Will the individual photons generate an interference pattern as in case of the continuous wave with maximum intensity distribution in the middle of the screen, and multiple secondary peaks at the edge? Or is the emerging situation the doubling of the single slit pattern? The experiment shows that, also in the case of the double slit, the random photon distribution converges to the intensity distribution of continuous laser light of the double slit. We conclude that interference also occurs if only a single photon is detected pm to the screen after passing the double slit. This means that the individual photons must interfere with themselves. The combination of particle and wave properties leads us to solve the riddle of “self-interference of the photon”, taking us to the heart of quantum mechanics in the next station.

1.6. The Heart of Quantum Mechanics - the spinning wheel (U1-06)

What happens if we combine wave interference and probability properties?

1.6.1. Interference and Probability [Link to U1-6-01](#)

The photon as a wave – the photon as a particle. The two statements appear to us to be contradictory, especially if we perform experiments involving a large number of photons. The two specifications become blurred there, because many light quanta look, together, like a wave. The two representations supplement one another, and, pursuing the train of thought further, lead to no contradiction.

1.6.2. Single and double slit with classical light [Link to U1-6-02](#)

Let us compare the interference pattern of the single slit with that of the double slit.

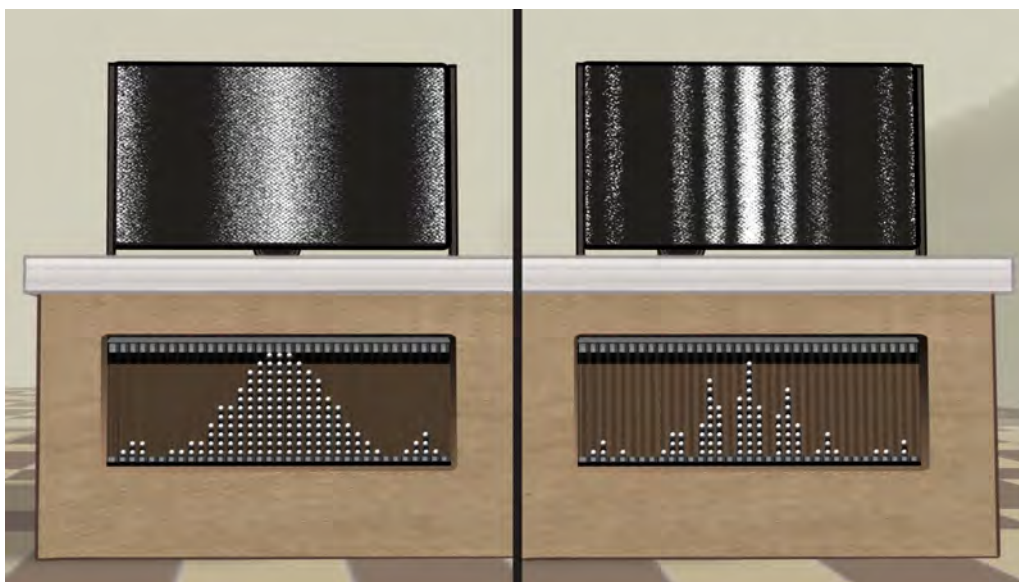


Figure 7. U1-6: Comparing single and double-slit experiment.

Firstly, after opening the second slit, we see more minima and maxima. Secondly, at point P, the light intensity on the screen in case of a double slit decreases compared to the single slit. Thirdly, the light intensity in the centre of the screen is higher in case of the double slit.

1.6.3. Vectors sums describing interference [Link to U1-6-03](#)

We consider a continuous laser beam on the single slit, and explain the interference pattern based on the wave theory. The laser is, in that context, described as an electromagnetic wave. Light travels in all possible directions. Starting with the straight path, we will divide the slit into six segments of equal size, and consider the phase differences that emerge. For the straight path, there is no phase difference, that is, all vectors point in the same direction. Let us now observe the red point on the screen. The six partial waves interfere there. Adding up the six vectors, we obtain the square root of the intensity I_S , which constitutes the maximum. Next, we consider the first minimum. What path difference Δ do the six partial waves take on at this location? After adding the six vectors, we see that the vector sum is zero. Thus, the phase difference between two successive partial waves is 60° . The resulting phase difference is $\Phi = 6 * 60 = 360$ or 2π . The phases of the six vectors always keep rotating in a circle, depending on the path difference Δ . The first secondary maximum is reached once the path difference has increased by a further half wavelength to $\Delta = 3/2\lambda$. Once the second slit has been opened, it can be seen that the path difference between the individual partial waves at the central maximum is zero again. In case of the double slit, the first minimum emerges much closer than in the case of the single slit. At the first minimum, the path difference Δ is half a wavelength. The partial waves of the first slit and the partial waves

of the second slit exactly eliminate one another. If the path difference Δ between the two slits corresponds exactly to one wavelength λ , we obtain the secondary maximum. Overall, the intensity distribution measured can be well explained based on this model of interfering partial wave.

1.6.4. *Single and double slit with single photons* [Link to U1-6-04](#)

Each photon hitting the screen is counted with a ball, which drops at the corresponding position on the screen, and is picked up in a pipe. Although the individual hits occur in a purely random manner, a ball distribution gradually forms, which allows for discerning a pattern. This pattern corresponds to the intensity distribution of the electromagnetic wave discussed in the previous slide. In the case of the double slit, we are likewise selecting a small number of photons. Again, the random distribution of the balls converges to the intensity distribution. In comparison to the single slit, we have considered only half the number of photons, so that the distribution maximum in the centre of the screen is equally high in the case of either the single slit or the double slit.

1.6.5. *Probability distribution* [Link to U1-6-05](#)

The position of a photon on the screen is determined by chance. Let us, for example, consider the red pipe in which 6 out of 150 balls have landed. The probability $P(x)$ in this pipe is $6/150 = 4$ percent. The position x of the photon can only be determined with an accuracy of δx , which corresponds to the width of the individual pipes. For any given point x within the pipe, we can only specify a probability density of $\rho(x) = P(x)/\delta x$. In any given location x , the number of balls is equal to $N_S \times P(x)$. The ball distribution in the pipes is thus a representation of the probability distribution $P(x)$ of each individual ball. As the ball distribution is proportional to the intensity distribution, it follows that $I(x)\delta x$ is proportional to $N\rho(x)\delta x$ equal $NP(x)$ - for both the single slit S and the double slit D. If we place the two curves of the single and double slit that emerge from the ball distribution on top of one another, we see that additional minima arise once a second slit is opened. So how do we get from the intensity distribution $I(x)$ to the probability density $\rho(x)$ of an individual photon? As $I(x)$ is proportional to $\rho(x)$, we only need to adjust the scale. In other words, the scale of the y-axis changes, but not the shape of the curves. As we have only observed $N/2$ photons at the double slit, the corresponding curve on the y-axis is doubled when the scale is adjusted. The areas underneath the curves correspond to the overall probability of 100 percent, as the photon will impact upon one point or another on the screen.

1.6.6. *Wave Interference and Particle Probability* [Link to U1-6-06](#)

On our journey to the heart of quantum physics, next, we compare the wave picture with the particle picture of light. In the wave picture, we can calculate the interference

pattern which corresponds to the intensity distribution of the light as square of the amplitude of the electromagnetic wave.

In comparison to that, in case of individual photons, the intensity $I(x)$ on the screen is proportional to the probability density $\rho(x)$ multiplied by the number N of photons. We combine the equation $I(x) = N\rho(x)$ with the equation $I(x)$ is equal to the square of the amplitude. In combination, we obtain an unfamiliar, new expression: The square root of the probability density $\rho(x)$, multiplied by the number N of photons. What can be concluded from this ‘squaring of the circle’? Let us take a look at an individual photon, i.e. set $N=1$. For the individual photon, the probability density $\rho(x)$ can then be calculated in a similar way as intensity distribution of a wave: it is the square of a rotating wheel with a rotation frequency, an amplitude, and a phase. Thus, we have found a fundamental, new description of light: A probability wave, symbolised by a rotating wheel. The radius corresponds to the square root of the probability density. The vector may be either positive or negative, owing to the phase. We can, however, not directly observe the phase. We can only indirectly recognise the phase based on the impact on the interference pattern if the path difference Δ between various different partial waves leads to phase differences. This “square root probability” with an invisible phase is termed, in quantum mechanics, as wave function Ψ . Mathematically speaking, the observation probability $P(x)$, the probability density $\rho(x)$ and the wave function $\Psi(x)$ relate to one another as follows. This equation yields the probability of detecting the photon in the range from x to $(x + \delta x)$. The spinning wheel symbolises an oscillation in the quantum dimension that cannot be directly observed, and thus forms the heart of quantum physics.

1.7. Paths into the quantum dimension - the path integral (U1-07)

What are the key ideas of the path integral ansatz first proposed by R. Feynman?

1.7.1. Turning the wheel [Link to U1-7-01](#)

A combination of many probabilities will never lead to a decrease of the total probability in classical physics. A rotating wheel, on the other hand, fluctuates between positive and negative values. In such a way, two principles can be combined in quantum physics: probability and interference. The phase of the spinning wheel remains hidden from us in a space which will only be revealed to us indirectly via digital measurement data and a fascinating mathematical description in the Hilbert space, which we call - the quantum dimension.

1.7.2. The laser beam in the empty space [Link to U1-7-02](#)

At Point A there is a laser light source, which rotates around an axis like a lighthouse, and emits a beam. Let us imagine a Point B in the room. Which way does the laser light travel from A to B?

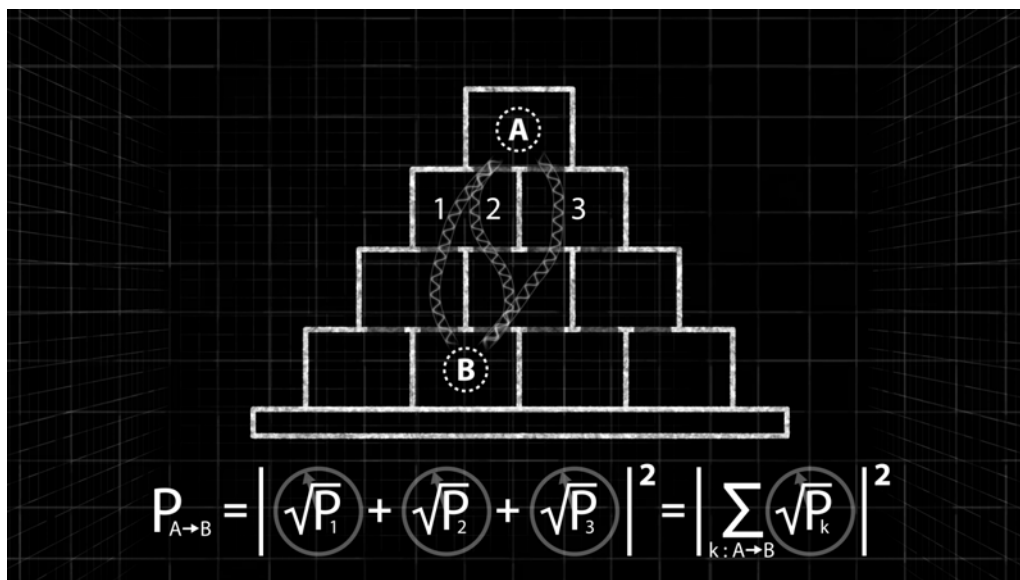


Figure 8. U1-7: Visualization of the key idea of the path integral: To each possible path which cannot be distinguished upon measurement, an amplitude is associated. The absolute square of the sum over all possible paths determines the transition probability. Compare to U1-1 for the "classical" case of the Dalton-Board.

1.7.3. Paths and probabilities in the quantum dimension [Link to U1-7-03](#)

Let us recollect the stepped pyramid and the possible routes, i.e. paths, that a classic particle can travel from A to B. The probability that the particle falls on one of the three paths into Box B is calculated as the sum of the individual probabilities for all paths to said box. Our laser light, however, must be described based on the rules of quantum physics. That means that we need to carry out a complex extension of the observation probability $P(x)$, to transform it into a probability capable of interference, in order to be able to make a statement on the probable location of a given light quantum. How do we achieve that? We associate a rotating wheel to each possible path. In such a way, we can form a vector sum on the square root probabilities of all possible paths to B. We thus add the vectors of the rotating wheels, and, in that way, obtain the amplitude in Box B. The square corresponds to the detection probability in Box B. With this so-called path integral formulation, Richard P. Feynman developed an important theoretical pillar of quantum physics.

1.7.4. The Cornu spiral [Link to U1-7-04](#)

If the photon is sent from A through an empty room and arrives at B, we do not know how it reached B.

We can, however, calculate the detection probability. For that purpose, we consider a selection of 11 potential paths. The paths become longer compared to the direct, straight path in the centre when moving outwards, leading to an increasing phase shift.

Summing over the amplitudes of all paths, we obtain the so-called “Cornu spiral”. The resulting red vector corresponds to the amplitude for the transition probability from point A to point B. We see that the direct, straight path and the directly adjacent paths are dominant. The contributions of the other paths mutually cancel one another out. Using the Cornu spiral, we can also depict any further interference patterns that photons can generate. Should, for example, a single or double slit exist in space as a scattering centre, some of the potential paths between Point A and Point B are cut off. Thus, other contributions from the Cornu spiral, which then no longer cancel one another out, suddenly become relevant.

1.7.5. *The Michelson interferometer* [Link to U1-7-05](#)

Besides the single and double slit, there are also many other important interference experiments in physics. Here, we see an interference pattern generated by the Michelson interferometer. If we hold hands into various points in the laser light, routes are blocked and we can discern the change in the interference pattern. If we block Path A and Path B, no light falls onto the screen. If we block either Path A only or Path B only, no interference pattern appears. As we have held a hand into the beam to suppress a path of light, an interference pattern now and then flashes into the close-up shot. That occurs due to the small gap between the fingers, through which a photon wave can again run through Path A, which then interferes with the wave from Path B. Here we see an interference pattern, which is generated by the so-called Michelson interferometer.

A laser light hits a beam splitter. Before the photons hit the observation screen, they travel along two possible paths via the mirrors A and B. Depending upon the difference in the wavelengths or the path difference between two routes, bending minima and maxima emerge on the screen, which we perceive as interference rings.

If we block off Path A and Path B with the hand, no light makes it to the screen. If we block either Path A only or Path B only, the light only falls on the screen via the remaining path, and the interference pattern disappears. As, in order to suppress the one path of light, we have held a hand into the beam, if a small gap remains between the fingers an interference pattern now and again flashes into the close-up shot, and in fact both paths can contribute.

1.8. **Polarisation of light - an interplay of vibration nodes and antinodes** (U1-08)

*How can we describe the polarisation of a single photon in the quantum dimension?
How can Malus' Law be generalized from classical light to single photons?*

1.8.1. *The polarisation* [Link to U1-8-01](#)

At this station we examine the theoretical and experimental properties of linear polarised light.

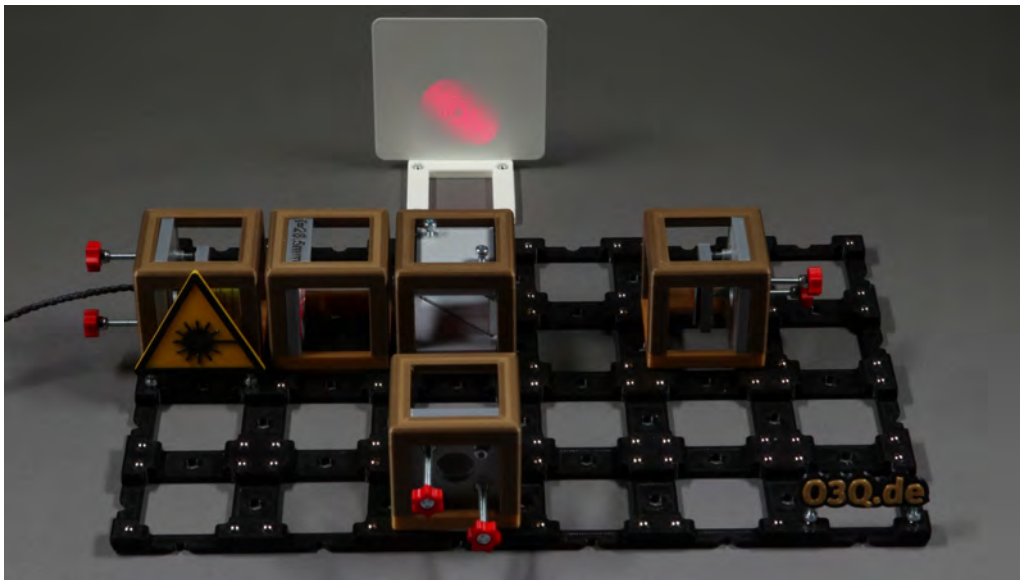


Figure 9. Low-Cost [Michelson-Interferometer](#) based on 3D-printing.

1.8.2. Experiment with a single polarisation filter [Link to U1-8-02](#)

In this experiment we observe light passing two polarisation filters. The first filter defines a polarization axis. Only the component of light polarized parallel to that axis can pass the filter.

If the polarization axis of the second filter is parallel to the first one, the light intensity does not change. If we alter the angle of the second filter, we see that the light intensity decreases. If the filters are orthogonal, no light will pass any more. The light intensity increases again if the angle increases towards 180° . The filters are then once again parallel to one another. In such a way, we obtain the angle-dependent “intensity distribution, shown as a red ellipse.

1.8.3. Polarisation filters and polarisation rotators [Link to U1-8-03](#)

The angle α between the two polarisation filters shown here can be rotated freely.

Using a rotating wheel, we can describe linearly polarised monochromatic light as a continuous wave. The direction of polarisation can be rotated freely on the plane. What will happen if we change the angle α of the second filter axis? Only the component of the electric field vector parallel to its axis can pass the filter. If the direction of polarisation of the incident light wave is vertical to the filter axis, the resulting field vector is exactly zero. There are two different types of polarisers: polarisation filters and polarisation rotators. In both cases, the light is polarised along the predetermined axis. In contrast to the filter, the amplitude of the light wave passing the filter does not change in the case of the polarisation rotator.

1.8.4. Polarisation of single photons [Link to U1-8-04](#)

The behaviour of single photons is determined by chance. What does this mean when determining the polarisation of single photons? Behind the polarisation rotator, the photon encounters a polarising beam splitter. Due to the crystal structure of the polarising beam splitter, a horizontal and a vertical axis are defined. If the incident photon is polarised along the vertical axis, there is a one hundred per cent probability that it will be transmitted, and that it will encounter the “White” detector.

We will now turn the direction of polarisation of the incident photon out of the vertical axis in 15° stages. A black-and-white random pattern emerges, that has a constantly increasing number of black measurement results, and a constantly reducing number of white measurement results. If the incident photon is polarised along the horizontal axis, it will, with one hundred per cent certainty, be reflected, and will encounter the “Black” detector.

1.8.5. Probability distribution [Link to U1-8-05](#)

If we measure the behaviour of a single photon at the polarising beam splitter, we obtain as answer either transmission or reflection.

Only when performing many individual measurements, the probability distribution for reflection and transmission in dependence on the angle alpha can be deduced. For that purpose, we sort the white and black fields at each given angle.

As a result, we obtain the probability distribution for transmission – “White” - and reflection – “Black” for all angles. Note that the probability distribution for “transmission” is proportional to the intensity distribution.

1.8.6. Probability and interference [Link to U1-8-06](#)

Let us recollect the introduction of the “heart of quantum mechanics” in station U1-6. There we saw that the behaviour of photons can be described by the combining probabilities with interference.

Probabilities are always positive numbers, which cannot become smaller when added. Thus, the phenomenon of the interference cannot be described by classical probabilities only. We are thus leaving the “classical dimension”, by extending the probabilities P-White and P-Black by an invisible oscillation in the quantum dimension, visualised by rotating wheels. The radius corresponds to the square root of the probability for transmission P_{\square} and reflection P_{\blacksquare} . The phase of the rotating wheel may be either positive or negative, depending on the angle, thus allowing for constructive and destructive interference. We cannot observe it, and yet it is important once again to remind ourselves: PRIOR to measuring – in other words, prior to the interaction with the detectors – the photon is neither transmitted nor reflected. The amplitudes for both possibilities are in a superposition state, and it is not possible to say where the photon is localized.

1.8.7. Polarization of a single photon in the quantum dimension [Link to U1-8-07](#)

Let us consider the probability distribution $P_{\square}(\alpha)$, displayed as red oval line. At each angle, we replace the probabilities by amplitudes, symbolised by rotating wheels. Thus, we obtain an oscillation in the quantum dimension, which is shown here by a luminous, white, oscillating circle. This oscillation has a nodal line on the x-axis, corresponding to horizontal polarization, and an antinode on the y-axis, corresponding to vertical polarization. Thus, the amplitude for vertical polarization is maximal when measured in the y-axis, and decreases to zero on the x-axis.

1.8.8. Summary [Link to U1-8-08](#)

We can summarise the results of station U1-8 by applying our scheme of four quadrants. In the first quadrant, the polarization of many photons is measured simultaneously. An intensity distribution emerges, which depends on the difference in the angle between two polarisation filters. In the second quadrant, the polarization of individual photons is measured. A black-white random pattern for transmission or reflection emerges. The probabilities for transmission and reflection depend on the angle. For 45° , the probabilities both are 50 percent. In the third quadrant, we sort the number of transmitted and reflected photons and arrange the resulting probabilities on a circle. In such a way, we obtain an angle-dependent probability distribution for transmission, which is proportional to the intensity distribution. Before the interaction with the detectors, we cannot describe the state of the photon just using probabilities, as probabilities cannot interfere with each other. In the fourth quadrant, we thus embark into the quantum dimension by generalizing probabilities by amplitudes, visualized by rotating wheels. An oscillation with one nodal line emerges, which describes the amplitude for transmission. The amplitude for transmission is zero at the nodal line, meaning that the photon is reflected in this angle with 100 percent probability.

1.9. Correlation function - searching for order in randomness (U1-09)

What kind of random patterns emerge when Alice and Bob perform experiments with two coins, or with a single coin?

1.9.1. Tow random patterns [Link to U1-9-01](#)

When the janitor and Alice go into the next room, they pass two chess boards. Black-and-white random patterns emerge on these flickering chess boards. At this station we will be concerned in a more in-depth manner with various black-and-white random patterns. If “White” has been measured, how great is, in that case, the probability of “Black”, or of “White”, if a second measurement is taken?

1.9.2. Two coins, one coin [Link to U1-9-02](#)

Alice throws one coin, and Bob the other. The first three results match one another. Is that mere coincidence? Or is there a secret connection between the two coins? We can only answer this question once Alice and Bob have carried out a lot of experiments. We vary the experiment, and take only one coin with one black side and one white side. Alice and Bob are looking at a single coin on a glass table from two different perspectives. Alice carries out her measurement. Based on her result, she can immediately conclude that Bob will measure black, irrespective of when, and how far removed from Alice, Bob takes his measurement. After 64 throws, both of them obtain a random pattern. Every random pattern, in itself, appears just as random as in the first experiment with the coin. When the two random patterns are compared, however, we see the difference to the first experiment with two coins.

1.9.3. Correlation function [Link to U1-9-03](#)

Without exchanging their measurement results, Alice and Bob cannot decide whether there is a specific connection between their random patterns, or not. Thus, they need to compare their measurement results with one another. A connection exists between the measurements, for example, if the results always match one another, or if they never match one another. To establish that, we count up, how often the measurements of Alice and Bob match, and how often they differ. The difference between the number of matching and different measurement results in the experimentally determined correlation function C . By dividing by the total number of all measurements, the value of C gets normalized and ranges between minus one (anti-correlation) and plus one (perfect correlation). If we compare the two random patterns from a coin, all fields become grey. We then obtain the result that the Correlation C is equal to -1 , that is, anti-correlation. The correlation function specifies to what extent the random patterns depend upon one another.

1.9.4. Theory and experiment [Link to U1-9-04](#)

Let us compare the theory and experiment of the two coin experiments. There are four possible measurement results. Each of the combinations has a certain probability. Let us calculate the correlation function for the case of two different coins. $P(\text{Black})$ equals $P(\text{White})$, equals $\frac{1}{2}$. The probability for two independent coins can be seen as the product of the individual probabilities. The greater the number N of measurements is, the smaller will be the fluctuations around the theoretically calculated expected value. As we have already seen in Stations U1-3, chance is averaged out if the number N approaches infinity. Certainty thus arises from an infinite number of chances. The experimental value always approaches exactly the theoretical value - however, only if the theory is true. In this simple example, that is, of course, the case.

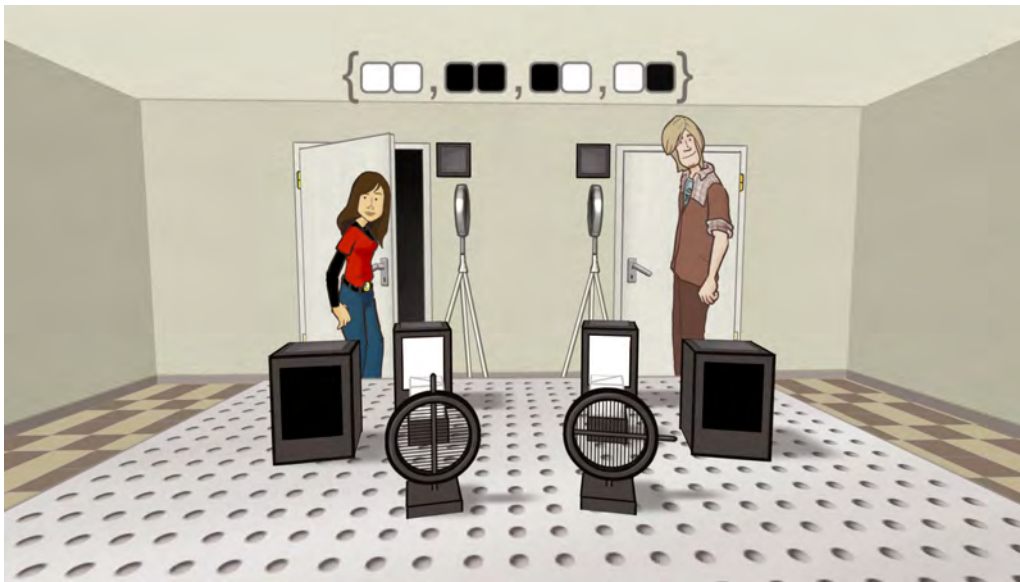


Figure 10. U1-10: Both doors can be either open or closed - representing the four possible measurement outcomes from Alice and Bob.

1.10. Combined measurement of polarisation - The two-doors metaphor (U1-10)

The two doors that are either open or closed, corresponding to transition of reflection of the measured pair of entangled photons at the detectors Alice and Bob. What determines the measurement results?

1.10.1. Two-doors metaphor [Link to U1-10-01](#)

The two doors to Prof. Omega's room are correlated. Alice discovers that Bob's door is closed if her door is open. If Bob's door is open, Alice's door stays closed. Chance decides which door opens in each trial. From the four possible combinations, only two are realized in this experiment. In other words, Alice and Bob's door locks are anti-correlated. Each door is associated to a polarisation filter. In the beginning, the polarization axes are parallel. After a while, Bob rotates the axis of his polarisation filter to the vertical position. By doing so, he alters the correlation between the doors. Alice's door now behaves exactly the same way as Bob's door - both locks are correlated with one another. What is behind this two-door metaphor? Why is the correlation between the doors altered by rotating the polarisation axis?

1.10.2. The detectors "Alice" and "Bob" [Link to U1-10-02](#)

The two-door metaphor symbolises an important experiment with pairs of photons in quantum optics. The polarisation of the pairs of photons is measured in the following experimental set-up. On Alice and Bob's side, there are a polarisation rotator, a

polarising beam splitter and two detectors, respectively. The “White” detector registers the transmitted photons – door open – and the “Black” detector reflected photons – door closed. Depending on the relative position of the polarisation rotators, the correlation between the measurements of “Alice” and “Bob” gradually changes from correlation to anti-correlation.

1.10.3. Correlation function [Link to U1-10-03](#)

Depending upon the angle of the polarisation rotators, one of the four possibilities $((\square, \square), (\blacksquare, \square), (\square, \blacksquare), (\blacksquare, \blacksquare))$ is realized in each measurement. Alice and Bob can, independently from one another, choose the measurement basis with their polarization rotator. Let us now determine the correlation function between the random patterns of Alice and Bob. In the case of a parallel position, the measurement results are identical, and thus fully correlated. At 45° , the measurements are uncorrelated. At 90° , they are anti-correlated.

1.11. Entangled photons - before and after measurement(U1-11)

What happens to Omega upon observation? How can we reconstruct the entangled state $|\Omega\rangle$ in the quantum dimension from the measurement results?

1.11.1. Birefringence [Link to U1-11-01](#)

The birefringence of light has already been known since the 17th century, and was discovered with calcite. Here we show a calcite crystal, lying on a chessboard pattern. If the light ray hits the crystal, it splits into two polarised parts, that are perpendicular to one another, resulting in a double image. Using a linear polarisation filter, we can select the two components individually. The horizontal polarised part can be discerned here. Upon rotating the polarisation filter, the slightly offset vertical polarised part becomes visible.

1.11.2. "Non-local or local chess": Omega's shadow on the wall [Link to U1-11-02](#)

Alice and Bob are surprised about the two chessboards at the end of Omega's room, opposite the two doors. Just like the doors, the two chessboards stand for the experimental results from pairs of entangled photons. In this metaphor, the two figures of Alice and Bob become detectors of photon pairs. In the film, Bob starts the experiment with the press of a button. We see an object in the centre of the room, which is illuminated from the two doors, each one by a flickering headlight. Thus, Alice and Bob see, on the opposite wall, two flickering shadows of a single object. In that respect, the shadow metaphor shows the following: when projected onto the wall by two headlights, the three-dimensional object loses the third dimension, and is shown as a pairs of two-dimensional shadows.

1.11.3. Experiments with entangled photons [Link to U1-11-03](#)

Here we see a simplified representation of the experimental set-up. The aim of the experiment is to produce pairs of entangled photons. BBO crystal: The crystal is optically birefringent. In this crystal, some of the incident ultra-violet photons, create pairs of two photons, each having half energy and reverse polarisation, i.e. once horizontally polarised, and once vertically. Two polarisation rotators, two polarising beam splitters, a pair of detectors at Alice and Bobs side, respectively. Alice and Bob each define their respective “vertical” and “horizontal” measuring axis by adjusting their polarisation rotators. A huge number of ultraviolet photons run through the BBO crystal, without pair creation. Only with very small probability, pairs of entangled photons are created, leaving the crystal along the two red lines.

1.11.4. The entangled quantum state Omega [Link to U1-11-04](#)

The entangled photons leave the BBO crystal, due to the special crystal structure, somewhere along the upper (R) and lower (L) green cone. R and L stand for two orthogonal polarisation directions. Depending upon the incidence angle of the laser beam to the BBO crystal and other optical components in the beam path, various different polarisations of the photon pairs can be generated. In this experiment, instead of linear polarised photons, circular polarised photons are used. Each photon pair leaves the crystal somewhere along these two cones. The photons are detected at exactly opposite positions, with circular polarisation (R: clockwise/L: anti-clockwise). Something quite special occurs at the two points where the cones intersect: It cannot be distinguished whether photon L is found at the left-hand intersection, and photon R at the right-hand intersection of the two cones, or vice versa. Both possibilities are in superposition in the quantum dimension leading to the entangled photon pair Omega. The detectors Alice and Bob are positioned in such a way that they can measure entangled photon pairs. Only on the red lines, a superposition and thus entangled photons are created. Only a minute fraction of the photons that hit the BBO crystal lead to such entangled photon pairs. The vast majority of ultraviolet photons pass through the crystal without interaction - see the blue line. Of the photon pairs that have emerged, in turn, almost all are not entangled but just product states, as they do not leave the crystal at the intersection lines of the two cones - compare the green circles. Only at the intersection of the two cones, the states LR and RL are indistinguishable and thus in superposition, resulting in the emergence of the entangled photon pair Omega.

1.11.5. Rotating coin [Link to U1-11-05](#)

How can we describe the entangled quantum oscillation $|\Omega\rangle$? Tentatively, we compare it with a coin, which is observed from the perspective of both Alice and Bob. Both possibilities are equally probable. In the quantum dimension, the two probabilities are in superposition. The measurement result is not defined prior to the measurement

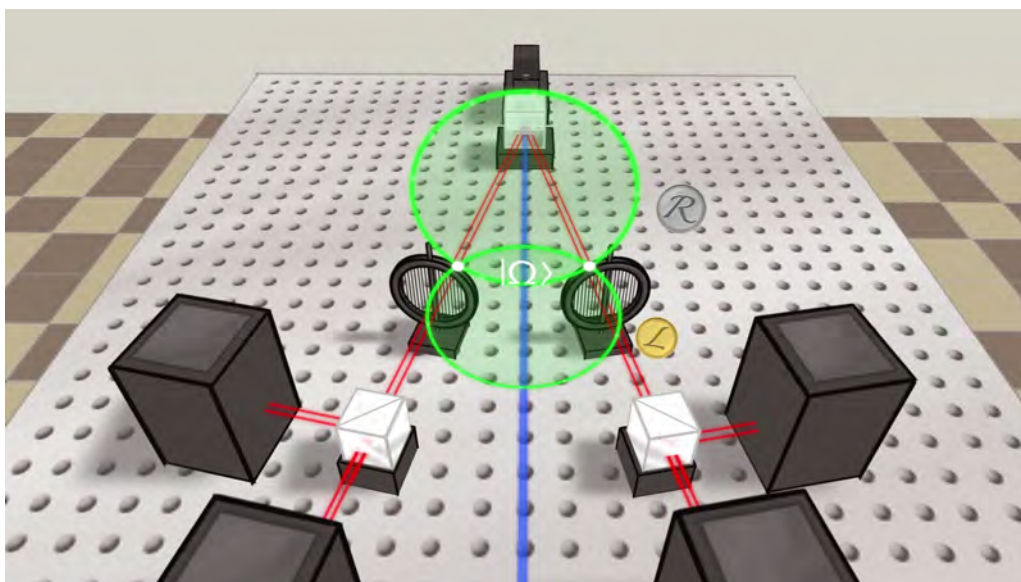


Figure 11. U1-11: Creation of entangled photons in experiment.

being taken. Therefore, the probabilities $P = 1/2$ for both possibilities must be generalized to rotating wheels with a radius of $1/\sqrt{2}$, meaning that the probabilities can interfere. Since Alice and Bob observe a single rotating coin from different perspectives, Alice’s measurement at this coin immediately influences Bob’s potential measurement result, as the measurement disturbs the superposition of the two probabilities. Note that the spatial distance between Alice and Bob it is irrelevant for this influence on the quantum superposition.

1.11.6. The “Omega Donut” in the quantum dimension [Link to U1-11-06](#)

Just as with the linear polarised photon from Station U1-08, we substitute the probability $\frac{1}{2}$ in every angle by rotating wheels having the radius $1/\sqrt{2}$, which oscillate on a circular axis between $+1/\sqrt{2}$ and $-1/\sqrt{2}$. This oscillating 3D circle delineates the form of a symmetrical baked donut. If a right-hand circular polarised photon is in superimposition with a left-hand circular polarised photon, the rotations are equalised. That means that superposition state must be rotationally invariant. Thus, Omega is then simply described by an oscillating circle. All amplitudes have the same length $1/\sqrt{2}$. As a next step, we will break down the Omega Donut in such a way that we can introduce the “horizontal” and “vertical” measuring axes as a coordinate system. Thus, we will perform a basis transformation from the basis R, L to the basis H, V. In a simplified notation, we are showing here the direction of the antinode. As Omega is rotationally symmetrical, the V/H coordinate system can be rotated at will. The double arrow axes indicate the directions of the antinode. This, again, is a basis transformation. The direction of the antinode is then marked as “V hat” and as “H hat”.

1.11.7. Visualization of the measurement process [Link to U1-11-07](#)

When “projected” from the quantum dimension into the three-dimensional world, the rotationally symmetrical oscillation Omega throws two “shadows” to Alice and Bob, describing the probability distributions for transmission (white ring) and reflection (black ring) in every angle of the polarisation rotator. When mapping the rotating wheel to the probability, the phase information is lost, and in turn, one dimension of Omega. Next, suppose that Alice performs a measurement. What is the impact of Alice’s measurement to Bob?. Alice initially selects her horizontal and vertical measuring axes by an angle of the polarisation rotator determined by her. The angle of Bob’s polarisation rotator is, for the time being, irrelevant to the following discourse. In the measuring axis selected by Alice, the entangled photon pair Omega interacts with the “White” and “Black” detectors from Alice. Prior to taking the measurement, Omega is, from Alice’s perspective, a superposition of two vertically and two horizontally polarised photons (cf. the red/brown double arrow pairs). For the outcome “White” (□) or “Black” (■), there is always the probability of 1/2. Prior to taking the measurement, the outcome is not yet certain – the two probabilities are in superimposition. If Alice measures “White” (□) equals transmission, the photon has been vertically polarised in relation to Alice’s measuring axis. When Alice measures “Black” (■) equals reflection, the photon was horizontally polarised. To put it another way: the measurement is the projection of the photon onto either the vertical or the horizontal component at Alice side. Alice measures again – and her “Black” (■) detector registers a photon, meaning that...

1. the photon measured was horizontally polarised.
2. the vertical portion of the photon pair is destroyed.
3. the remaining photon of the photon pair has the same horizontal direction of polarisation as Alice’s photon.
4. Bob’s oval-shaped probability distribution now describes the observation probability of a horizontally polarised photon.

According to quantum physics, Alice’s choice of her measuring axis has a direct influence on Bob’s potential measurement result, without any time delay. Alice cannot influence whether she obtains the result “Black” or “White”. After taking the measurement, Alice can, however, state with certainty how Bob’s photon will be polarised. However, whether Bob measures Black or White is something that she can only ascertain by comparing the measurement results, as Bob can likewise freely select his measuring axis independent of Alice.

1.11.8. Quantum mechanical calculation of the correlation function [Link to U1-11-08](#)

Without exchanging their measuring data, Alice and Bob cannot state whether their results are correlated with one another or not. The correlation function can, however, be calculated from quantum theory based on the assumption that Alice and Bob observe the entangled state Omega. We have to determine the four combined

probabilities: $((\square, \square), (\blacksquare, \square), (\square, \blacksquare), (\blacksquare, \blacksquare))$. The top row of representations relates to Alice's white measurement result, the bottom row to Alice's black measurement result. On the right-hand side at the top, we see the probability distribution $P(\text{White, White})$ - a white oval, and implicitly also $P(\text{White, Black})$ - black crescents - of Bob. On the right-hand side at the bottom the probability distribution $P(\text{Black, White})$ can be seen - a white oval, and implicitly also $P(\text{Black -Black})$ - black crescents - of Bob is shown. Moreover, the probability distribution for Bob's photon depends on the difference in the angle $(\beta - \alpha)$ of his and Alice's measuring axis. Should, for example, the difference in the angle be zero, then the probability of $P(\text{White, White})$ is 100 percent for Alice's "White" measurement. We now see two curves for Bob's probability distribution, depending on the difference in the angle both for matching measurement results, and for for different measurement results. If we work out the difference between the two probability distributions, we obtain the theoretically calculated correlation function C .

1.11.9. Alices and Bobs series of measurements [Link to U1-11-09](#)

Alice and Bob first of all select matching measuring axes, i.e. both angles α and β of the two polarisation rotators are at 0° . Whereas Alice does not change her measuring axis, Bob rotates his directions of polarisation on up to 90° in 15° steps. For every angle combination, 64 measurements are carried out, and recorded as Black/White random patterns.

1.11.10. Experimental determination of the correlation function [Link to U1-11-10](#)

Alice and Bob can only determine the correlation by comparing their random patterns after the measurement. For that purpose, we compare the corresponding random patterns and subtract, for every angle difference $(\beta - \alpha)$, the coinciding combinations (White/White, Black/Black), from the non-coinciding combinations (Grey boxes). The resulting correlation depends upon the angle difference $(\beta - \alpha)$. For identical angles, we obtain total correlation, for $\beta - \alpha = 90^\circ$, anti-correlation. For 45° , the measurement results are uncorrelated. If we compare the correlation obtained by experimentation (white dots) with the theoretical predictions of quantum physics (red curve), there are still minor deviations occurring after 64 measurements, but, overall, we already recognise a good accordance. In the actual experiment, approx. 100,000 photons per second are measured. Theory and experiment then match perfectly, constituting the correlation function of $|\Omega\rangle$. The correlation function describes the connection between Alice's and Bob's measurement results. Here, the difference between correlation and information can be seen: We visualise information as chess boards, correlation as the overlay of both chess boards. Correlation emerges without any time delay. However, In order to recognize this correlation, Alice and Bob need to exchange the digital information of their measurement data. This is only possible with a time delay, and not faster than with the speed of light.

1.11.11. *Shadow world and quantum dimension* [Link to U1-11-11](#)

The concept that digital data swims on a “sea of oscillations”, on the surface of the quantum dimension has far-reaching consequences. On the one hand, at least in principle, any information may be invisibly connected with any other information. Such correlations exist, even if we are not aware of them. In the microcosm, the world does not appear to be getting smaller, but larger and multi-dimensional, however, at the expense of loss of direct observation. On the other hand, the awareness of such correlations can enable new technological paths in quantum communication, e.g. in quantum cryptography, and more general, in quantum technology.

1.12. **Bell’s inequality (U1-12)**

Is it possible to model the correlation between Alice and Bob without quantum dimension? Can the “spooky action at a distance” be avoided using a theory of hidden variables? Can we avoid the concept of a quantum dimension?

1.12.1. *“Maybe he was murdered”* [Link to U1-12-1](#)

Omega murdered? There is no quantum oscillation at all in the quantum dimension? Doubt was cast upon the concept of Alice and Bob being connected non-locally through the quantum dimension by Albert Einstein in 1935. For that purpose, he conducted one of his well-known thought experiments, and published his doubts under the name of the EPR paradox. Einstein designated the mysterious connection between Alice and Bob “spooky action at a distance” and was convinced that quantum physics predicting this connection must be incomplete, and would be replaced by a hidden variables theory in future. At that time, Einstein’s considerations could not yet be verified experimentally. The modern measurement results with entangled photons show that the theoretical prediction of quantum mechanics are consistent with all experiments so far. Did Einstein then err at that time? Or is there in fact an alternative explanation, which gets by without the non-local interference of quantum physics?

1.12.2. *Experimental determination of the correlation function* [Link to U1-12-2](#)

Determining the correlation function experimentally, or “Quentin, the bantam of solace” We begin with the search for an alternative explanation by reconsidering the experimentally determined correlation function. Alice and Bob have each chosen an angle, and thus their measuring axis, using their respective polarisation rotators. The detectors register the signals of the transmitted and reflected photons. Alice and Bob each register random black-and-white patterns. Consider an individual measurement of Alice and Bob. How photons really look is not known by either Alice or Bob, or by anyone else. What we, or our technical aids, perceive is only indirect messages of the photons, which are transmitted to us by various “messengers”. The senders

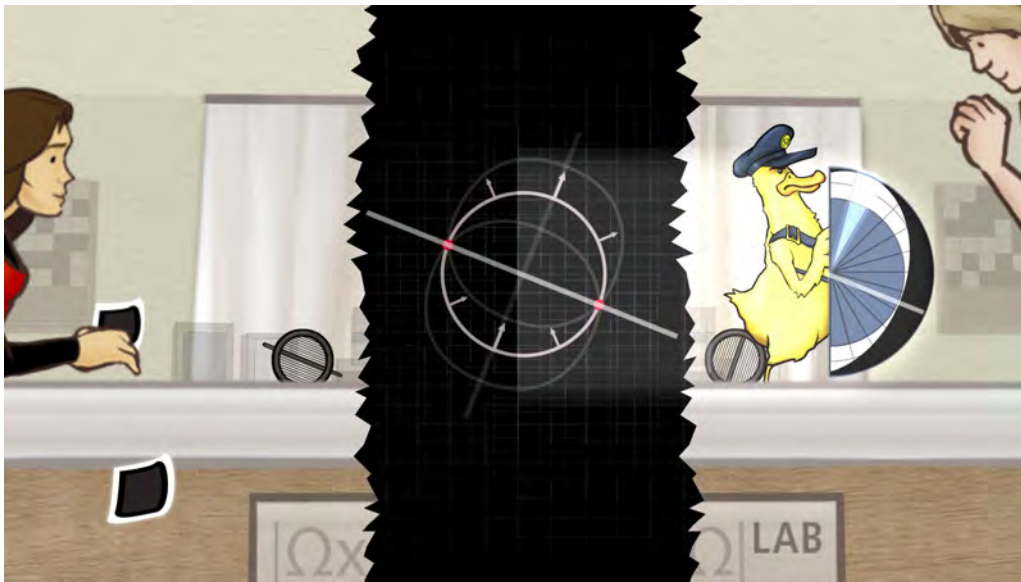


Figure 12. U1-12: Are Alice and Bobs really connected via the quantum channel?

remain hidden and invisible. As a messenger from the quantum dimension, we imagine “Quentin”, the bantam of solace. Any other messenger would have just as much or as little to do with the sender as Quentin. A postman also only brings the mail to where it is supposed to be left, is, however, not responsible for the content of the mail. Next, Alice carries out her measurement. She can only access a single angle pouch α of Quentin. When digging into the pouch, Quentin immediately disappears. Only a black or a white card remains in Alice’s hand, as a symbol of transmission or reflection. After the measurement, it is impossible to retrace which measurement result would have been realized, had Alice chosen a different angle pouch. Quentin the postman cannot draw any conclusions about it, because he irrevocably disappeared with the measurement. Next, Bob carries out his measurement. Also he can only access a single angle pouch β of Quentin. The quantum once again disappears once the measurement is taken. Only a black or a white card remains in Bob’s hand. Alice and Bob next conduct a lot of measurements. In this example, they always select angle pouches that are at an angle of 90° to one another. Alice and Bob can only compare their measurement results with one another in order to determine the correlation function C if they exchange the information on their measurement results. The two patterns are anti-correlated at this angle.

1.12.3. The “spooky” quantum dimension under close scrutiny [Link to U1-12-3](#)

Once again, we consider Einsteins “spooky action at a distance” which, in his opinion, actually may not exist. According to quantum physics, the probabilities in the angle pouches of Quentin are predetermined by the joint quantum oscillation Ω – 50 percent for black and 50 percent for white in each compartment. Alice carries out

her measurement, and, in the process, destroys one of the two photons of Omega. The remaining photon is then polarised either vertically or horizontally to Alice's measuring axis, depending upon Alice's measurement result. The choice of her measuring axis therefore has a direct impact upon the remaining photon, the signal of which is recorded by Bob. Now, with Bob, the nodal line of the polarisation of the remaining photon is located exactly on the measuring axis chosen by Alice. Bob carries out his measurement. In his angle compartment that is rotated through 90° towards Alice, he now, with 100 percent probability, finds the result "White" (\square).

1.12.4. *Hidden variables* [Link to U1-12-4](#)

Now, we assume that there is no "spooky action at a distance", and no quantum oscillation Omega. Metaphorically speaking, we kill with our classic the quantum oscillation Omega. We assume that the measurement taken by Alice cannot have any impact on the potential results seen by Bob. That means, that the probabilities of two independent events can be multiplied by one another, as they are independent from each other. With these assumptions, the correlation function emerges as a product of the differences of the individual probabilities for Alice and Bob. For just any angle, the difference arising from $P(\text{white})$ minus $P(\text{black})$ is a number between -1 and +1. How must the different polarisation directions of many different photons need to be distributed in order to match with the experimental correlation function? In case of success, we would have found an alternative explanation without any spooky long-range effect, and Omega would not exist. We are therefore looking for a suitable mixture of predetermined directions of polarisation. Every photon pair is labeled with a number and an associated polarisation direction, established prior to measurement. The two photons of a pair have the same direction of polarisation, which, as shown here, is symbolised by the oval in a numbered box. The hidden parameters, as Einstein called them, are, in our example, the label of the photon pair and its specific polarisation direction. Alice carries out the first measurement. According to the alternative theory, this does not influence Bob's measurement result. Bob carries out his measurement independent of Alice. After taking an average of many experiments, or an average of the hidden parameters, again we obtain a random black-and-white pattern. By determining the probabilities alone, we cannot yet rule out our alternative theory. We will only obtain certainty if correlations at various different angle combinations are investigated.

1.12.5. *Bell's inequality* [Link to U1-12-5](#)

We now need a general criterion in order to test any desired theory that assumes the independence of Alice and Bob's measurements. The general criterion we get from Bell's inequality, and similar inequalities based on the same key ideas. Alice and Bob each choose two different angles (α_1, α_2) , as well as (β_1, β_2) . On the board, we see two angle pouches, which show the angles chosen, α_1 or β_1 . Next, we will test the validity of the product ansatz for the correlation function. We assume that the product

ansatz is correct, and check whether there is a combination of correlation functions that contradicts this assumption. We begin with the statement that the mathematical expression shown is never greater than two. The difference illustrated here is likewise never greater than two. As an example, we select the extreme case. The sum is $2 + 0$ equals 2, and is thus likewise not greater than 2. This also applies in general. We use the values from the angle pouches in this inequality. Finally, we multiply out the brackets. After averaging over many measurements, the respective correlation functions in the four angle combinations arise. This inequality is a variant of the well-known Bell's inequality - the CHSH inequality. It was deduced based on the assumption that the measurements of Alice do not influence Bob's results, and vice versa.

1.12.6. Comparing theory and experiment [Link to U1-12-6](#)

We compare the inequality deduced from the assumption of independent measurements with the experiment results.

$$|C(\alpha_1, \beta_1) + C(\alpha_1, \beta_2) + C(\alpha_2, \beta_1) - C(\alpha_2, \beta_2)| \leq 2$$

By comparing their random chessboard patterns, Alice and Bob determine the experimental correlation function. We select four angle combinations. Based on the correlation function, $4 \times 0.71 = 2.84$ emerges. And that is no longer smaller than 2. Thus, the inequality is not fulfilled in this angle combination. The product approach in regard to the correlation function contradicts experimental findings. The assumption that the measurements do not mutually influence one another is wrong. Quantum physics can successfully describe this experimental result by non-local interference of amplitudes of product states, whereas the local hidden parameters theory cannot.

1.12.7. The truth is... interpretations of quantum physics [Link to U1-12-7](#)

Quantum physics describes the measurement results observed most successfully. This not only applies to the experiments introduced here, but goes far beyond that. Quantum mechanics does not, however, have any claim to finality, but actually derives its strength from its incompleteness. The quantum dimension will always be more complex than what we can ultimately imagine.

1.13. On the high pass of quantum mechanics (U1-13)

This station is at the border between well-known results of quantum physics and terra incognita. Before proceeding, we should test our understanding by looking back at the past 12 stations with test questions. Are you ready?

1.14. Quantum computation (U1-14)

Which dimensions open up if we generalize probabilities to amplitude? What happens in the first "chessboards" when entering the realm of non-local correlation? What discoveries can we expect in the future?

1.14.1. Checkerboard patterns [Link to U1-14-1](#)

A classic computer processes and stores digital data, based on electrical voltages and currents. Digital data can be symbolised by the numbers 0 and 1. As visualization, we have selected black and white fields on a chess board. In order to process digital data, arithmetical operations need to be carried out, such as the binary addition of numbers: $1 + 1 = 0$.

What distinguishes the classic computer from a quantum computer? What significance does Alice and Bob's experiment have in this respect? And why should secret services, state authorities and banks pursue the development of a quantum computer with a keen interest? These are the questions that we pose at the last station of Line 1 in "Omega City".

1.14.2. Classical computing [Link to U1-14-2](#)

Classic computers process information based on simple logic operations, i.e. by binary addition or multiplication. Let us look at a simple metaphor, a light switch. The switch can be "on" and "off", representing the digital data "1" and "0". The operations are accordingly called "Change switch" and "Do not change switch". That means that the equation $1 + 1 = 0$ can be interpreted either as an operation, that is, as an action at the switch, and as resulting data, that is, switch positions. Let us take a look at the truth tables for binary addition and multiplication. The neutral element of the addition is zero (0), that of the multiplication is plus one (+1). In both cases, we interpret the neutral element as "Do not change switch". The number one (1), in case of addition, or minus one (-1), in case of the multiplication, are interpreted as "Change switch". Carrying out two operations consecutively ($x + y$ or $x \times y$) leads to the truth tables shown here. In particular, the operation "Change switch twice", is identical to "Do not change switch". The calculations of a classic computer are based on these simple rules. Thus, the operation "Change switch" on a single bit is termed a "NOT gate" in information technology. The truth table of the binary addition shown here corresponds to the CONTROLLED NOT gate.

1.14.3. Space of probabilities [Link to U1-14-3](#)

The number of atoms which are involved in storing a "Black" or "White" bit state was 10^{17} , in the year 1960, and has been exponentially reduced in the course of computer development. At present, we are at a point where only a few atoms are needed

for this sort of data processing. However, with further miniaturization, we face quantum effects. Consequently, we can only operate with probabilities and interference, which means that we enter the quantum dimension. Here, we discuss general conclusions resulting from the basic principles of quantum mechanics, viz. “probability” and “interference”, which applies to any quantum computer, independent of its explicit physical realization. Each field on this chess board corresponds to one bit, that can assume either the value 1 or 0, or the colour “Black” or “White”. In contrast to the quasi-deterministic computer, where the value is either black or white, in case of a quantum computer, we operate with probabilities $P(\text{Black})$ and $P(\text{White})$ for black or white. For one bit, due to conservation of probability, $P_{\blacksquare} + P_{\square} = 1$, only one of the two probabilities can be freely selected. That means that one parameter is free. For the special case of $P_{\blacksquare} = 0$ and $P_{\square} = 1$ or $P_{\blacksquare} = 1$ and $P_{\square} = 0$, we obtain a deterministic computer. Thus, the classic computer can be considered a special case of the quantum computer. For 2 bits, four combinations $((\square, \square), (\blacksquare, \square), (\square, \blacksquare), (\blacksquare, \blacksquare))$ arise, with four probabilities $(P_{\square, \square}, P_{\blacksquare, \square}, P_{\square, \blacksquare}, P_{\blacksquare, \blacksquare})$. Due to conservation of probability, three free parameters suffice to describe these probabilities. For 3 bits, we obtain eight combinations. Due to conservation of probability, seven free parameters suffice to describe the probabilities. The number of possible combinations doubles with each field, and is generally 2^N . The number of free parameters for the probabilities is $2^N - 1$ for N bits or N chessboard fields.

1.14.4. Quantum dimension of a single qubit [Link to U1-14-4](#)

In station (U1-06) “Heart of quantum mechanics”, we revealed the link between probabilities P_{\blacksquare} and P_{\square} and amplitudes in the quantum dimension capable of interference. Thus, the two probabilities are extended each to become a rotating wheel with two parameters: a radius and a phase. This generalisation defines the transition from a classic bit to a quantum bit or qubit. As a specific example, consider a photon passing a polarising beam splitter Whether the detector “Black” or the detector “White” records the photon is decided by chance. The rotation frequencies of the turning wheel is proportional to the energy E of the photon. Overall, four real parameters emerge. The “Black” and “White” phases are independent of one another. From conservation of probabilities $P_{\blacksquare} + P_{\square} = 1$, it follows that the number of free parameters or degrees of freedom of a qubit in the quantum dimension is reduced to $4 - 1 = 3$. As only phase differences are observable, all observable states can be represented on a two dimensional sphere – the so-called Bloch sphere.

1.14.5. Two qubits [Link to U1-14-5](#)

Let us consider the combinations of two photons and the potential measurement results $((\square, \square), (\blacksquare, \square), (\square, \blacksquare), (\blacksquare, \blacksquare))$. If the photons are not entangled, the measurement results are independent of one another. Let us begin our considerations with this case. Probabilities from two independent events can be multiplied. In the

quantum dimension, we obtain a three-dimensional parameter space for each photon (or qubit) in this case. As a result, obtain a six-dimensional parameter space of all product states of two independent photons in the quantum dimension. Were the photon pairs thus always to be independent of one another, the quantum dimension would have six dimensions. However, photons can be entangled with one another. What can be concluded from the latter in regard to the actual number of dimensions? To infer the quantum dimension behind the measurement results, the four combined probabilities ($P_{\square,\square}, P_{\blacksquare,\square}, P_{\square,\blacksquare}, P_{\blacksquare,\blacksquare}$) need to be generalised to become complex amplitudes. Thus, each probability is generalized to a turning wheel. Each turing wheel has a phase and a radius. Overall, the number of parameters is thus doubled, from four to eight. Due to conservation of probability, the number of free parameters for two qubits in the quantum dimension equals $8-1=7$. The quantum dimension of two independent photons does, however, only have six dimensions. How can the difference be interpreted? The fact of a seventh dimension in the quantum dimension shows that two photons cannot always be considered independent of one another. Photons that have a polarisation oscillation that can be found in this seventh dimension are entangled. The seventh dimension is defined by the parameter c , concurrence. It specifies the degree of entanglement: For $c = 0$, the photons are independent of one another, for $c = 1$ they are maximally entangled. The polarisations of the two photons that are not to be found on the intersection lines of the two cones are not entangled. The photon on the upper cone has a clearly defined polarisation; likewise the photon on the lower cone, $c=0$ applies. The measurement of the polarisation of one photon does not influence the polarisation of the second photon. The detection probabilities of the two individual photons can be multiplied by one another, that is, are described by a product state. These two independent amplitudes are visualized in the $c = 0$ plane. On the intersection lines of the two cones, the photons are maximally entangled, $c = 1$. Only through the measurement of the polarisation of one photon is the polarisation of the second photon determined. The detection probabilities of the individual photons cannot be described as a product state. This entangled state is visualized in the $c = 1$ plane.

1.14.6. The four Bell states in the “Seventh Dimension” [Link to U1-14-6](#)

Die maximal verschränkten Zustände sind die vier Bell-Zustände. Mit dem BBO-Kristall lassen sich alle vier Bell-Zustände erzeugen. Dazu müssen zusätzliche, passende Polarisationsdreher im Strahlengang installiert werden. Die rotationssymmetrische Schwingung Omega, $|\Omega\rangle$ wird in der Fachliteratur als Bell-Zustand als $|\Phi^+\rangle$ bezeichnet. Der Bell-Zustand $|\Phi^-\rangle$ ergibt sich aus der Überlagerung von Photonen, die in plus 45° bzw. minus 45° -Richtung linear polarisiert sind. Der Bell-Zustand $|\Psi^+\rangle$ ergibt sich aus der Überlagerung von Photonen, die in vertikaler und horizontaler Richtung polarisiert sind. Der Bell-Zustand $|\Psi^-\rangle$ ist etwas Besonderes: Er ist antisymmetrisch unter Vertauschung der Polarisation von Photon 1 und Photon 2.

The basis for all maximally entangled states is given by the four Bell states. All four

Bell states can be created experimentally using the BBO crystal. Additional polarisation rotators need to be installed in the beam path for that purpose. The rotationally symmetrical entangled state Omega, $|\Omega\rangle$ is usually termed as Bell state $|\Phi^+\rangle$. Here we shown the Bell-state $|\Phi^-\rangle$ describing the superposition of plus 45° and minus 45° polarized photons. Here we shown the Bell- state $|\Psi^+\rangle$ describing the superposition of horizontal and vertical polarized photons. The Bell state $|\Psi^-\rangle$ is something special: it is anti-symmetrical when photon 1 and photon 2 are interchanged.

1.14.7. Local and non-local dimensions [Link to U1-14-7](#)

One qubit: Of these four parameters, only 3 can be freely chosen, as the sum of both probabilities is normalized to 1. These 3 parameters are locally assigned to one chessboard field. Two qubits: In the case of two chessboard fields, there are four possible combinations. The corresponding 4 probabilities are generalised, in the quantum dimension, to amplitudes with a total of 8 real parameters. As the sum of the probabilities is 1, in general, a 7-dimensional space arises in the quantum dimension. Three dimensions are assigned locally to the first or second chessboard field, respectively. The four Bell states can be found in the non-local seventh dimension c , irrespective of whether we are looking at the polarisation of a photon pair, the spin of an electron pair or any other quantum states. Three qubits: We dive deeper into the quantum dimension and consider at three chessboard fields. In this case, 3 detectors, A, B and C, would record eight possible measurement results. How many non-local dimensions can be found in the quantum dimension behind 3 chessboard fields? And how large is the quantum dimension associated to a quantum computer with 64 qubits?

1.14.8. The metaphor of the “non-local grains of rice” [Link to U1-14-8](#)

We epitomise the dimensions of a qubit using grains of rice. Thus, each grain of rice corresponds to a free parameter, that is, a single dimension within the quantum dimension. The first qubit has four dimensions. Based on the condition $P_{\blacksquare} + P_{\square} = 1$, there are three freely selectable parameters. These three dimensions, two phases and one probability, are locally assigned to the one qubit. Next, we assign a number to each chessboard field. We designate the first field qubit 13,0. Only two of these three dimensions can be observed in the experiment, as only phase differences lead to observable effect. The so-called “Bloch sphere” is often used to describe observable states of a single qubit. The combination of two Q-bits has eight dimensions; only seven of them are independent of one another. Three dimensions are assigned locally per qubit. One red grain of rice, that corresponds to a non-local dimension, is left over. The state Omega $-\Omega_i$ represents this dimension. All other quantum states in this seventh dimension can be derived from Omega by local, complex rotations. We can think of this as a family tree, with relatives connected with one another via certain routes. In particular, all other Bell states can be generated from Omega in this way.

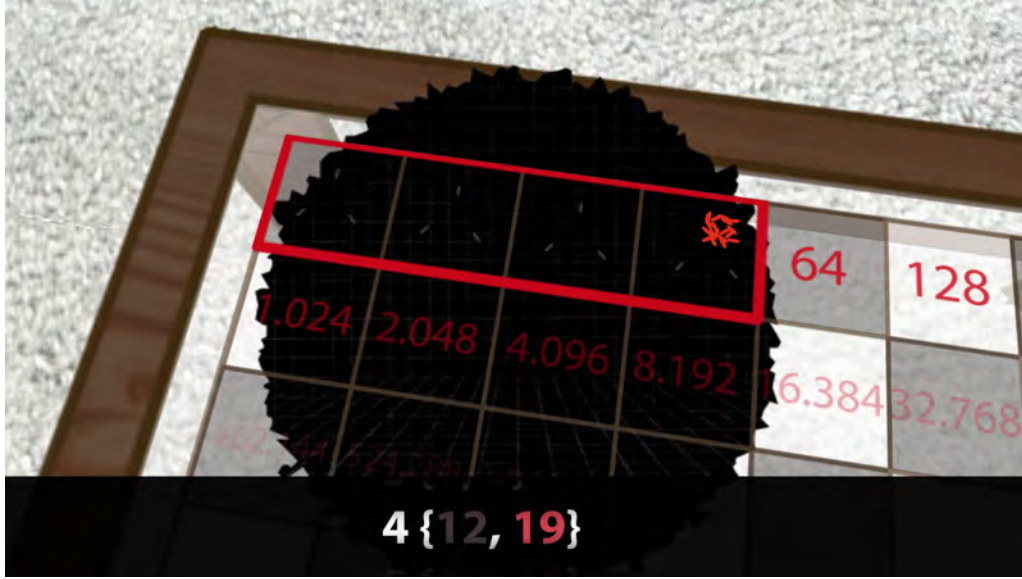


Figure 13. U1-14: The number of nonlocal dimensions (red cones of rice) is growing exponentially, while the number of local dimensions only grows linearly, when the number of qubits is increased.

$$|\Phi^+\rangle = \frac{1}{\sqrt{2}}(|00\rangle + |11\rangle) \equiv |\Omega\rangle$$

$$|\Phi^-\rangle = \frac{1}{\sqrt{2}}(|00\rangle - |11\rangle)$$

$$|\Psi^+\rangle = \frac{1}{\sqrt{2}}(|01\rangle + |10\rangle)$$

$$|\Psi^-\rangle = \frac{1}{\sqrt{2}}(|01\rangle - |10\rangle)$$

It is therefore sufficient to associate Omega to this non-local dimension, as a representative of the family, so to speak. Alice and Bob are always assigned locally to one chessboard field. The quantum state Omega is assigned non-locally to both chessboard fields. We describe the two first fields, as a unit, with the number qubit 26, 1, where the first number in curly brackets describes the number of local dimensions, and the last number the number of non-local dimensions. Now we proceed a step further, and look at the combination of three qubits with 16 dimensions, of which 15 are independent. Three dimensions are assigned locally per qubit. Six red grains of rice are left over, as representatives of the non-local dimensions. Which quantum states arise in these six non-local dimensions? There are 3 possibilities for selecting 2 fields out of these 3 chessboard fields. For each of these 3 combinations, there is one respective Omega-like quantum state, which connects these two fields. These are the first three red, non-local dimensions. Three non-local dimensions are left over. Oscillations which

connect not only two, but all three, fields non-locally can be found in these dimensions. It has been shown that there are exactly two types of entangled states that can connect all three fields with one another. The first type is represented by the so-called GHZ state. “GHZ” is short for the three physicists Greenberger, Horn and Zeilinger.

$$|GHZ\rangle = \frac{1}{\sqrt{2}}(|000\rangle + |111\rangle)$$

The GHZ state was realized experimentally for the first time in 1998. The second type is represented by the W state. “W” stands for the physicist Wolfgang Dür.

$$|W\rangle = \frac{1}{\sqrt{3}}(|001\rangle + |010\rangle + |100\rangle)$$

These two states describe the entanglement of three particles. To observe them, therefore, not only the detectors Alice and Bob would be necessary, but also a third detector at a further location. The sixth non-local dimension, being an irrelevant phase, does not lead to any observable effect. Thus, we have completely described the entanglement of a system consisting of 3 qubits. As a next step, we will look at 4 qubits. Here, something exciting happens: For the first time, the number of non-local dimensions prevails. Out of the $32-1 = 31$ dimensions, $4 \times 3 = 12$ are local, and $31-12 = 19$ non-local. We designate the combinations of four chessboard fields with the qubit number 412,19. The deeper we explore the quantum dimension, the more dimensions are non-local. Whereas the number of local dimensions only increased by three per qubit, the number of non-local dimensions increase exponentially. The invisible dimensions are doubled with each further field, and point the way to a gigantic quantum world, many aspects of which are still unknown. Expressed in our metaphor of the red grains of rice which increase exponentially, the “volume” that the grains of rice absorb is doubled with each field. The comparison with the volume of billions and trillions of grains of rice can only show what exponential growth means. Each red grain of rice is, in itself, a small universe, a dimension that is interwoven with these billions of other dimensions in a complex and fascinating way.

In the non-local quantum dimensions, we distinguish between two types: Type A consists of states that would be experimentally accessible, and Type B states which are inaccessible according to current knowledge. Most states belong to Type B, and could only be generated by an exponentially large number of two-qubit operations when starting from a product of local states. The larger part of the quantum dimension appears, for this reason, to be inaccessible for local observations from the present-day perspective. But also Type A, where only a finite but large number of two-qubit operations would be necessary, is unbelievably large, and large parts of it have not yet been investigated.

On the one hand, we have vast mathematical and experimental evidence for the non-local, unobservable quantum dimension. On one hand, further properties of the quantum dimension are understood and penetrated, through theory and experimentation, due to global research activities. On the other hand, many aspects of the properties of the quantum dimension contradict our local, classic world view. In spite of all our understanding, an insurmountable barrier between the dimensions of non-local, non-directly observable quantum states and our local, observable space will persist.

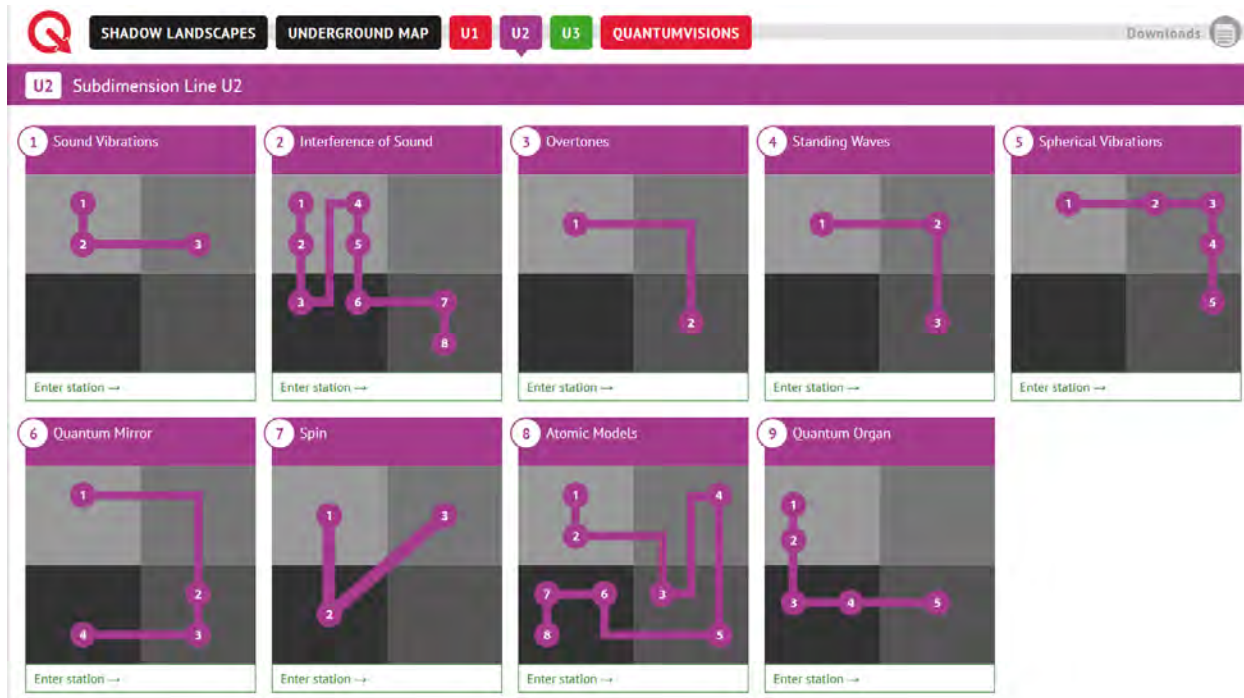


Figure 14. The stations of U2: [Quantum Reflections](#) and their relation to the four quadrants: experiment (many qubits/single qubits) - theory (amplitudes/probabilities).

2. U2: Quantum Reflections

What is the relation between the overtones in music and the table of elements? In U2: Quantum Reflections we start with classical waves, and discuss nodes in standing waves. The positions of nothingness - the nodes will show up again in the quantum dimension, while the nature of the standing wave has changed substantially, as we are dealing with quantum wave functions. Starting with the simple spectrum of standing waves in one dimension, just by rotations, reflections and Hopf mapping, we end up at the complete table of elements.

2.1. Visualizations of sound waves (U2-1)

In this station we show how to make a snapshot of a sound wave.

2.1.1. Spinning wheels [Link to U2-1-01](#)

Is the three-dimensional world a shadow world? Could it be a surface phenomenon of a much higher-dimensional space? Maybe the shadow world and the quantum dimension are mutually dependant, and only exist in a symbiosis? Enter my dimension. The last station of the U1 Quantum Dimensions subway line serves simultaneously as an



Figure 15. The search of Alice and Bob for $|\Omega\rangle$ is ongoing in the subway line U2: *QuantumReflections* of Omega-City.

introduction to the U2 Quantum Reflections line. In the following nine stations on the U2 line, we will search again for images, modellings, and visualizations of the shadow world and the quantum dimension.

Omega's house features the shadow of a spinning wheel, which will also be a leitmotif on our journey through quantum reflections. The spinning wheel changes its character on the journey between the U2 stations. It is first used to describe classical vibrations in one, two, and more dimensions. It then changes to represent quantum states, and the structure of the periodic table. However, in the first two stations, the spinning wheel serves initially as a symbol of phase, frequency, and amplitude of sound waves.

2.1.2. Sound wave and sound intensity [Link to U2-1-02](#)

Sound waves are invisible; we can only hear them. But is there a way to visualize them somehow? Sure, here they are! All right; it's not quite so simple. In order to make sound visible, we need a speaker, a frequency generator, and an amplifier. We then record the sound from the speaker using a microphone, and send the signal to a lamp via the amplifier. The lamp's brightness is a measure of the sound volume. The greater the distance between the microphone and the sound source is, the lower the sound, and the dimmer the lamp.

We can symbolically represent a sine wave having a certain frequency using a spinning wheel whose rotation frequency corresponds to sound frequency, and radius to sound amplitude. The microphone picks up the sound, and transmits it via the amplifier to the lamp in the form of an electrical signal. Since the volume decreases

with the distance, the radius of the wheel becomes increasingly smaller. But where exactly is the wave? To make the wave visible, we need the so-called phase difference, that is, the displacement of the pointer, which occurs due to the distance between the speaker and the microphone.

2.1.3. Phase of a sound wave [Link to U2-1-03](#)

The further away the sound wave is from the speaker, the longer it has travelled. The phase has therefore shifted more, relative to the initial phase of the sound wave, when it was close to the speaker.

The following trick will help us to “freeze” this phase displacement, so to speak. We can copy the speaker’s output signal and paste it at the position of the lamp and the microphone. We can then add the outcome to the signal that is received by the microphone. The angle between the spinning wheels, that is, the phase difference, is now fixed. It stays as if it were frozen, even when the wave propagates. With increasing distance, the lamp is now periodically emitting bright and dim light, depending on the phase difference between the two spinning wheels. At the minimum, that is, with a phase displacement of one-half wavelength, the two spinning wheels are directly opposed to each other. At the maximum, that is, with a phase displaced by one full wavelength, they point in the same direction. The phase difference grows steadily, with the result that bright and dim light alternates at intervals of one-half wavelength of the sound wave.

If we wave the bar up and down, we can scan the sound wave in the room, so to speak, and after long time exposure we get a pattern of the minima and maxima of the sound wave!

2.2. Sound interference (U2-2)

The station U2-2 coincides with U1-01, as both subway lines cross each other - or shall we say: are in superposition?

2.3. Overtones (U2-3)

In this station, we use the Fourier transformation for an frequency analysis of sound waves.

2.3.1. From wave to source [Link to U2-3-01](#)

We can hear the sound wave, but the instrument used is hidden in the dark. Is there a clear connection between the sound wave and its source, which would allow us to infer detailed characteristics of the musical instrument from the acoustic signal? We shall investigate this topic in the present station, and in the following one. Recording the sound wave using a computer will allow us to study the time course of the amplitude

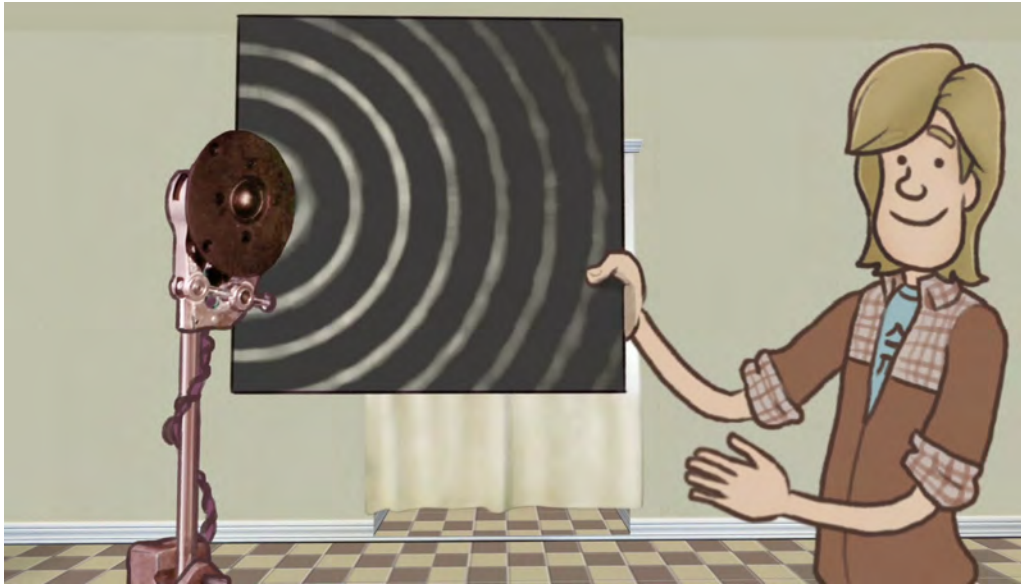


Figure 16. U2-1: Is it possible to take a "snapshot" of sound waves?

in more detail. If we refine the time resolution further and further, we will see the individual fluctuations in pressure and density of the sound wave. Compared to a sine wave with a fixed frequency, which is shown here in the form of a spinning wheel, the time course of this amplitude is much more complex. Is it possible to present this sound wave as a superposition of many different frequencies and amplitudes, that is, of many spinning wheels having matching rotation frequencies and radii?

2.3.2. *Fourier transformation* [Link to U2-3-02](#)

Let us consider a superposition of spinning wheels, which are arranged in a very specific way. We have a fundamental frequency f , along with double, triple, quadruple, quintuple, and sextuple of that frequency. The amplitudes of the spinning wheels decrease to one-half, one-third, one-fourth, one-fifth, and one-sixth of the amplitude of the fundamental frequency f . What is the time course of this superposition? The spinning wheels, with their respective frequencies and amplitudes, form a kind of a sawtooth wave. This is the time course of the sawtooth wave. It is possible to present the same information in a different way. Let us consider the specific spinning wheels with their rotation frequencies. Let's start with the fundamental tone having the frequency f and the amplitude r , that is, with the radius of this wheel. Let us now add the amplitudes of the multiples of the fundamental frequency. We get the so-called spectrum of the wave, which covers all frequencies with their respective amplitudes that are present in the wave. The spectrum helps us to reconstruct the time course of the wave.

The mathematical operation that associates the frequencies and their respective amplitudes with the time course is the so-called Fourier transform, named after French mathematician Fourier. Nowadays, it is very easy to investigate frequencies of sound

waves using a computer. We can thus describe the wave either over time, or in the so-called frequency domain. The Fourier analysis is one of the key methods of analysis used in the natural sciences. Let us return to the issue of unambiguity. Is it possible to infer the sound source from the sound wave? Is the frequency spectrum a unique fingerprint for the musical instrument used? We shall answer this question in the next station.

2.4. Good vibrations (U2-4)

In this station, we discuss the relation between the overtone spectrum and the number of nodes in standing waves.

2.4.1. Vibrating guitar string [Link to U2-4-01](#)

The key elements of this station are classical musical instruments, such as a guitar. Let us analyze the spectrum of a single vibrating string. But this is not an ordinary guitar. The reflections suggest a reinterpretation of the fundamental vibration pattern of the guitar string. The key lies in nodes, nodal lines, and nodal surfaces of standing waves, as well as in interplay between dimensions and symmetries. Those elements will reappear in all subsequent stations, like a theme and variations.

2.4.2. Spectrum of the guitar string [Link to U2-4-02](#)

Let us answer the question whether the spectrum is a unique fingerprint of the musical instrument used. It is best explained using a single vibrating string, the so-called monochord. Plucking causes the string to vibrate. We cannot, however, hear the oscillation directly. The vibrating string must be surrounded by air, so that the air molecules can carry the vibration to our ears, at the speed of sound, in the form of fluctuations in pressure and density. We can record the time course of the sound wave using a computer. The Fourier transform reveals the mixture of frequencies that form the sound of the string.

It is evident that there is a lowest frequency f_0 - the so-called fundamental tone. Moreover, there is an equidistant spectrum. That means, all other amplitudes have a frequency that is two times, three times, four times, or, in general, n -times the frequency of the fundamental tone. All these overtones - along with the fundamental tone - form the spectrum of the oscillating string. Is it possible to infer the characteristics of the oscillating string, such as its length, based on this spectrum? Can we use the wave to draw unequivocal conclusions about the source?

2.4.3. Standing waves [Link to U2-4-03](#)

What is the relationship between the frequency spectrum of the sound wave and the vibration on the string? Let us first consider only the fundamental tone f_0 . Plucking

causes the string to vibrate. This vibration travels through the air at the speed of sound. Let us consider two points: point A in the air, and point B on the string. In the air, there is a sound wave that is propagating. The fundamental tone has the frequency f_0 , which corresponds to a wheel with a rotation frequency f_0 . Its spatial and temporal course is visualised here.

The situation at point B on the string is different, because the vibration is reflected back and forth at the two end points of the string. There are thus two waves which travel in opposite directions and overlap, forming a standing wave. The frequency of this standing wave is also f_0 . There are two nodes at the edges, where the string does not move. An antinode forms in the middle. This standing wave on the string, with the length l , is equivalent to one-half a wavelength on the string. This is the vibration behind the fundamental tone with the frequency f_0 . When the frequency doubles, the wavelength is halved. This happens because the product of frequency and wavelength is always equal to the wave propagation rate on the string. That means there are now two antinodes on the vibrating string. There is also one additional node, which is located precisely in the middle of the string. The wavelength is reduced again when the frequency is tripled. There is exactly one additional antinode on the vibrating string, and, correspondingly, there is also another node.

Let's sum it up. Standing waves are formed when multiples of one-half wavelength fit within the length of the vibrating string. In the simplest scenario, there are only two nodes at the edges, and one antinode, which is also the fundamental tone. The first overtone has one node more than the fundamental tone; the second has two nodes more, and so on. Doubling the frequency halves the wavelength relative to the fundamental tone. Tripling the frequency reduces the wavelength to one third. It goes on like this for all the multiples of the frequency of the fundamental tone. Let us now return to the question of unambiguity. Is this spectrum a unique fingerprint for the vibrating string with the length l ? Well, it might seem to be the case at first, since there is an apparent correlation between the frequency and the string length l , such that $l = n\lambda/2$. Let us consider two different vibrating strings having different lengths and different wave propagation rates, c_1 and c_2 . At first, the longer string sounds lower. That means, we have an equidistant spectrum again, but the fundamental tone f_0 has moved down a little. All multiples of f_0 , or overtones, have moved down with it.

However, if we increase the string tension of the longer string, thus adjusting the wave propagation rate c_2 such that the ratio of wave propagation rate and length is equal for both vibrating strings, the result will be an identical spectrum. That is, the fundamental tone is equal, as are the overtones, even though the strings have various lengths. Of course! You can, for example, tune a guitar so that two different strings will have the same fundamental tone. If just one vibrating string does not allow us to draw clear conclusions on the instrument used, it will certainly not be the case with more complex instruments. I am sorry, Bob!

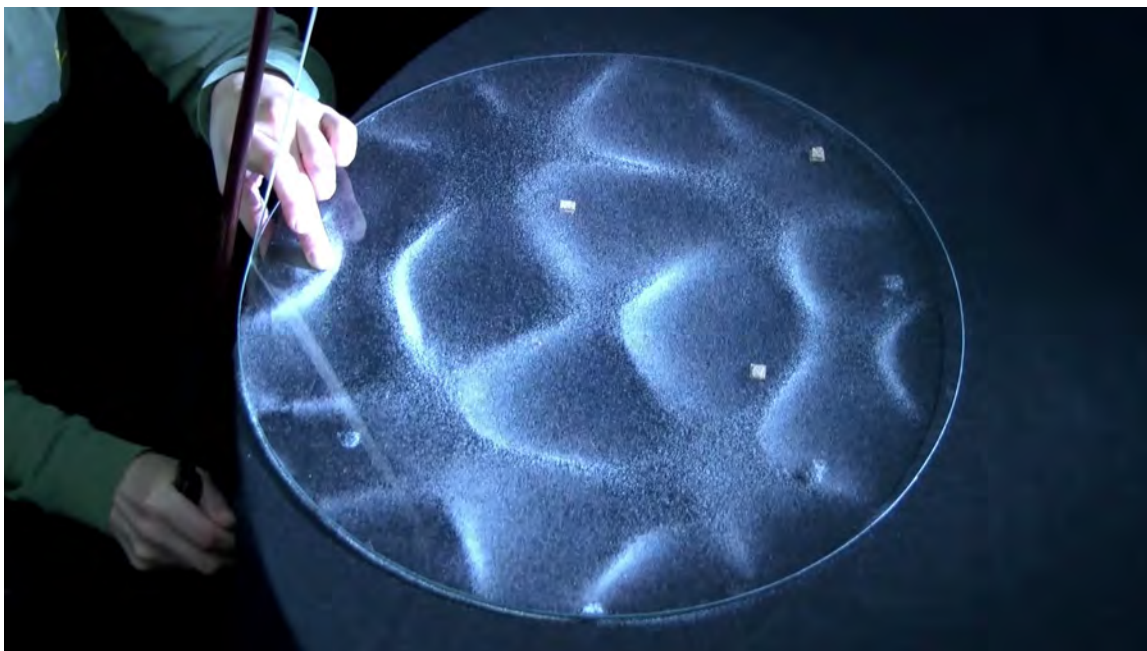


Figure 17. U2-5: Using Chladni sound figures on a glass plate, nodal lines can be directly visualized.

2.5. Spherical Vibrations (U2-5)

In this station, we discuss standing waves in one and in two dimension, leading to the generalization of nodal points to nodal lines.

2.5.1. Water waves [Link to U2-5-01](#)

The search for Omega, or the quantum vibration, in the classical media is a complete failure. However, in this station, Alice and Bob leave the one-dimensional world of vibrating strings, and start considering two-dimensional vibrations. They are looking for Omega, but only find the caretaker. The vibrating glass plates, cups, and soap bubbles presented in this station are a fascinating and aesthetic visualization of two-dimensional vibrational patterns. At the same time, they will offer important clues on our subsequent search for Omega in the quantum reflections.

2.5.2. Chladni sound figures [Link to U2-5-02](#)

The vibrating string of the monochord is an example of a one-dimensional standing wave. The potential basic modes on the string can be classified according to the number of nodes. As early as in the 19th century, Chladni investigated potential vibrational modes in two dimensions. Two-dimensional nodes form nodal lines. Chladni had a simple and ingenious idea of how to make those lines visible. For example, we can use a violin bow to make a round glass plate vibrate. Let's sprinkle the plate with fine powder.

If we hold the plate at the appropriate point, we will obtain a so-called Chladni figure. How can this be explained?

The stationary granules reveal the places where the plate does not move, that is, where nodal lines are formed. If we cut the glass plate in the middle, we will see a one-dimensional standing wave with two nodes. Antinodes are at the edges, and in the middle of the glass plate. The granules do not accumulate there. They only stay where the nodes are. As a result of rotation, the nodes form a nodal line. This vibrational mode of the glass plate creates a so-called radial nodal line with a radius r_1 . If we hold the plate at the appropriate point at the edge, we get a pattern. Which vibration mode does this figure correspond to? Now, let us consider the vibration on the outer semicircle, with the corresponding nodes and anti-nodes. A standing wave with four antinodes is created at the edge of the glass plate. This pattern continues throughout the entire glass plate, that is, for all radii. The nodal lines are therefore located at fixed angles; that's why they are called azimuthal nodal lines. In this case, the angle Φ between the two azimuthal nodal lines is equal to 90° . Nodal lines with a fixed angle are called azimuthal lines. Nodal lines with a fixed radius are radial lines. Of course, there are also vibration modes that combine both types. To demonstrate this, we shall use a glass plate with a slightly greater radius. With fingers positioned appropriately, we obtain a vibration mode with both a radial and an azimuthal nodal line.

The larger the glass plate, the more place for nodal lines, and the more complex the vibrational patterns. If we draw the nodal lines, we obtain this figure. This is just one example of hundreds of complex vibration modes that can be produced on a glass plate. Chladni analysed many of them. All these intricate patterns can be attributed to superposition of simple basic modes, in line with the Fourier transform. These basic modes can be described using the number l of azimuthal nodal lines, and the number r of radial nodal lines. That is: $l = 0, 1, 2, 3$, and $r = 0, 1, 2, 3$, etc., and combinations of r and l . On the other hand, it is possible to describe any potential vibration on the glass plate by superimposing these basic modes. For example, here we can see the combination of the basic mode $r = 2, l = 2$ and the basic mode $r = 3$. In this way, the Chladni figures come back as a superposition of basic modes.

2.5.3. *Vibrating cup* [Link to U2-5-03](#)

We can use a simple coffee cup to generate interesting variants of Chladni figures. All we need is a spoon. If the cup is struck opposite the handle, it sounds like that... Now, strike slightly offset to one side, and it sounds like that... Here, the cup sounds deeper, and there, higher. Why is that? Apparently, the angle between the handle and the place where the spoon strikes is essential.

We can illustrate the phenomenon using a figure of standing waves. A standing wave forms on the cup rim. In the simplest scenario, the rim fits four antinodes, or two wavelengths. When an antinode forms at the handle, more mass is vibrating. The frequency decreases, and the sound becomes lower. When a node forms at the handle,

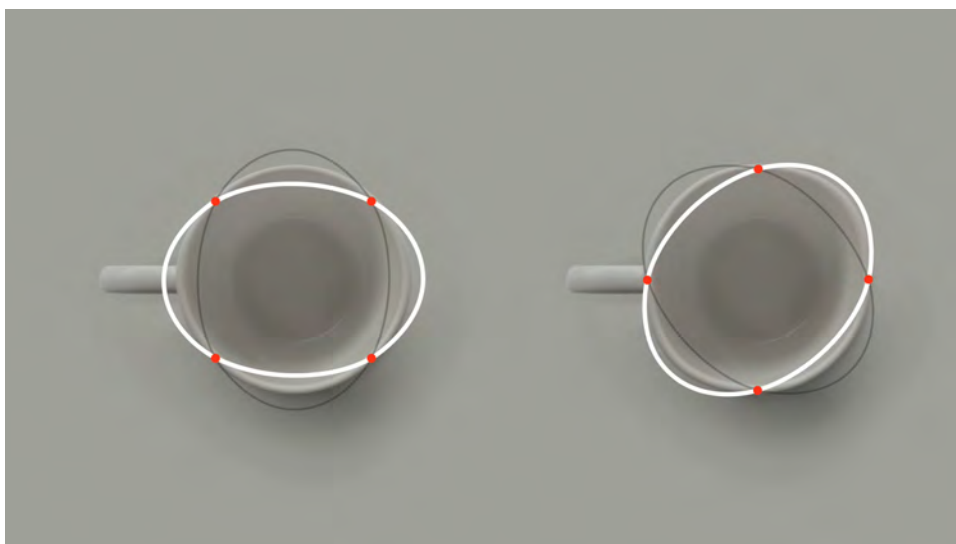


Figure 18. Standing waves on the cup rim. Why does the frequency of the sound depends on the position where the spoon hits the cup?

less mass is vibrating. The frequency increases, and the sound becomes higher. How can we prove this theory? To do that, we need to adequately visualize these standing waves. Let us fill the cups with coffee. Let us strike the cup directly across from the position of the handle. A standing wave having four antinodes forms and spreads across the surface of the coffee. We can see that a lot of coffee is stirred at the four antinodes, and a wave is running into the centre of the cup. Indeed, the antinode is located at the handle.

Let us now strike the cup 45° from that position. What will happen on the surface of the coffee? Again, a standing wave with four antinodes forms. However, we can clearly see that the node is located at the handle. We have thus found an explanation for the mystery of the two tones emitted by the vibrating cup. Either the handle vibrates with the cup, or it stands still. Let us now consider the entire spectrum of the vibrating cup. We have already observed that standing waves with four antinodes can be formed in two ways. Exactly two wavelengths, that is, 2λ , fit on the cup rim. In the vibration $2\lambda^+$, the handle vibrates with the rim; in $2\lambda^-$, it does not. Are there more frequencies in the spectrum? If so, what do they mean? One obvious possibility would be that the rim can fit not just the double wavelength, but the triple wavelength as well. It would look like this. Again, either the node, or the antinode is positioned at the handle. To create these standing waves, we need to strike the cup at the appropriate place.

With a little practice, it is indeed possible to generate standing waves having six antinodes. Let's start with striking the cup 60° from the handle. Indeed, we can see six antinodes forming at the cup rim. The antinode is located at the handle. Let us strike the cup 30° from the handle. Again, the cup rim vibrates with six antinodes, but this time the handle is positioned precisely between two antinodes. It thus lies directly at the node. The hexagon has shifted by 30° , and the frequency is slightly increased.

We have thus explained the spectrum of the cup. We can create double peaks with two times, three times, and, with some effort, even four times the wavelength. Try it out, Bob!

2.5.4. *Vibrating soap bubble* [Link to U2-5-04](#)

The number of nodes is a key feature for the classification of spectra in one dimension. We have seen that in the case of the vibrating string and the cup rim. Let us now apply this concept to two-dimensional vibrations in order to investigate vibrations on a spherical surface. It is easy to create vibrating spheres. For example, in the form of soap bubbles. In order to make the vibration visible, let us consider a hemisphere. We can excite this hemisphere using a vibration generator. The vibration looks usually quite wobbly and irregular.

If we change the frequency with which we provoke the vibration, the Fourier transform will show specific points where the so-called resonant frequencies are formed. What does that mean? Let's look at a specific resonant frequency. If the bubble is excited with this frequency, the result is a very regular, periodic vibration. We can superimpose this vibration upon itself. If we do this with a time delay of half a period, we will obtain the following picture. The nodes remain constant, and each antinode is maximally deflected. By rotating the nodes around the vertical axis, we can form nodal lines on the two-dimensional soap surface. We obtain five nodal lines in total. The following applies: $l = 5$.

How does the subsequent resonant frequency look like? If we adjust the frequency appropriately, we'll obtain this regular vibration. Again, we can superimpose the vibration upon itself, with a time delay of half a period. We can thus see the positions of the nodes and the antinodes again. By rotating the nodes, we can form nodal lines on the spherical surface. There are seven nodal lines in total. It is possible to describe the entire spectrum of resonant frequencies using the number of nodal lines. For reasons of symmetry, there can only be an odd number of nodal lines, since the vibration must always be its own mirror image by design.

2.5.5. *Spherical Harmonics* [Link to U2-5-05](#)

The spectrum of the vibrating string consists of multiples of the fundamental frequency f_0 . These specific modes of vibration can be classified according to the number of nodes. There are generally two different types of framework conditions. There can be either nodes or antinodes at the edge. Physically, this corresponds to either a closed end, or an open end. Let us consider the simplest mode of vibration having two open ends. It has one node in the middle, and one antinode per each of the two edges. Let us now bend this vibration to form a semicircle. Rotating this semicircle around the z-axis will result in a sphere. There is an azimuthal nodal line at the equator of the vibrating sphere. We can perform the same steps for the following resonant frequency, which has two nodes. Let us bend the vibration to a semicircle, and, again, let the semicircle

rotate around the z-axis. This results in a vibrating sphere having two azimuthal nodal lines. We can repeat this on and on. Bending and rotating the vibration with l nodes results in a vibrating sphere with l nodal lines. By definition, these sphere vibrations are rotationally symmetric. They are also their own reflection. Positioning the mirror plane exactly in the middle will result in an identical mirror image. l specifies the total number of azimuthal nodal lines. There is no nodal line for $l = 0$. There is one nodal line for $l=1$; however, this exceptionally symmetrical vibration does not reveal the full range of possibilities, because we can also rotate the nodal line on the sphere. Let's rotate that nodal line to the right, or reflect it to the left. There are now two new modes of vibration on the spherical surface with one nodal line. Those are vibrations with an azimuthal nodal line that is rotating clockwise or anti-clockwise. In case of two nodal lines, there is an option to rotate not just one, but both nodal lines to the right, and reflect their image to the left. In case of three nodal lines, we can rotate first one line, then two, then all three nodal lines to the right, and reflect their image to the left. There are thus $(2l + 1)$ potential modes of vibration on the spherical surface with l nodal lines. We can generate any number of basic modes on the two-dimensional spherical surface by adding and rotating nodal lines, starting from the simplest vibration.

2.6. Plancks constant as key to the quantum dimension (U2-6)

In this station, we dare to enter the quantum dimension by replacing standing waves in real space by standing waves in the quantum dimension. Nothing remains the same!

2.6.1. Candle and Mirror [Link to U2-6-01](#)

Finally, light dawns on Bob. At this point, since nothing is what it seems, we could as well speculate whether Bob's hair is real. In this station, we pass through the quantum mirror to enter the quantum dimension for the first time. A pattern of nodes and nodal lines is all that remains from the classical vibrational states we have seen in the previous stations. It forms a kind of skeleton for the vacuum. The vibrating matter is gone. It is recreated in the form of a complex wave function.

2.6.2. Rotation operator [Link to U2-6-02](#)

Simple rotation operations allow us to generate all kinds of vibrational modes on the two-dimensional spherical surface. Using suitable rotating operations, we can convert the total number of azimuthal nodal lines into m nodal lines that rotate clockwise or anti-clockwise. The sphere we are considering here has a fixed radius. This is why we can leave radial nodal lines out. Let's now take a closer look at the rotation operator. An operator manipulates properties of a state. A state is generally a complex object with a variety of properties. It could be a banana, for example. Let us express this state with B . The state "banana" has many different properties, such as a shape, a colour, and a taste. Of course, we can also rotate the banana.

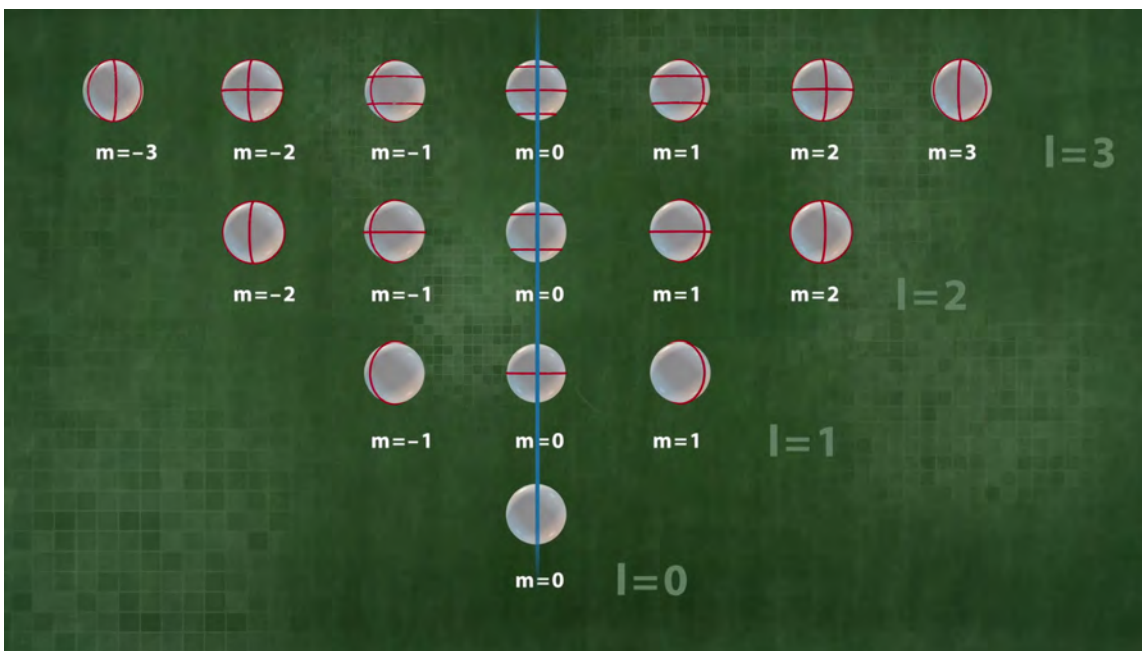


Figure 19. U2-6: The angular momentum quantum number l counts the total number of azimuthal nodal lines, the magnetic quantum number m defines the arrangement of the nodal lines on the surface of the 2D-sphere.

Three-dimensional objects have three different axes of rotation: the x-axis, the y-axis, and the z-axis. The rotation operator D manipulates only the banana's rotation property. The banana will not change its taste just because you rotate it, for example, by 90 degrees about its z-axis, right? We can also perform several rotations one after another. For example, we can first rotate the banana by 90 degrees about its z-axis, and then by 90 degrees about its y-axis. The banana is now lying on its back. Rotation operators have a curious feature. To demonstrate this, let us perform the same rotation operations in reverse order. We first rotate the banana about its y-axis, and then about its z-axis. The final state of the banana is different, although the initial state was the same as before. The banana is not lying on its back now. It has been turned to the side. Rotating operations do not commute. It means that the order in which they are applied plays a crucial role. Let us now consider a slightly different state: a banana that is rotating about its z-axis. Let us express this state with R-z-B. Applying a rotation operator along the rotational axis of the banana does not change its state. This banana has a so-called eigenstate. Generally speaking, the eigenstate does not change when the corresponding operator is applied. Be careful, though. The only rotation operator that does not change the state is the one that rotates it along the specified axis. Rotation about an incorrect axis will surely change the state. Therefore, Bob is an eigenstate only with respect to rotation about his z-axis ... or rather... he was an eigenstate ...

2.6.3. The spectrum of the rotation operator [Link to U2-6-03](#)

We shall now examine the spectrum of the rotation operator, that is, the complete set of its eigenstates in three dimensions, in more detail. To do this, let us take $l=2$ as an example. The most symmetric state, $m = 0$, is completely rotationally invariant. This state does not change at all when it is rotated about the z-axis at any given angle α . It is thus obviously an eigenstate with respect to the operator $D_z(\alpha)$. Its eigenvalue is 1. Is this also true for $m = 1$? This state is rotating about the z-axis. Rotating it additionally by a fixed angle α therefore only changes the phase of its rotation. It does not change the state itself. This is another eigenstate of the operator $D_z(\alpha)$. For rotation by the angle α , the eigenvalue is $e^{i\alpha m}$. This is true for all m . All states shown here are thus eigenstates of the rotation operator about the z-axis. What happens when we rotate one of these states about the y-axis? Let us take $m = 0$. In this case, the state does change. It is thus not an eigenstate with regard to the operator "rotation about the y-axis". This is also true for all m . Let's sum it up. The vibrations on the spherical surface in three dimensions can be classified using the number l of azimuthal nodal lines. This gives us all possible real eigenstates of the rotation operator about the z-axis. We can only construct eigenstates with regard to rotations about one specific axis. In this example, we have selected the Z-axis. These vibrational states on the sphere are therefore not eigenstates with regard to rotations about the x-axis or the y-axis. However, we can use these two rotation operators, D_x and D_y , to form two new and important operators. Let us call them nodal rotation operators. We shall describe their role in the next slide.

2.6.4. Quantum Mirror [Link to U2-6-04](#)

We use candles and mirrors here to represent states and operators. Particularly symmetrical states are their own reflection. They are located right in the middle, dividing the mirror plane. All other states are not their own mirror image; instead, they come in pairs. In this case, there can only be an odd number of states: three, five, and so on. Let's have a closer look at the scenario where there are seven states. Here, we have a total of $l = 3$ azimuthal nodal lines. In the most symmetric case, the three nodal lines are horizontal. The nodal rotation operators rotate one nodal line from horizontal to vertical. They thus generate the state m equals plus 1 from the state m equals 0, with one nodal line rotating clockwise. This is reflected as m equals minus 1, with one nodal line rotating anti-clockwise.

If we apply the nodal rotation operator again, it will rotate another nodal line from horizontal to vertical. If the nodal rotation operator is applied once more, it will generate states in which all nodal lines are rotating about the z-axis, clockwise or anti-clockwise. There are no more horizontal nodal lines. Applying the nodal rotation operator again will result in zero. The state will be destroyed. We have thus discussed all potential vibrational states on the spherical surface in three dimensions. All the states shown here are eigenstates, when classified with regards to the D-z operator. The nodal rotation operators d^+ and d^- rotate nodal lines from horizontal to vertical, generating the states

m-plus and m-minus from the state m. We start from the most symmetric eigenstates of the D-z operator on the mirror plane. We can then obtain all other eigenstates by applying the nodal rotation operators. There is one free parameter in the figures of both operators and states on the spherical surface, which we have yet to analyse: If we change the distance between the states and their mirror images, everything else will remain the same. We can choose the distance arbitrarily without destroying the symmetry between the eigenstates.

In case of classical operators on the spherical surface, this distance delta has no greater significance. It varies depending on the application. In quantum physics, however, this is the crux of the matter. This distance is a universal physical constant \hbar , that is, 10 to the power of minus 34 joule-seconds. This value is absolutely immutable. It is equally valid on the Earth, in the Sun's core, and inside a black hole. Therefore, in the transition to quantum physics, the operators are "only" scaled. The main difficulty lies not in the mathematical structure, but in interpreting this scaling. Let's compare operators and states on the spherical surface in quantum physics with those in classical physics. In quantum physics, the distance between the states is a universal physical constant. In classical physics, it is random. But how do things stand in case of states? In both cases, the eigenstates can be classified as vibrations on a spherical surface, using the number and location of nodal lines. In this example, we have $l = 2, m = 0$. There is one crucial difference, though. In classical physics, vibrational states are directly observable. They are real vibrations on a spherical surface, such as a soap bubble. In quantum physics, we have a vibration that is not directly observable. We could interpret it as a square root of a probability, or as a wave function. When we cut the sphere in half, we obtain a vibration on a circular line. In the quantum dimension, however, the result is a section of a complex wave function.

For historical reasons, in quantum mechanics, the operators L_z, L^+ , and L^- are called angular momentum operators. However, the only thing these operators have in common with the classical angular momentum is the physical unit joule-second. They have more similarities only in very few special cases.

2.7. The middle mirror (U2-7)

One small step for an individual mirror, a giant leap to a new dimension - the 720°-quantum dimension.

2.7.1. Haunted Mirror [Link to U2-7-01](#)

Alice and Bob observe their own mirror image in the chessboard bar. The black and white squares represent zero and one, that is, the digital data we use on a daily basis to create our media reality. The quantum mirror opens the door to a world beyond the digital world. A single candle and its mirror image represent a qubit. It's the simplest possible quantum system, a generalization of a bit.

2.7.2. Spin [Link to U2-7-02](#)

The figure with a candle and a mirror, which serves to illustrate states and operators, can be manipulated by changing the distance between the states. Another way to manipulate it is by changing the position of the mirror plane. The mirror should reflect states onto further states, and the distance between the states should always be equal. This can only be achieved in two ways. We already know one solution: if a state is its own mirror image, the number of states will always be an odd number.

If the mirror is positioned exactly in the middle between two states, the number of states will be even, and no state will be its own mirror image. The simplest scenario thus includes two states. The transition to quantum physics is performed by scaling the distance between the two states by \hbar . These two states have an important function. They can, for example, describe the spin of the electron, spin-up and spin-down, with $\pm\frac{1}{2}$ in \hbar units. What modes of vibration correspond to these two states? Those cannot be vibrations on the two-dimensional spherical surface, since they have been fully classified already.

Something new is happening here. It is possible to demonstrate mathematically that, in the simplest scenario, those are vibrations in four dimensions on a three-dimensional spherical surface. This spherical surface is a complex geometrical object. In quantum physics, such a four-dimensional state is possible because it cannot be directly observed, and only has an indirect impact. In classical physics, such a state is simply not possible. This is because four-dimensional vibrational modes that can be directly observed do not exist. The spin is the first and the most important example of a state that cannot exist in real space, and therefore represents a purely quantum mechanical phenomenon. What we are able to see is, so to speak, a projection into the real three dimensions. Let's define the z-axis from the bottom up, as usual. In relation to the z-axis, the spin-up state points upwards, and the spin-down state points downwards. We can project the three-dimensional spherical surface onto a conventional, two-dimensional spherical surface, whose north and south poles correspond to the states spin-up and spin-down. These two basic spin states exist alongside the potential superposition states of these vibrations, such as spin-up plus spin-down, or spin-up minus spin-down. The geometric representation would be a spin pointing in the direction of plus y or minus y. By way of analogy, the spin can also point in the direction plus x or minus x. The spin in the three-dimensional space can thus point in any direction. This is indicated here by the direction of the large red arrow. Each point on the sphere corresponds to the spin state which points in that spatial direction. All potential spin orientations of this so-called qubit yield a two-dimensional spherical surface, the so-called Bloch sphere.

2.7.3. Stern-Gerlach experiment [Link to U2-7-03](#)

The Stern-Gerlach experiment, performed in 1922, delivered the first experimental proof of the fascinating degree of freedom of an electron spin. A beam of silver atoms was generated in an atomic beam furnace. It was then sent towards an inhomogeneous

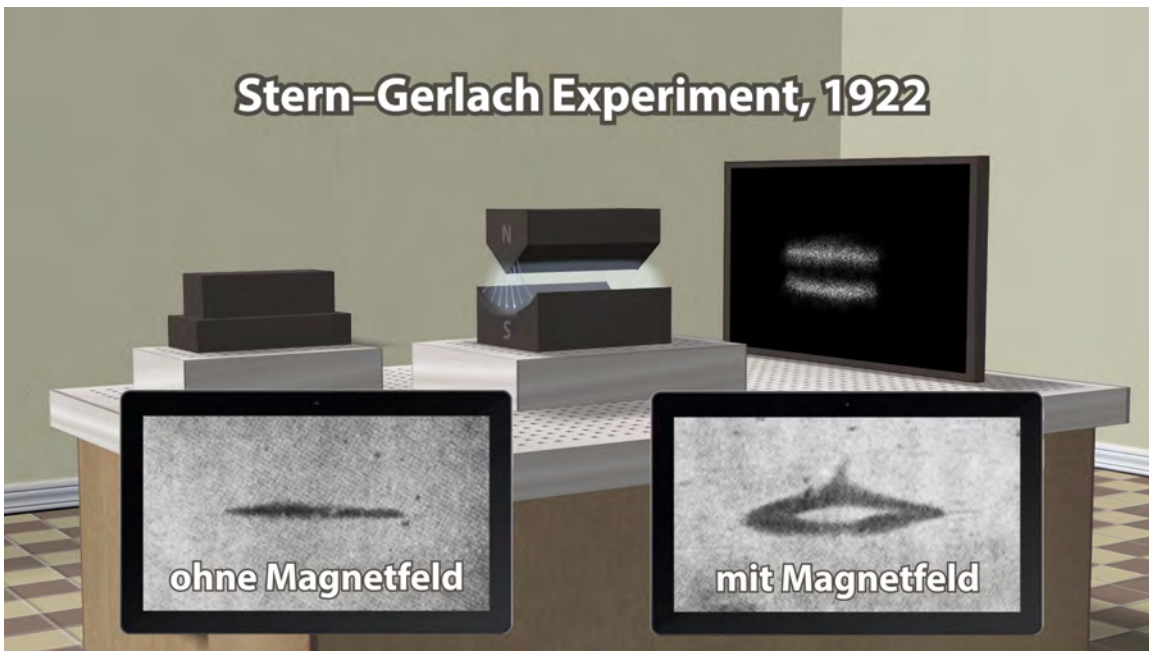


Figure 20. U2-7: The Stern-Gerlach experiment.

magnetic field. According to classical physics, one would expect the magnetic moments of silver atoms to be randomly oriented. They should be deflected in the inhomogeneous magnetic field by different amounts, depending on their orientation.

However, the researchers observed that the beam was split in two possible states, which were later named spin up and spin down. How can this be explained? Let us first analyze the electron configuration of a silver atom. One silver atom has a total of 47 electrons. In 46 of these electrons, each spin up is paired with one spin down. The spins neutralize each other. There is only one unpaired spin - the spin of the 5s electron. It can be either in spin up or spin down, or in any superposition of these two states. We can represent this spin state using a Bloch sphere. The spin can point in any random direction. The spins of all silver atoms are randomly distributed. They are, therefore, not polarised. In fact, there is a close connection between this experiment with a single electron spin and the experiment with single polarized photons. Here, the polarizing filter corresponds to the inhomogeneous magnetic field. Just like with photons, in a single experiment it is completely random whether the spin points in the direction of the polarizing filter, or in the opposite direction. The result is a black and white random pattern. Let's have a closer look at the quantum mechanical measurement process in the Bloch sphere. The spin has some arbitrary orientation before it interacts with the inhomogeneous magnetic field. The inhomogeneous magnetic field acts as a filter. It is presented here as a slot. It forces the spin to take a random orientation, either in line with the inhomogeneous magnetic field, or in the opposite direction. If the basis state is close to "up", it is very unlikely to change the direction in "down"; however, it may still do so. When performing their canonical experiment, Stern and Gerlach were unable to

use single silver atoms. Therefore, they could not demonstrate the role of chance in each experiment. However, they were the first to demonstrate that the spin is quantized, or separated in “up” and “down”. It was a sensational achievement in their time.

2.8. From Bohr to the quantum dimension (U2-8)

In this station, we compare Bohrs atomic model to the approach based on quantum physics. We show that in the model of quantum mirrors in the quantum dimension, counting the number of quantum states helps to understand the composition of the table of elements.

2.8.1. Stair steps [Link to U2-8-01](#)

Alice and Bob go down the stairs. The candles and their mirror images are arranged along these energy levels. In this key station, the spinning wheel is running at full speed. Our journey will start with historical experiments on atomic spectra. It will take us through first atomic models, to the representation of all elements of the periodic table on the quantum organ.

2.8.2. Atomic spectra [Link to U2-8-02](#)

Sir Isaac Newton split white light into spectral colours using a prism. We have built a similar experiment. The white light falls on the prism, which splits it up into its constituent colours forming a rainbow. However, if we choose a specific gas as a light source - in this case it is neon - only certain spectral lines will appear. This is why the light emitted by a neon tube is not white, but yellowish-orange. For helium, we will obtain a different set of spectral lines. Hydrogen emits only four spectral lines in the visible range. Joseph von Fraunhofer used a similar set-up to study the spectrum of sunlight. He discovered dark lines in the colour spectrum. Today, we call those lines Fraunhofer lines. Apparently, specific frequencies in the solar spectrum are absorbed before they reach the Earth. Each element has a unique emission spectrum, similar to fingerprints. We can thus infer which elements are present on the solar surface, based on the black absorption lines. This is how the element helium was discovered on the Sun’s surface at the end of the 19th century. Nowadays, we can observe the sunlight in different wavelengths, or spectral ranges, directly from outer space.

Spectral lines are fingerprints and distinctive properties of elements, and can be measured as such. Following this discovery, we are faced with the obvious question: what causes these spectra? We shall discuss the key milestones, which have led to the current explanation offered by quantum physics, in the following slides.

2.8.3. Balmer-formula [Link to U2-8-03](#)

The four visible lines of the hydrogen spectrum correspond to electromagnetic

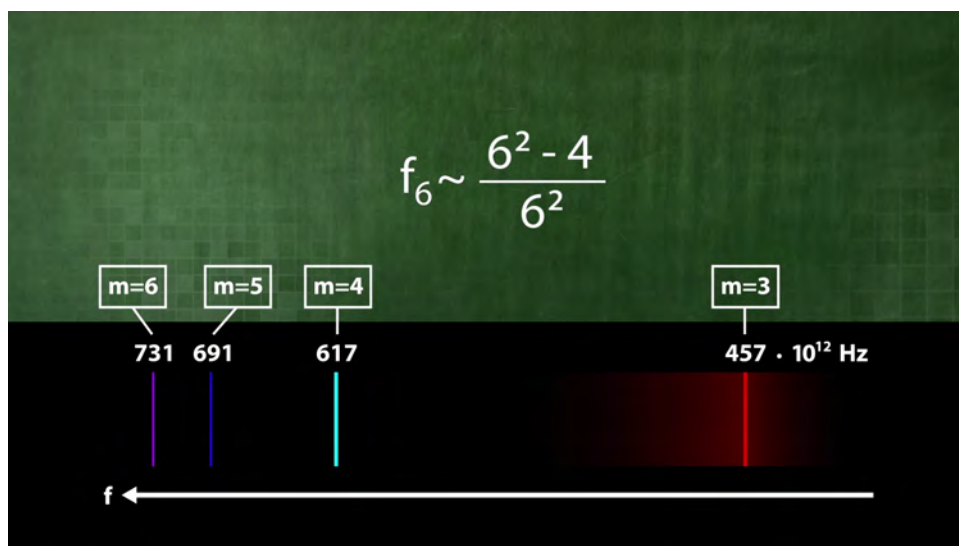


Figure 21. U2-8: Balmer was the first to guess a mathematical relation for the measured spectral lines of the hydrogen atom.

oscillations with frequencies in the order of magnitude of one million times one billion oscillations per second, namely, 731, 691, 617 and 457 times 10 to the power of 12 Hertz. Anders Jonas Angstrom measured this as early as in 1862. He could not, however, explain it theoretically. Can we describe this spectrum using a mathematical formula? To do this, we need a specific concept. Johann Jakob Balmer, a Swiss teacher, proposed using natural numbers m in his formula. He did so perhaps by analogy with the spectrum of a guitar string, because it involves multiples, that is, m times a fundamental frequency. We could assign natural numbers to each of these frequencies, and check whether this will allow us to create a useful formula. We do not know how Balmer came up with his formula. He discovered that the combination of m squared minus 4 divided by m squared correctly describes all frequencies for m equal to three, four, five, and six.

Rydberg rewrote Balmer's formula as a difference between 1 divided by 2 squared minus 1 divided by m squared. This means that Rydberg assigned TWO natural numbers to each frequency. In this case, 2 and 3, 2 and 4, 2 and 5, and 2 and 6. Using the Rydberg constant, we can obtain the following numbers: 457 times 10 to the power of 12, 617 times 10^{12} , 691 times 10^{12} , and 731 times 10^{12} . Johannes Rydberg extended his formula for use with any m and n . It can thus be used to predict frequencies in the hydrogen emission spectrum that are outside the visible region. With this prediction, he hit the mark.

2.8.4. Rutherford-scattering [Link to U2-8-04](#)

In order to understand atomic spectra, we need to start with the structure of an atom. Already at the beginning of the 20th century, it was known that atoms were made up of smaller particles with a positive and a negative charge. However, it was

not yet clear how an atom looked on the inside. Were negative and positive particles distributed evenly? Or, maybe, negative particles were on the outside, and positive ones inside? If so, how far apart were they?

You could ponder over these questions as much as you want, but the only way to really find out is by performing an experiment. The ingenious experiment of Rutherford was essential for finding the answer. Radioactivity had just been discovered, and Rutherford could use an alpha emitter, that is, fast atomic nuclei of helium, which are emitted by radioactive radium. Rutherford chose a gold foil as a target for fast alpha particles. The foil was extremely thin, and had only a few atomic layers. To measure how alpha particles were deflected in the gold foil, Rutherford used scintillation screens. The experiment was performed in complete darkness. The screens gave off tiny flashes of light when struck by alpha particles. Detecting the alpha particles, which were scattered at all angles, helped to figure out the structure of a gold atom. It turned out that most alpha particles passed straight through the gold foil. Unexpectedly, only a few alpha particles were deflected by the foil. Some of them, however, were bounced back with a considerable force. What did that mean? Electrons are very light, and do not present a significant obstacle for alpha particles. An alpha particle will move onwards practically undisturbed. Only heavy, positively charged atomic nuclei can deflect alpha particles. It appears that atomic nuclei must be astonishingly small; otherwise, many more alpha particles would be deflected. Deflected particles with positive charge follow hyperbolic paths. Those paths are more sharply curved when the alpha particles are nearer to the nucleus.

Any distance between an alpha-particle and the nucleus is equally likely. In other words, alpha particles passing close to the nucleus, which are scattered through large angles, occur as often as those that are slightly less close and are less scattered, or those that are further away still and are even less scattered, and so on. The hyperbolic paths have already demonstrated that particles were much less likely to be scattered through large angles than through smaller ones. Most alpha particles pass far away from the tiny nucleus. Their hyperbolic paths are hardly deflected, and they come straight through the gold foil. This is true as long as the nucleus only acts on the particles through its force of repulsion, that is, the Coulomb force. The closer an alpha particle comes to the nucleus, the larger the scattering angle. The particle deflects from its hyperbolic path only when a new force, that is, the nuclear force, comes into play. Rutherford was able to specify a limit at which such deflections occur. He also inferred the size of the atomic nucleus from the respective scattering angle. That size is $10^{-15}m$. This is how we know that most of the atom is empty. The electron shell is almost a hundred thousand times larger than the nucleus. It is thus clear that the binding energy of the nuclear force must be over a hundred thousand times that of the Coulomb energy; otherwise, the positively charged nucleus would come apart. If an atom were as big as a football stadium, we would find its electron orbits in the spectator stands. The nucleus would be roughly the size of a pin.

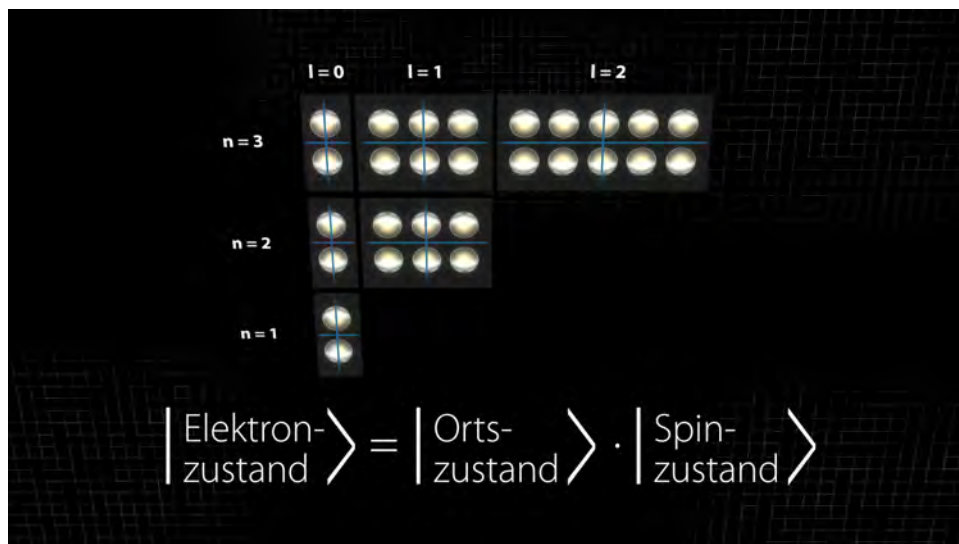


Figure 22. Visualization of the relation between the four quantum numbers n, l, m, s in the model of bound states of the electron in the Coulomb-potential. The spin s doubles the number of states, indicated by the horizontal quantum mirror. The quantum number m counts in every "block" from $-l$ to $+l$. In total, $2n^2$ state for fixed principal quantum number n arise. The octet rule $6 + 2 = 8$ can be understood just by counting all possible quantum states in the s- and p-orbitals.

2.8.5. Bohrs atomic model [Link to U2-8-05](#)

In 1913, Niels Bohr proposed his famous atomic model. According to this model, electrons can assume only certain orbits around the nucleus. But first things first. Bohr put together the knowledge blocks available to him at that time, and created a kind of a recipe book.

We know from the Rutherford scattering experiment with a gold foil that the atomic nucleus is tiny relative to the electron shell. But how are the electrons moving around the nucleus? A possible, albeit naive, explanation would be comparing an atom to a planetary system. The nucleus would correspond to a sun, and the electron to a planet which is held in a circular orbit by electrical attraction. The problem with that theory is that an accelerated charge would have to radiate energy like an antenna. The electron would lose energy, and eventually spiral into the nucleus. Such an atom would be unstable from the classical point of view. Bohr postulated that atoms were stable, but could not explain why. He assumed that electrons could follow only certain discrete orbits. But it follows that only certain discrete electromagnetic radiative transitions are allowed. Transitions are radiationless when the electron jumps one orbit closer to the nucleus. When the electron stays in the smallest orbit, the so-called basic state is reached.

According to Bohr, the permissible orbits are characterized by the angular momentum. The angular momentum must be a multiple of Planck constant \hbar . What about the energy of the electron? Generally speaking, a bound state is characterized by

negative energy. The electron receives positive energy and can leave the atom only when this so-called binding energy is overcome. The atom then becomes ionized. However, we are talking about bound states, in particular the basic state, and the smallest orbit with $n = 1$. The next higher orbit $n = 2$ has more energy, the orbit $n = 3$ has even more energy, and so on. When talking about transitions in which electromagnetic radiation is released, let us recall the Balmer equation as generalized by Rydberg. We are now able to interpret the difference between the numbers n and m as the difference in energies, for example, between shell No. 2 and shell No. 3. As we can see, Bohr proposed an ingenious interpretation of Rydberg's findings. Bohr's postulate of discrete orbits thus allows a new interpretation of the discrete absorption and emission spectrum. During the transition in hydrogen, for example from shell 3 to shell 2, a photon is released. The opposite happens when the electron jumps from shell 2 to 3: a photon of that frequency is absorbed. The absorbed or emitted light corresponds in each case to the energy difference between two permitted energy levels in the atom. Bohr's postulate of certain permitted electron orbits helped to explain why only certain emission and absorption energies of photons were possible in the atom. However, Bohr could not explain why only these electron orbits were permitted. A step in that direction was made later by Louis de Broglie, who postulated that matter, and electrons in particular, had wave properties. This changed our understanding of an electron, from a particle travelling either left or right, to overlapping waves travelling both left and right. These overlapping waves may form a standing wave, which, however, would need certain constructive interference conditions.

According to de Broglie, a wavelength λ is assigned to each pulse P . A constructive interference between waves travelling right and left is given when a multiple of these wavelengths is equal to the circumference, thus $2\pi l = l\lambda$, in this example for $l = 2$. This revolutionary idea allows interpreting Bohr's postulate as a necessary condition for standing waves. The next step towards quantum physics is the question of what this Oscillating Thing, a term that seems fitting for an electron, is supposed to be; and, in particular, in how many dimensions it is oscillating. That standing wave is certainly not two-dimensional, as in the Bohr atomic model. It is at least three-dimensional; but that's just the beginning, the dawn of the quantum dimension.

2.8.6. States, operations and the hydrogen atom [Link to U2-8-06](#)

Quantum physics has advanced since Bohr developed his atomic model over 100 years ago. An important step in developing the Bohr atomic model was introducing operators and states to describe and manipulate an electron in the quantum dimension. How do these two models relate to each other? The Bohr atomic model was first refined by De Broglie, who assigned standing waves to electron orbits. In this example, we have $l=2$. Accordingly, there are electron positions with two nodal lines in the quantum dimension. In quantum physics, we interpret the postulate $L = n\hbar$ differently. Angular momentum becomes a rotation operator. In order to analyse electron states, let us start

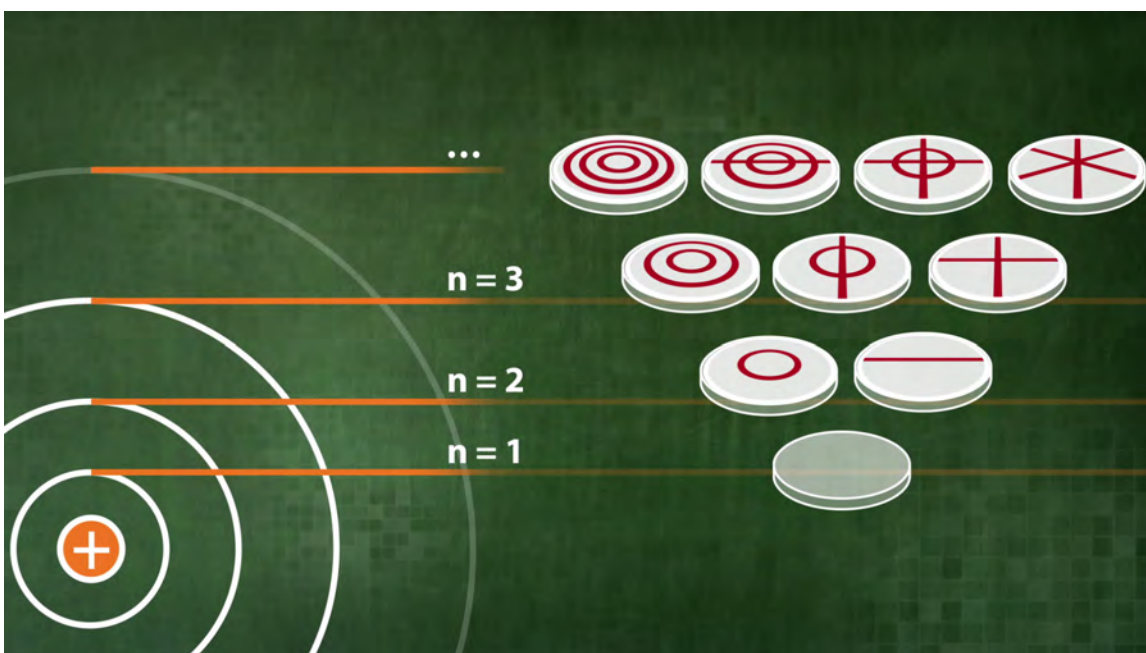


Figure 23. The s/p/s-orbitals are defined by the number $l = 0, 1, 2$ of azimuthal nodal lines.

with eigenstates with regard to the rotation operator about the z -axis.

In quantum physics, $L = n\hbar$ does not hold. General superposition states do not have a specified angular momentum. They have only their respective eigenstates. Therefore, \hbar is the smallest possible measurable difference of the angular momentum. Analysing classical vibrational states and operators will help us to understand quantum states. Between all possible vibrational states on a glass pane, let us consider the eigenstates of the energy operator. These eigenstates have two types of nodal lines: radial or azimuthal, or combinations of both. These fundamental frequencies will help us understand the respective quantum states, even though we cannot know what these states are really like.

In a hydrogen atom, vibrational states have roughly the same binding energy on each orbit $n = 1, 2, 3$, and so on. That means they have the same number of nodal lines. The innermost orbit $n = 1$ does not have any nodal lines. The next orbit, $n = 2$, has one nodal line, either radial or azimuthal. The third orbit, $n = 3$, has two nodal lines. Those can be two radial lines, or one radial and one azimuthal, or two azimuthal lines; thus $l = 0, 1, 2$. If the electron were a two-dimensional object, this is how its spectrum would look like in the quantum dimension. In three-dimensional space, the spherical symmetry rules out other options for radial nodal lines. In case of one azimuthal nodal line in three dimensions, there are more possibilities, because that nodal line can be horizontal or vertical to the z -axis. Each new azimuthal nodal line will result in two additional states. If the electron were a three-dimensional object, this is how its spectrum would look like in the quantum dimension. In fact, the quantum dimension has more to offer. A spin

is an additional vibrational mode of the electron state. In three dimensions, it has two possible eigenstates with regards to the rotation operator: “up” and “down”. This additional degree of freedom of the electron is visualized here using another mirror plane. The number of eigenstates doubles. The electron state is thus a product of position and spin state in the quantum dimension.

The Bohr atomic model could therefore be developed as follows, so that it can be applied in the quantum dimension: First, the angular momentum becomes the rotation operator. \hbar thus represents the smallest possible measurable difference of the angular momentum. Secondly, by counting nodal lines, we can explain why there are exactly $2n^2$ eigenstates per orbit or energy level n , where n is equal to 1, 2, 3, and so on.

2.8.7. Atomic orbitals [Link to U2-8-07](#)

How does chemistry describe electrons in an atom? The so-called atomic orbitals are a visualization of the probability of finding an electron at a specific location in the atom. Here, we can see the locations of maximum probability for the s, p, and d orbitals. Behind this probability, there is the invisible vibration in the quantum dimension. This vibration has interference properties. It is visualized here in the form of a spinning wheel. The s orbital is based on the vibration without nodal lines. The p orbital is based on the vibration with one nodal line, thus $l=1$. Let's analyse the context of the p orbital in more detail. We have already seen the vibrational state $l=1$ on a single spherical shell. If we slice the space like an onion, we obtain many spherical shells. In space, the nodal line becomes a nodal plane. The maximum vibration amplitude decreases at a very large distance from the nucleus. Chemistry does not describe the entire vibration in space, only the location of maximum probability of finding an electron. It corresponds to the points with the greatest vibration amplitude. The result is this representation of the p orbital. This also applies to all other orbitals. Atomic orbitals in space inherit the nodal lines, or nodal surfaces, from the quantum dimension. Thus chemistry and physics go hand in hand.

2.8.8. Table of elements [Link to U2-8-08](#)

The elements of the periodic table are arranged according to the number of electrons. The Bohr atomic model cannot explain the number of electrons in the respective periods, or shells, very well. What about our vibrational modes of electrons in the quantum dimension? Can we explain the periodic table by counting nodal lines? Let us assign the possible vibrational states to the keys of an organ. The organ manuals correspond to the energy levels $n=1, 2, 3$, and so on. An electron can excite a specific vibrational state. The key is then pressed, so to speak, and the corresponding vibration is activated. Two electrons press two keys - at least! The more electrons are present, the more keys are pressed.

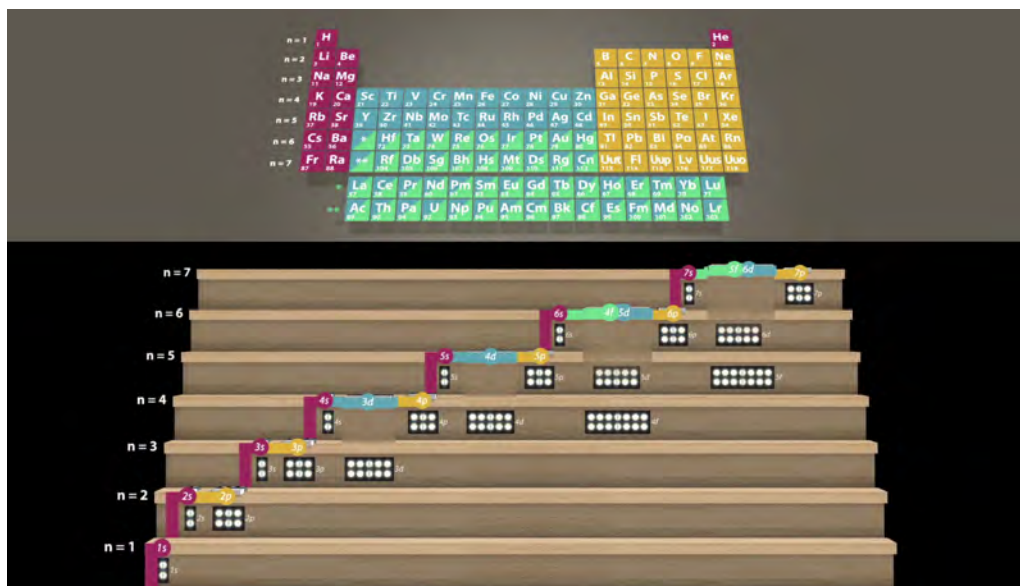


Figure 24. The structure of the table of elements can be modeled using the concept of quantum mirrors. While symmetries of the quantum states $|j, m\rangle$ lead to a prediction for the *number* of quantum states, the calculation of the *binding energy* is highly non-trivial. However, using the simple rule that radial nodal lines are preferred compared to azimuthal nodal lines (for fixed total number of nodes), many features of the table of elements can be grasped without any calculation.

But first things first. The first electron occupies the vibrational state at the lowest energy level, that is, $n=1$. In a $1s$ orbital, spin up and spin down have almost the same energy. The spin can thus point in any direction. Superpositions may happen. The hydrogen atom, which is the simplest atom, having only one electron, is also the most frequently occurring chemical element in the universe. According to the so-called Pauli Exclusion Principle, a second electron cannot occupy exactly the same state as the first. When there are two electrons in the $1s$ orbital, they occupy two different spin states - up and down. We have thus filled the first shell. The corresponding element with two electrons is the noble gas helium. The third electron has no place left in the bottom shell. It must occupy a state with one nodal line in the second shell; again, this is due to the Pauli Exclusion Principle.

Radial nodal lines are more advantageous than azimuthal lines in terms of energy. This is why the $2s$ orbital is occupied first, and not the $2p$ orbital. This single electron is very reactive. It is thus, significantly, the highly reactive alkali element - lithium. The fourth electron occupies the other spin state in the $2s$ orbital. This corresponds to the element beryllium.

For the first time, an electron occupies a state with an azimuthal nodal line: It is the fifth electron, which corresponds to the rare semimetal boron. Six electrons correspond to carbon. Negative electrons repel each other, and the p orbital can take more states. That is why, at this step, the electron does not complete the spin, but fills the next p

orbital instead. This happens according to the so-called Hund's Rule. With nitrogen, all p orbitals are filled once. It is only with oxygen that a p orbital is filled twice. The next in line is fluorine. Finally, the noble gas neon completes the second shell. We have thus explained the arrangement and number of elements of the first two periods of the periodic table. S orbitals can accommodate a maximum of two electrons; p orbitals a maximum of six electrons. The far right section of the periodic table lists noble gases. The shells of those elements are filled completely. Here, a lot of energy is required to free an electron from its ground state.

Let us now fill our third shell with electrons, following the same principle. For a better overview, let us pull the organ manuals apart a little. We have, again, two elements with 3s electrons, six elements with 3s and 3p electrons, and another 10 elements with 3s, 3p, and 3d electrons.

Wait a second! You may have noticed that two elements are missing. Where are the elements 19 and 20 - potassium and calcium? How can we explain the break in the arrangement between argon and scandium? We have seen a similar situation at the 2s orbital. Radial nodal lines are more advantageous than azimuthal lines in terms of energy. Thus, electrons prefer to fill them first. Even though, in this case, we have one nodal line more, the electrons prefer the 4s orbital with two possible states. This arrangement corresponds to the two missing elements. But why doesn't the 21st electron simply continue at the 4p orbital, but switches to the 3d orbital instead? Once more, we are presented with the question: what is more favourable for an electron: one azimuthal and two radial nodal lines, or two azimuthal nodal lines? In this case, the lower total number of nodal lines proves to be more advantageous. We lift, so to speak, our organ manual, and the 3d states can be filled in logical order. The 3d orbital consists of 10 so-called sub-group elements. All of them are transition metals, such as iron. Only then the six 4p orbitals follow, up to krypton, which has a total of 36 electrons.

In the 4d orbital, two azimuthal nodal lines and one radial nodal line are available for the 37th electron. However, this electron also follows the previous pattern. The 4 radial nodal lines of the 5s orbital are more favourable for the electron in terms of energy, and it prefers to fill the 5s orbital. The electron starts a new period. For the 39th electron, again, the lower total number of nodal lines proves to be more advantageous than the number of nodal lines on the 5p orbital. The 4d states are filled with 10 further sub-group elements. All of them are transition metals, such as palladium. The six 5p orbitals follow up to the noble gas xenon with 54 electrons. The 55th electron can now fill a 6d orbital with 10 states, and, for the first time, a 4f orbital with 14 states. What decision will it take? Three azimuthal nodal lines, or two radial and two azimuthal nodal lines?

When two people quarrel, a third rejoices. The 6s orbital with 5 radial nodal lines is still more favourable than the two opponents, and is gets filled. The energy levels of the 5d and 4f orbitals mix, and form the basis for the next 24 elements. This is followed by six elements. The 6p orbital gets steadily filled. The 87th electron also occupies the 7s orbital without azimuthal nodal lines. The 6d and 5f orbitals mix again,

and form the basis for the elements 89-112. Finally, the 6 states of the 7p orbital are filled. The elements 113-118 of the periodic table are thus complete. None of these elements has stable isotopes. They all decay radioactively within a short time. The Bohr atomic model described the shell structure of the atom for the first time. It could not, however, explain the exact structure of the periodic table. With Chladni's help, we have managed to extend the model, and to rediscover the s, p, d, and f orbitals in the quantum dimension.

But that is not the end of the story. It is just the beginning of the music of a quantum organ.

2.9. Quantum organ - dancing electrons (U2-9)

In this last station we present some selected quantum melodies.

2.9.1. Quantum organ [Link to U2-9-01](#)

The organ is considered the queen of musical instruments. It offers almost unlimited wealth of musical possibilities. In analogy, a quantum organ serves as a basis for the composition of quantum states. The wealth of quantum melodies is inconceivable in every sense of the word. In this last station on the U2 line, we will contemplate a few examples of such quantum melodies.

2.9.2. Helium-Neon-Laser [Link to U2-9-02](#)

How do lasers actually work? It's simple; you just need to press the button, and the show goes on. In the physical sense, however, there is much more to it. Let us discuss the helium-neon laser as an example of a gas laser. There are two parallel mirrors at each end of a glass tube, which contains helium and neon. The mirrors must be perfectly parallel to each other; otherwise, the laser will not turn on.

Helium atoms are excited by shock waves created by electric discharge. The interesting feature here is that helium cannot give off energy by emitting radiation; it needs collisions to do so. This is because helium atoms are metastable. When a helium atom collides with a neon atom, it gives its energy off. The neon atom, in turn, can immediately emit a photon to its surroundings. It then returns to its ground state. The so-called inversion is a key mechanism in lasers. Excited helium is very durable. That's why it is possible to generate many excited helium atoms simultaneously. Excited helium atoms give energy off to many neon atoms, which then generate many photons - in stimulated emission. These coherent photons are reflected back and forth in the resonator by the two mirrors. That creates a standing wave, which is amplified further and further. A section of this standing wave is decoupled by the mirror, which does not reflect at 100 percent. That is the laser beam we can see.

Why is a helium atom unable to make a radiative transition? According to the Bohr atomic model, each electron should be able to jump from a higher shell to a lower

one, emitting radiation in the process. We can see that Bohr cannot help us here. In the model of a quantum organ, we specify not only shells $n = 1, 2, 3, \dots$, but also the orbitals within the shells; that is, the s, p, d, and f orbitals, each with an additional azimuthal nodal line in the wave function. An electron in the p orbital can emit a photon only by changing the orbital; for example, during the transition from 3p to 2s. These movements along the diagonal line are possible, while all other movements are forbidden. For example, a transition from 2s to 1s is forbidden. These are the so-called “selection rules”. We can compare these rules with the movement of a bishop on a chess board. A white bishop can only move diagonally; it remains on white squares. The black bishop must move according to similar rules, so that only the transitions shown here are allowed. Where do these selection rules come from? To explain this, we must consider the spatial wave function of the electron. At first, the spin plays no role here. We begin with the s and p orbitals. The wave function has no azimuthal nodal line in the s orbital; it has one in the p orbital. Here, we represent the three spatial orientation possibilities of the nodal line as one nodal line that rotates anti-clockwise, one that rotates clockwise, and one horizontal nodal line.

The wave function of the photon has one azimuthal nodal line. The electron “inherits” this line, so to speak. This is because this transition creates vertically polarized light, and the p orbital becomes an s orbital with less energy and with one azimuthal nodal line less. From the anti-clockwise vibration in the p orbital, the photon inherits the anti-clockwise nodal line. This creates a left-circularly polarized photon. The electron can choose an s orbital with less energy, and with one azimuthal nodal line less. From the clockwise vibration in the p orbital, the photon inherits the clockwise nodal line. The result is a right-circularly polarized photon. The electron can choose an s orbital with less energy, and with one azimuthal nodal line less. A single photon is polarized, that is, it has a nodal line. When the electron has no nodal line initially, and it also has none afterwards, a photon won’t be created. This is because it must get its nodal line from somewhere. And yet, an electron can emit radiation starting from the 3s orbital. We have seen a similar situation in U1 station 11 slide 6. A rotationally symmetric wave function without a nodal line can be understood as a superposition of orbitals that rotate clockwise and anti-clockwise. If an electron emits a right-hand polarized photon, it will get a p orbital rotating anti-clockwise. If an electron emits a left-hand polarized photon, it will get a p orbital rotating clockwise. We have thus explained the significance of the selection rules. The bishop moves along the diagonal, because an azimuthal nodal line can only be transferred to the photon when orbitals are changed. It is precisely for this reason that an excited electron in the 2s state is metastable. A photon cannot be emitted in the transition to the 1s orbital. The white bishop stays on the white square. This is exactly what happened with the excited helium atoms. A helium atom can return back to its ground state without emitting radiation only when a so-called “collision of the second kind” takes place. It means the helium atom must transfer its excitation energy to the neon atom. The many technical applications of gas lasers would be unthinkable without this subtle interplay of nodal

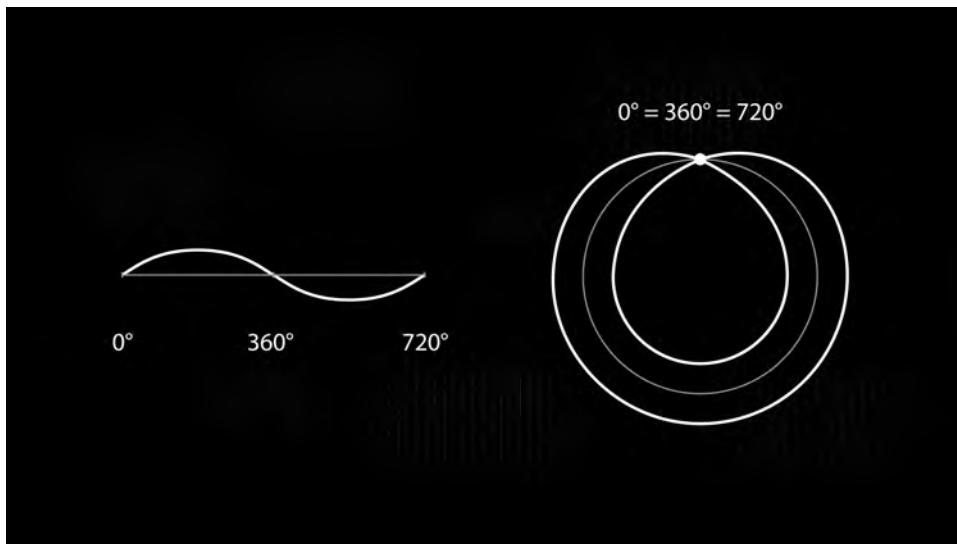


Figure 25. U2-9: In the 720° -quantum dimension, the spin is simply a standing wave - the Pauli principle only emerges due to the Hopf-mapping to the 360° -world. Due to the Hopf-mapping, the double-valued spin wave function arises, which in turn can only be occupied once.

lines between electrons and photons.

2.9.3. Quantum nodes [Link to U2-9-03](#)

An electron state combines position and spin state. Both components can be derived from the spectrum of a guitar string. Let us analyze the fundamental frequency and the first overtone. All other overtones follow the same model. The key lies in the geometry of space, in which the state swings. Let's start with a simple circle, like we have done in U2 station 5 slide 5. If we connect the starting point with the endpoint, we obtain this vibrational state on a circular line. Such a vibration with a "twist", however, cannot be stable. Hence, this state does not exist. Let us now consider the first overtone. When we wind this vibrational state on a circle by connecting the starting point with the endpoint, we obtain a familiar result. This state has one nodal line, thus $l = 1$. In the quantum dimension, all vibrational states on a spherical surface are in at least four dimensions. Some large circles in four or higher dimensions can be divided into 720 degrees, instead of 360 degrees. This is how the fundamental and harmonic frequencies look like in the quantum dimension. Everything is doubled! Let us wind this state on a circle in three-dimensional space. All vibrational modes are doubly wound. What implications does that have? For the fundamental frequency, the double winding results in the following vibrational state with one node. The "twist" has disappeared. This state is, in fact, possible. For the state $l = 1$, the double winding makes no difference. In this case, it does not matter whether we project the state from four dimensions, or just analyze it directly in three dimensions. The double-wound fundamental mode has

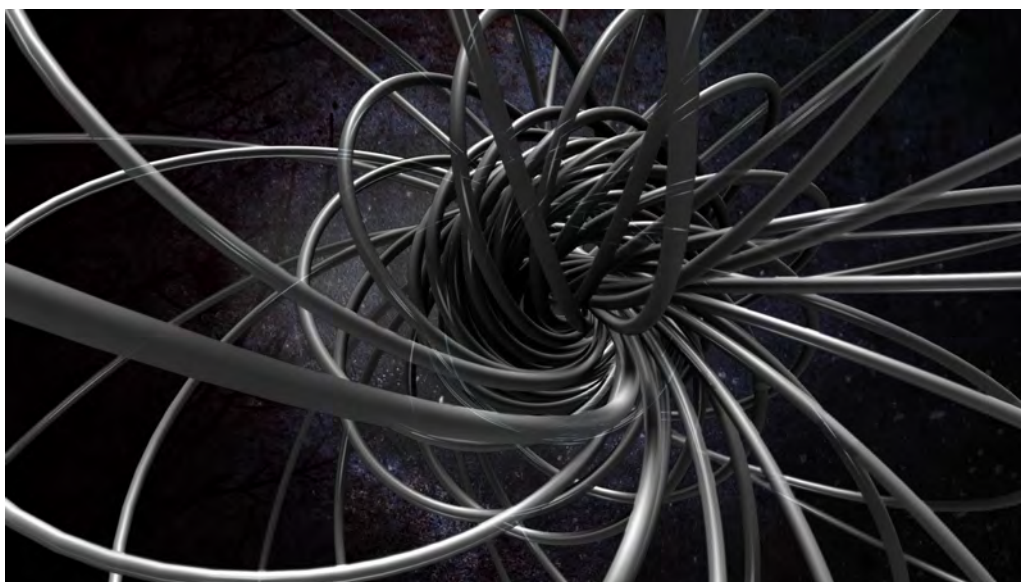


Figure 26. 720° -geometry of the quantum dimensino: We show S_1 -fibres of the Hopf-mapping $S_3/S_1 \simeq S_2$. Using some software, e.g. the programme Antitwister, the time dynamics on S_3 can be visualized.

one node. It represents the spin state. The first overtone has one nodal line, as usual, and represents the state $l = 1$.

Let us now analyze the spin state with one node in more detail. The antipode of the node is the point with the maximum amplitude. On the Bloch sphere, this corresponds to the exact direction of the spin vector. In this projection, the spin "up" state is an exact mirror image of the spin "down" state. The distance between the states is specified by \hbar . The distance to the mirror plane is thus s equals plus one half and s equals minus one half respectively, in units of \hbar .

2.9.4. Pauli exclusion principle [Link to U2-9-04](#)

All quantum states originate from a mirror plane. We generate the spin states up and down by means of the double arrow shown here. We can generate combined states with two spins by shifting the double arrow to the respective position of the first spin. This shift gives us four combinations: up/up, up/down, down/up, and down/down. Symmetries under exchange are a key for a deeper understanding of double spin states, and multiple particle systems in quantum physics in general. We have seen such symmetries already when we analyzed classical vibrational states. Let us recall the cup with a handle. When we mirror at the handle on the plane shown here, the state with the antinode at the handle merges into itself. The state with the node at the handle, however, becomes its own negative. An exchange of A with B thus results either in symmetry, $A - B^+$, or antisymmetry, $A - B^-$.

Symmetry or antisymmetry under exchange of A and B can be found again as a

principle in two-particle states. Combinations of two indistinguishable spins overlap, creating joint vibrational modes that are either symmetric or antisymmetric under exchange of spins A and B. The three symmetrical spin combinations are called triplets. The antisymmetric combination is known as a singlet. The entire two-electron state consists of a position and a spin state. The symmetrical spin triplet joins with the antisymmetric position, and the antisymmetric spin singlet joins with the symmetrical position. This is the Pauli Exclusion Principle: the state of two electrons A and B must be antisymmetric! However, it also follows from the Pauli principle that each spin state can be occupied only once. This is due to the ambiguity: a rotation by 360 degrees changes the sign of a spin! The basis state is reached again only after 720 degrees. In case of a single spin, this is irrelevant, because the phase of the spinning wheel cannot be observed. However, if the same spin state is occupied twice, exchanging the particles A and B or rotating one of the two spins by 360 degrees will result in the exact opposite of the basis state. This is due to the ambiguity. An identical state, however, can only be its own opposite when it is equal to zero.

So far, we have only analyzed states on one great circle. The geometry of the quantum dimension is much more complex. On the left hand-side, there is the two-dimensional spherical surface in three dimensions, which we are familiar with. On the right hand-side, we draw the corresponding points of the three-dimensional spherical surface in four dimensions. We project them stereographically, that is, we distort them, so that we are able to present them at all. In fact, the great circle in four dimensions is completed only after it has revolved around the sphere in three dimensions two times. This projection converts the nodal line of the spin state in the quantum dimension to a node on the Bloch sphere. The antipode of the node is the point with the maximum amplitude. In fact, if we apply this projection, we will lose not only 360 degrees per great circle, but also an entire dimension - the invisible phase. One point on the Bloch sphere corresponds to an entire great circle in the quantum dimension. All invisible phases are hidden in intertwined great circles. Let us consider a group of points on the Bloch sphere. In the quantum dimension, this group corresponds to a fascinating system of intertwined rings. This is just the beginning; the dawn of the quantum dimension. May I introduce myself? My name is Omega.

2.9.5. Guitar reflections [Link to U2-9-05](#)

Alice and Bob coexist in superposition states until the caretaker, as an external observer, forces a collapse of those states. This confusing quantum imagery causes Bob to finally lose his patience. “Anyone who is not shocked by quantum theory has not understood it.” Today, this quote from Niels Bohr is certainly still true. The shock has lasted for over 100 years. Nowadays, it is slowly giving way to a more pragmatic approach. Applications of quantum physics are now found in almost all branches of industry. Our picture of the guitar mirror and the model of quantum organ derived therefrom represent this pragmatic approach to quantum physics. The models do not



Figure 27. All symbols of the movie *Shadow Worlds* are reassembled like puzzle pieces in the sub-dimension, where the actual plot of the film becomes clear. Within the *Shadow Worlds*, the true story remains invisible.

claim to be true; instead, they provide help for use in practical applications. Each model leaves room for interpretation. This reflects the strength of quantum physics, but also the fascination with the scientific research in general, because the truth is: open.

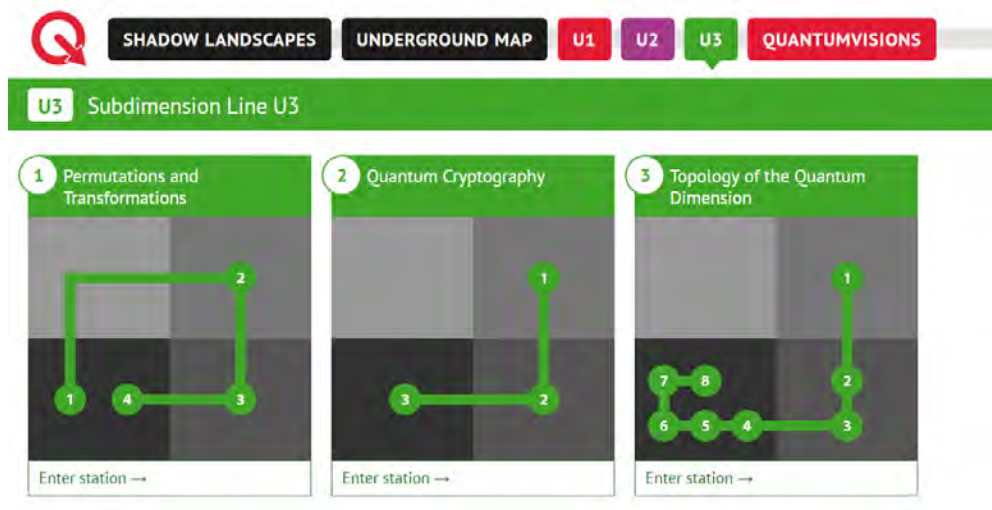


Figure 28. The stations of U3 [Quantum Symmetries](#) and their relation to the four quadrants: experiment (many qubits/single qubits) - theory (amplitudes/probabilities). In U3-3, a particular focus lies in the 720° -topology of the quantum dimension.

3. U3: Quantum Symmetries

3.1. Permutations and transformations (U3-1)

Is the future just a permutation of the past?

3.1.1. Shadow worlds [Link to U3-1-01](#)

The three-dimensional world – a world of shadows? A surface effect of a higher-dimensional space? Or are the shadow world and quantum dimension mutually dependent upon one another, do they exist because they form a symbiosis? Is the future just a rearrangement, a permutation of the past? How do new things enter the world? Follow me into my dimension. In combination with the U1 Quantum Dimensions and U2 Quantum Reflections, the U3 Quantum Symmetries reveals a topological view on the standard model of elementary particle physics, with symmetry groups U1, U2 and U3. However, first of all let us, at the first station, take a look at the permutation of information taking simple examples – based on pictures and music. The caretaker plays a xylophone that has had its bars swapped round. No wonder the music does not sound the way Bob is normally used to it sounding. Music scores always refers to a base – in this case the arrangement of the bars on the xylophone. We have played the co-ordinates – i.e. the notes of the piece of music – using the wrong base. Let us transform the base, by swapping around the bars. Then we return to the standard base, namely to the xylophone as we know it, with the notes in ascending order.

We might as well, however, also do it the other way around: If we transform the base, and say that that is supposed to be the proper base, then the coordinates are

wrong! Consequently, we not only have to transform the base, but also, accordingly, the coordinates. If we play the piece of music using the notes that match the base, we hear the same piece of music again! When subjected to this sort of transformation, the music is rendered invariant – meaning that the permutations are the corresponding symmetry group. With 13 bars, we obtain over 6 billion possible permutations of the base and coordinates. In the standard model of elementary particle physics, we will rediscover permutations as the core of all symmetry groups.

3.1.2. Sound permutations (U3-1-02) [Link to U3-1-02](#)

To play music in the wrong base is essentially a special type of encryption – of cryptography! This idea – i.e. encryption of a message using coordinates that are read in the wrong base – has previously actually been used, however not with musical notes, but with letters of the alphabet.

We are, however, interested in permutations for a quite different reason – because such permutations are the backbone of all operations in the quantum dimension. Let us get started with the simplest permutation of all – which is “interchanging two items”. Interchanging them once more takes us back to the original state. Now, suppose we add one more item. Then, there are three possibilities for transpositions: 123 can become 213, 321 or 132. If we operate with one more transposition, there are only two different options, namely 123 can become 231 or 312. The third option would once again give rise to the initial state, without any permutation.

In a similar way as in U1-1, a tree structure emerges, that always has two branches to the following generation: either adding one item without additional transposition, or adding an item combined with a transposition. This is repeated every time further items are added. At the 13th level, 13 faculty - in other words some 6 billion permutations - are classified in accordance with this scheme. Who would have thought that there would be so many different ways of writing musical notes ... All the permutations can be understood if we grasp the simple transposition of two items! Transpositions are, however, not as easy as they seem – as a sneak preview of that, imagine the objects 1, 2 and 3 as coordinate axes – the exchanges then correspond to 90-degree rotations. Similar as in U2-06 Slide 2, consider a banana as object to be rotated. The 90° rotation around the first axis corresponds to a transposition between coordinate axes 2 and 3. Next, we rotate around the third axis, which corresponds to a transposition between coordinate axes 1 and 2. The order of operations plays a crucial role. If we first rotate the banana around the third axis, and then around the first axis, the final state is quite different. In other words: rotating operators do not commute - just like the permutations. If we thus interpret the objects that are subject to a permutation as dimensions, we have encountered the basic structure of rotations in any number of dimensions desired. This is a further piece of the puzzle towards answering the question of whether the future is a permutation of the past – in the quantum dimension, the time evolution is actually described as a complex rotation, which is the core of the so-called Schrödinger equation.

The choice of base and the corresponding coordinates is, however, arbitrary. This idea leads to the so-called “gauge principle”, which is the cornerstone of the standard model of elementary particle physics.

3.1.3. Music operations [Link to U3-1-03](#)

The quantum organ introduced in station U2 - 9 provides a visualization of all possible vibration modes of the wave function of the electron, culminating in a model for the periodic table of elements. While quantum states and the corresponding wave functions are an essential trait of quantum physics, some of their basic properties can also be studied using sound waves ...for example, with a usual piano keyboard. We can apply operations to any melody, i.e. the notes and their temporal progression. If we apply the operator “derivative” on this melody, it sounds like this ... while the “integral” leads to this result... How can we apply a “derivative” or an “integral” operator on a piece of music? To do this, we have to code the music in numbers. First, we label the keys, starting with an arbitrary key. The music - here the melody of ”Brother John ” - becomes a sequence of numbers ... similar to a piano roll. Now, we apply the difference operator, which determines the height difference between two adjacent notes of the melody ...It starts at zero, then plus two, plus two, then down - minus four, zero - so the same pitch, then plus two, plus two, and so on. At first, this is just a sequence of numbers, but we can also interpret it as a new melody. In such a way, we obtain the sound of the derivative of Brother John. The integral operator sums up all numbers... Starting with the first number, -4, then plus -2, gives -6, then plus 0, stays -6, then plus -4, gives -10, then -4 again, gives -14, and so on. This gives us another sequence of numbers that we can interpret again as a new melody – the integral of Brother John! What happens if we first apply the integral operator and then the derivative operator to “Brother John”? So let’s look again at the differences in the sequence of stages, $-4, -2, 0, -4, -4$, and so on ... This sequence of numbers sounds familiar to us - that’s exactly the initial melody of ”Brother John”! From a mathematical point of view, this is nothing but the fundamental theorem of calculus. But we can also regard this as a special form of encryption and decryption, since - apart from transposition, i.e. a constant shift of the point of reference on the keyboard - no information is lost. And all these operations are examples for various possible operations on vibrational states, just as operations on wave functions are carried out in quantum physics. Of course, in contrast to usual music, quantum states are not audible ... And we certainly can’t observe them directly. Only by using mathematics, we can find a pathway into the quantum dimension.

3.1.4. Qubit operations [Link to U3-1-04](#)

In preparation for the application quantum cryptography in the next station, here, we first examine basis transformations for a single spin. This qubit describes spin ”up” - but is it an eigenstate? Yes and no - it depends on the rotation axis chosen! For

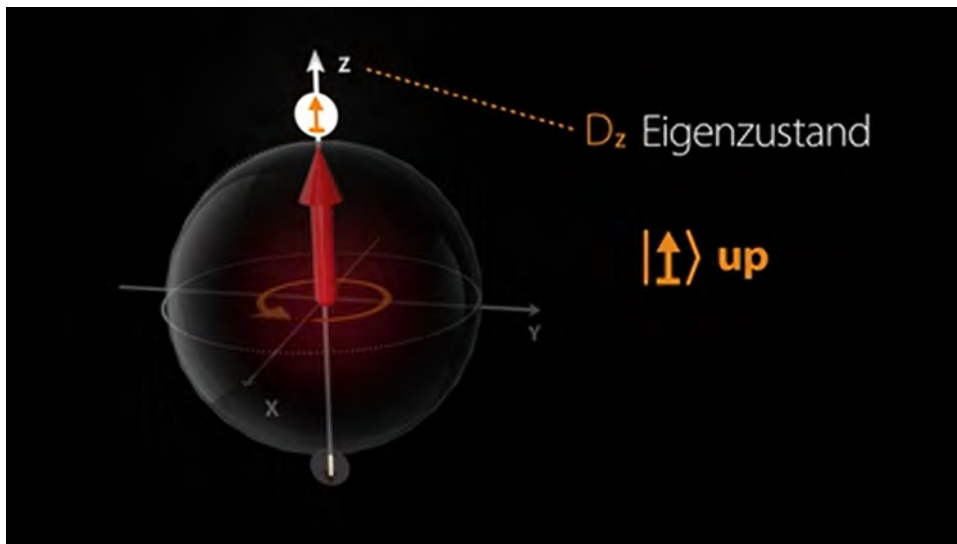


Figure 29. For the spin eigenstate, the position of the state on the Bloch sphere coincides with the rotation axis of the time dynamics determined by the Hamiltonian. As the rotation axis pierces the Bloch-sphere at antipodes, these two points represent the two eigenstates.

rotations around the y-axis, spin “up” is not an eigenstate, since the direction of the spin is changed upon rotation. Up becomes down - then up again ... a permutation! However, spin up is an eigenstate for a rotation around the z-axis: Spin “up” stays where it is - the direction of spin does not change. This is true in general: For a given qubit, the rotation around an arbitrary axis results in a cone. Only if the direction of spin and the rotation axis match, the state is an eigenstate! If the direction of spin is orthogonal to the rotation axis, the cone degenerates into a plane. In U2-7 Slide 3, we discussed the Stern-Gerlach experiment. The direction of the inhomogeneous magnetic field defines the z-axis. Due to the interaction of the arbitrary initial spin with the magnetic field, the spin direction changes to become an eigenstate. The initial state must, so to speak, align with the direction of the slot ... Why does the magnetic field have to be inhomogeneous? If the magnetic field were homogeneous, the spin would just rotate around the cone. The inhomogeneous magnetic field causes the arrow to spiral towards the z-axis and thereby to become shorter. The initial state is projected onto the z-axis. If the initial state is orthogonal to the z-axis, the length of the arrow becomes zero, leading to 50 percent probability for spin up or down - a completely mixed state. An eigenstate does not change at all upon projection. Here, the probability for spin “down” is 100 percent. Now we rotate the direction of the inhomogeneous magnetic field by 90 °.

Then, the same initial state is no longer an eigenstate. The projection results in a completely mixed state with a 50 percent probability for parallel or anti-parallel alignment of the spin with the magnetic field. Thus, depending on the measuring axis, the same initial state either leads to a predictable or to a random result! The state

corresponds to certain coordinates - which are interpreted in one basis or another. This basis transformation is the essential step for quantum cryptography, where this idea is realized with single photons, as we will see in the following chapter.

3.2. Quantum cryptography (U3-2)

A visual approach to quantum key distribution

3.2.1. Alice Chessboard-Code [Link to U3-2-01](#)

Alice decrypts the given random pattern by adding another random pattern, known as the one-time pad. How Alice can transmit and decrypt secret codes with the aid of quantum physics we will find out at this station.

3.2.2. One-time pad [Link to U3-2-02](#)

Alice would like to send Bob a message – say, this picture, for example. But watch out! Unencrypted messages are not secured on the Internet against eavesdropping! How can data be securely transmitted? There are various methods – the safest, which takes a lot of effort with current technology and is only rarely used yet, is the following: we encrypt the picture in 0 and 1, and add a random pattern Z . The random pattern is the key – it turns every bit around if $Z=1$, otherwise not. What emerges is a random pattern: $Z+B$ no longer contains any information. $Z+B$ can thus be publicly transmitted without any problem. Only those who know the key Z can turn garbled bits again back to its original form again. Secure data transmission is therefore possible if Alice and Bob share a secret random pattern Z , the so-called one-time pad. Thus, Alice needs to transmit the random pattern to Bob. It could be said that this would be the starting problem again – so the spy actually needs to eavesdrop on the random pattern in order to be able to decrypt the message. However, nothing can create random patterns better than quantum physics! In the next slide, we will explain how we can outsmart the spy through the quantum dimension.

3.2.3. Quantum cryptography [Link to U3-2-03](#)

In order to achieve data transmission that is absolutely safe from eavesdropping we need a secret random pattern – the so-called “one-time pad” – that only Alice and Bob know. Here, we show how we can transmit the one-time pad from Alice to Bob using polarised photons. The polarisation of the photon can be represented on the Bloch sphere, too: An upward arrow represents horizontal polarization, a downward arrow vertical polarization. In this base, horizontal or vertical polarized photons are eigenstates with a 100 percent predictable outcome. If the photons are, however, polarised in plus or minus 45° direction, we obtain a random result in the horizontal and vertical base – as can be seen here. Generating a random pattern is thus very easy

in quantum physics – however, how can we securely transmit a given random pattern as a one-time pad, so that only Alice and Bob can share it? Viewed naively, Alice could transmit horizontal or vertical polarised photons, and Bob could measure them in the same base and would, with 100 percent probability, obtain the same result.

If there were a spy, who measured the photons in the same base and then, depending on the result, re-transmitted the same polarisation, the spy would have won. Yet the spy does not actually know the measuring base. In the wrong base, that is in this case plus or minus 45° , he would obtain an entirely different random pattern, and Bob as well, for the spy would in fact then no longer transmit horizontally or vertically polarised photons to Bob, but photons polarized in plus or minus 45° . In addition, Alice and Bob would notice that somebody had eavesdropped on them – because their random patterns would be completely different from one another! If Alice and Bob were always to transmit and receive in the same base, the spy would only have to keep on trying to crack the code sufficiently long – until he received the message without changing it! Once the spy had found the right base, Alice and Bob would no longer notice that somebody had eavesdropped on them! Alice and Bob can, however, prevent that, using for example the so-called BB84 protocol, which we are now going to explain in more detail. Alice would like to send her key to Bob. For that purpose, she sometimes transmits photons polarised in the horizontal/vertical base, sometimes in the $+/-$ base. Bob is likewise constantly randomly changing the measuring base, without knowing the base used by Alice. In that way, Bob receives his measuring results. Which of them can be used as a one-time pad, then? This is where Alice can help. She now discloses only the respective measuring base, but not the polarisation state of the photon.

Next, Bob compares his respective base with that of Alice. Only the approx. 50 percent of cases where both have, by chance, taken the same basis give rise to identical data, which Bob can use as a key, that is, as a “one-time pad”. There is, however, no absolute certainty – because if the key is stored digitally on Bob’s PC, the quantum channel no longer helps . . . so that the cat-and-mouse game starts all over again.

3.3. Topology of the quantum dimension (U3-3)

Is it possible to find Omega?

3.3.1. Omegas’ Secret Lab [Link to U3-3-01](#)

Even if Bob’s naive way of looking for the key to the secret passageway to Omega brings forth a great deal of scepticism from Alice, Bob’s idea that he only just needs to “rotate” the key, to find Omega, is brilliant. Needless to say, Bob is not even aware of how brilliant his idea actually is. At this station we explain how, through complex rotations, Alice and Bob actually succeed in finding the secret passageway to Omega.

3.3.2. Complex rotation [Link to U3-3-02](#)

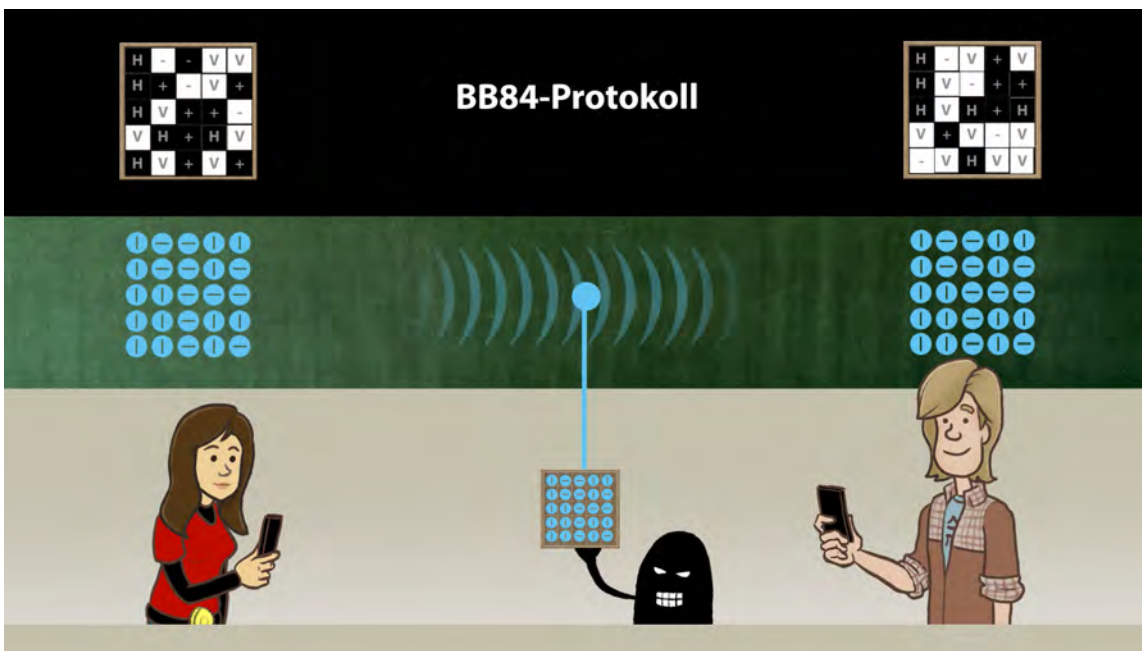


Figure 30. Visualization of the BB84-protocol on the Bloch-sphere. Horizontally and vertically polarized photon states correspond to antipodes on the Bloch sphere. Here, they are displayed on the north- and south-pole. The orthogonal basis states representing light polarized in $\pm 45^\circ$ direction lie on the equator of the Bloch-sphere.

A mirror image can be created as follows: each point x in the real world become a point minus x in the mirror world. Bob now sees the camera twice: through the direct optical pathway ... and from the mirror world. The light is reflected in the mirror in accordance with the principle “angle of incidence equals angle of reflection”. We can also think of this mapping from x to minus x as a rotation – in fact, as a rotation through 180° . Thus, the rotation through 180° corresponds to minus one. A further rotation takes us back to the starting point again, for twice 180° makes 360° . The key to the complex dimension is this: consider a rotation through 90° - so that two such rotations would make 180° , that is, correspond to minus one. That means, however, that the rotation through 90° must correspond to the square root of minus one - in other words, a number that does not exist in real numbers! The mathematicians have termed this generalisation of the real numbers “imaginary numbers”, or “complex numbers” ... In fact, the complex numbers are the key which will open the door to the quantum dimension.

3.3.3. Complexified function [Link to U3-3-03](#)

What does the complex extension of a real function $f(x)$ look like, for example for the function $f(x)$ defined as $f(x) = 1/(1 + x^2)$? First, we extend the real number x by the imaginary component iy . Each real function $f(x)$ can be extended to the complex plane, with x being replaced by $x + iy$, as can be seen in this example. From $f(x + iy)$,

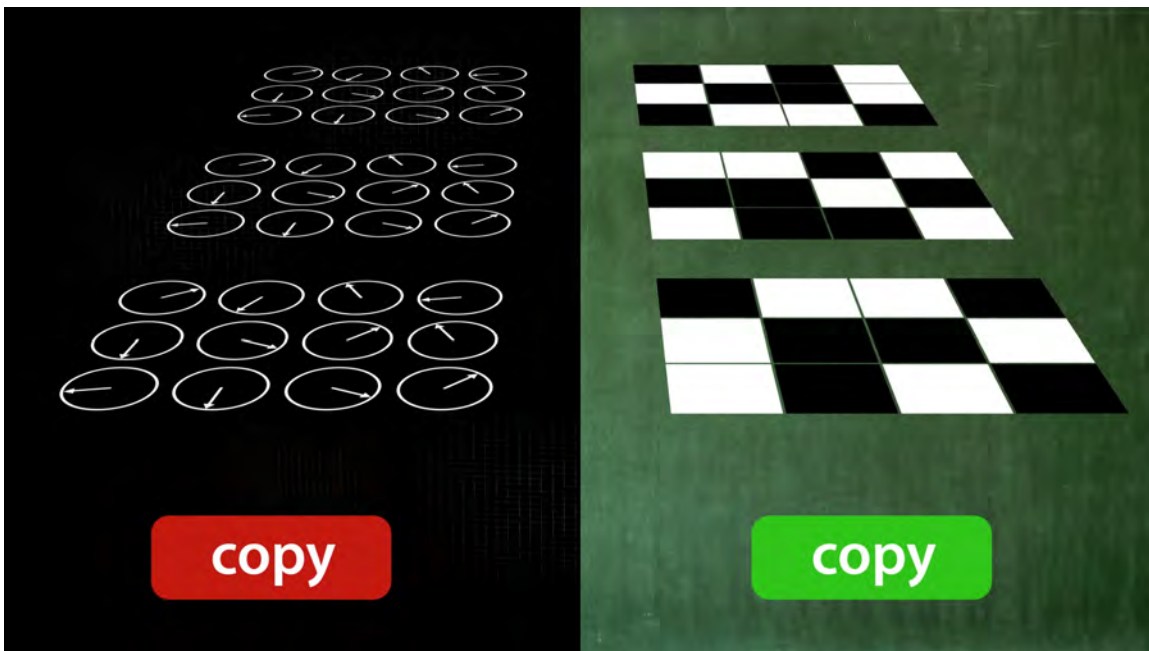


Figure 31. Zustände in der Quantendimension können nicht kopiert werden (links) - digitale Daten aber schon (rechts).

firstly, the real part emerges on the complex plane, which we are visualising here as a mountain landscape coloured in blue. An astonishingly rich mathematical structure arises. Two singularities can clearly be identified, at plus and minus i . Secondly, we display the imaginary part of $f(x + iy)$ on the complex plane. Next, we are showing the real and imaginary parts together. There is an interesting connection between the real part and the imaginary part of f : consider the altitude lines of the mountain landscape here, to start with, for the real part. Near the singularities at plus/minus i the altitude lines become increasingly dense - and this take shows the altitude lines of the mountain landscape for the imaginary part. It can be seen that the altitude lines of the real and imaginary parts always intersect at right angles. This also means, however, that the information of the real part is contained in the imaginary part - and vice versa! And the entire complex structure is already determined by the function $f(x)$ on the real axis - even if the deeper structure is somewhat concealed here, in particular that of the singularities. This complex extension of the function $f(x)$ helps us to understand this deeper structure much better. What about the quantum dimension? What is the situation there? Is everything specified by the real probabilities here as well?

No, not at all! Here the route is reversed, from the complex dimension into the real world. The invisible phase shows that there is no one-to-one connection between the complex wave function and real probabilities. We will be showing you the dramatic consequences of this fact in the next few slides.

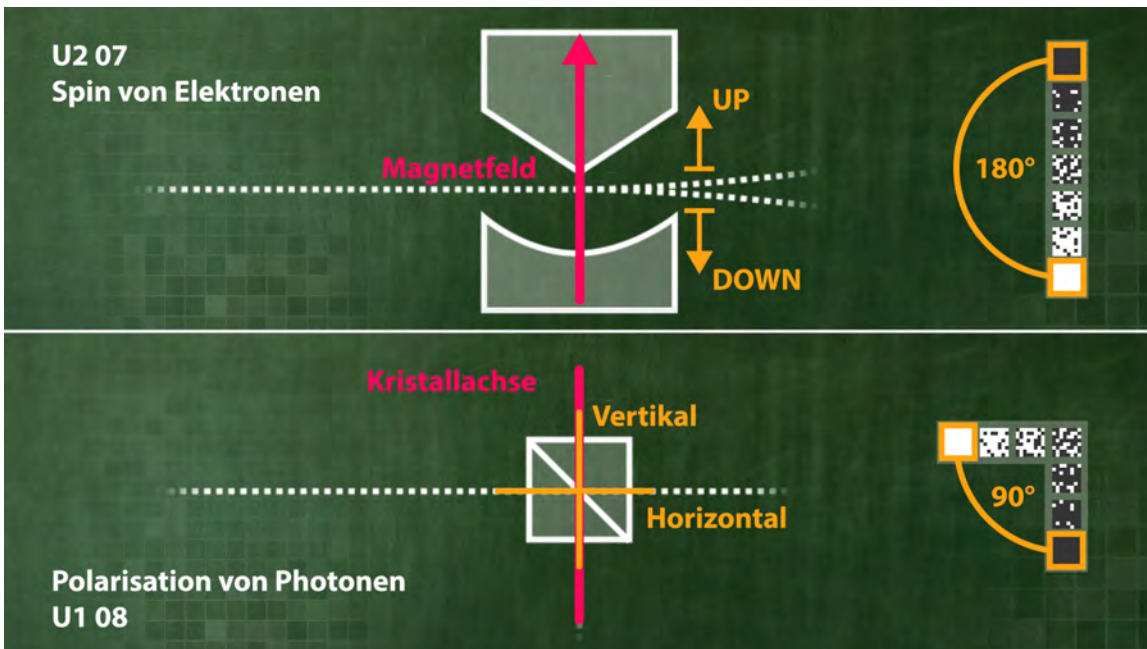


Figure 32. Comparing the geometry of spin and polarization states.

What is the relation between amplitudes in the quantum dimension and observable probabilities? The square of the absolute value of the rotating wheel defines the probability – this is a reduction of the wheel to its radius. The angle - in other words, the phase information – is lost in the process. An infinite number of different possibilities lead to the same probability – and even this is in fact only a probability, not a certain outcome! What is the conclusion? Digital data can, for instance, simply be copied; but the states in the quantum dimension cannot be copied! For we do not know which of the infinitely many possibilities we are supposed to copy, and, if we want to know, we once again arrive at the right-hand side, the digital data without any phase information. If we arrange the amplitudes like a string of pearls, and relate them to solid angles, we obtain a representation for Omega. Omega has many applications – for example, as part of the s-wave of a bound state of an electron in the atom. If we run once in a circle at a fixed radius – for example, at the Bohr radius – the probability density of the electron is constant. However, the rotating wheels do not need to turn synchronously, as long as the radii remain the same – for each of these representations leads to the same probabilities. This is a simple example of the so-called gauge principle: the phase of the wave function can be rotated locally to any value, and each of these infinitely many representations lead to the same observable probabilities.

3.3.5. Spin and polarization [Link to U3-3-05](#)

Viewed from a topological perspective, there is an interesting connection between the spin of electrons and the polarisation of photons. Let us first of all compare the

experiments: the Stern-Gerlach experiment measuring the spin of electrons as shown in U2-7, and the experiment measuring the polarisation of photons as shown in U1-8. Let's start with the spin: if the spin is aligned parallel to the magnetic field, the probability for "spin up" is 100 percent. The probability for "spin up" decreases if the angle between the initial spin direction and the magnetic field increases. After a rotation of 180° , the initial spin is aligned anti-parallel to the magnetic field. In this case, the probability for "spin down" is 100 percent. Compared to the case of polarisation, there is a small, but important difference: the "horizontal" polarisation only describes an axis, and, unlike the spin, does not have any direction. The horizontal and vertical polarisation axes are thus at an angle of 90° to one another. The probabilities for spin "up" and "down" differ compared to the probabilities for reflection and transmission in the angle by a factor of two. In U2-9, we have already discussed the corresponding amplitudes in the quantum dimension: in case of the spin, the standing wave is wound up on the circle twice, leading to one node in 360° . In the case of the polarisation, the amplitude is described by a single-valued standing wave with two nodes in 360° . Recall that all amplitudes originate from the 720° -quantum dimension, being unobservable for us until a projection has been made into the 360° -world. This doubling of the angle is the most important track in our further search for a topological interpretation of particles and interactions, as we will elaborate further in the next few slides.

3.3.6. Topology and quanten nodes [Link to U3-3-06](#)

In U2-5 we classified standing waves in a usual two-dimensional sphere by the number l of nodal lines. Consider a circular line on the equator of the sphere, always for the state $m=l$. Each of the " l " nodal lines crosses this circular line on the equator twice. Therefore, on this equatorial line, $2l$ nodal points arise, that is, always an even number. All other states can be reached by applying the d^- operator. In the 360° world, this is the full spectrum of standing waves on a sphere in three dimensions. If we scale the distance to \hbar , the quantum states arise, for example those from the orbitals as shown in U2-6. What happens, however, if we go from the 360° world to the 720° world, that is, to the three-dimensional sphere in four dimensions? Now, spin states arise, which, as we have seen in U2-9, are actually nothing but usual standing waves in the 720° -world. Only due to the mapping into the 360° -world by winding the amplitude twice onto a circle in 360° , a double-valued amplitude arises with a single nodal point. In 360° , the spin states thus fill the gaps: these states have an odd number of nodes in the 360° -world. The difference between quantum states with an even or odd number of nodes is huge: The so-called "bosons" are the states that are well known to us from the usual two-dimensional sphere, with an even number of nodes. At low temperatures, bosons can condense into the lowest quantum state; there is no ban on multiple occupations of the same state. The so-called "fermions" have an odd number of nodes. Due to the double-valuedness, which arises upon projecting four dimensions onto three, each state observed in three dimensions can only be occupied at the most once

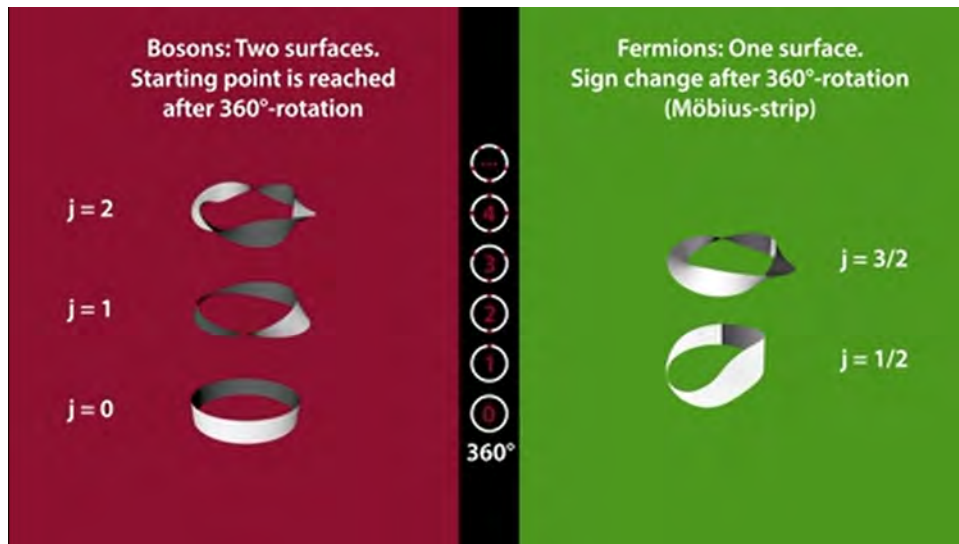


Figure 33. The spin j -state has $2j$ nodes on the Bloch-sphere. For fermions, (1, 3, 5... nodes), the states can only be defined in 720° -geometry.

- that is the so-called “Pauli exclusion principle”. The Pauli exclusion principle is the basis for the stability of matter, as discussed in U2-4. The deeper cause for the stability of the matter thus lies in the projection of the quantum states from the 720° -quantum dimension into the 360° world, and the associated double-valuedness of the spin, which we will examine more closely in the next slide.

3.3.7. Twists [Link to U3-3-07](#)

In order to better understand the difference between bosons and fermions, we will now take a look at the complex phase. We will begin with the simplest state, namely $j=0$. We associate a rotating wheel with each angle, with constant radius – yet, what about the phase? The phase can take any value, without the probability being changed. We are modelling these different phases for each solid angle using a paper strip. The direction of the arrows on the paper strip indicates the phase at the corresponding angle. Cut open, the constant phase in the paper strip model simply looks like this. The simplest change of the topology of the phase is one twist. We can twist either clockwise or anti-clockwise.

The superposition of the phases of the clockwise and anti-clockwise twist correspond to the sum of $e^{\pm i\phi/2}$, that is, $\cos(\phi/2)$. What happens if we first cut open the paper strip of the state $j=0$, then twist it, then glue it together again? Topologically speaking, a Möbius strip thus arises. The Möbius strip has only one surface. Following a rotation through 360° , we arrive at the reverse side, and only after 720° , do you get back to where you started! The superposition of the clockwise and anti-clockwise Möbius strip again leads to $\cos(\phi/2)$, where the angle ϕ runs from 0° to 720° . In such a way, the double-valuedness of the spin state with a single nodal point emerges. If we repeat the

“cutting open”, “twisting” and “gluing together” operations, all other spin states can be constructed starting with the state $j=0$ with trivial topology. The fermions with an odd number of twists are all Möbius strips with only one surface - in contrast to the bosons, which have an even number of twists. This is the main difference of the phase of the quantum states from bosons and fermions: only the fermions completely fill up the 720° space; the bosons are already satisfied with 360° .

3.3.8. Alice and Omega [Link to U3-3-08](#)

Alice has continued to think about Bob’s admittedly somewhat awkward search for the secret passageway, and has figured out the twist she needs in order to find Omega. Alice takes two paper strips, sticking them together on the longitudinal side, to make a strip that is twice as wide. With the “twisting” and “regluing” operations, she forms the well-known Möbius strip. If we run 360° in the Möbius strip, we get from the front to the back. Only after 720° , do we arrive at where we started. Here is Alice’s trick: She separates the two original paper strips, by cutting the Möbius strip longitudinally again. Alice obtains a strip that is twice as long and twisted four times, which is also known as “Dirac’s belt”, in honour of Paul Dirac, the scientist who discovered anti-matter. That is what a fermion in the 720° world looks like, before the two angle ranges are stuck together, in order to project them into the 360° world. Come on, Bob – it is your turn! Do the same for a boson! Okay: stick two paper strips together at the longitudinal edge – twist once ... twist twice, reglue both ends ... Yet, already after 360° Bob the boson comes back again to the starting point ... What happens, then, if we cut the double-twisted strip longitudinally again? ... we obtain two copies of the initial state, intertwined once. Oops! Oh, Bob - you will never make it to the 720° world of the quantum dimension this way ...

Alice got the twist: she takes her own hair in two thick tresses, making a plait, with one, two, three, four, five twists ... Do you like my hairdo? Watch out though, Bob! You need an odd number of twists ... Then put your hair back again, and look into the quantum mirror. Turn once through 360° there. Now all you need to do is to superpose with yourself ... and, hey presto, ... Alice is gone ... Alice?!?

Bob the Boson thinks to himself: What Alice can do, I can do, too! So, off we go – make a lovely plait, one, two ... Oh, you darn wig! The hair is much too short, this is getting me nowhere. ... Wow, now I look exactly like Alice! Put the hair back, and look into the mirror. Turn through 360° there ... Now all I will do is just superpose with myself ... and ... Nothing happens ...?!? Oh yes, it needs to be an odd number of twists – one, two, three, four – twist once more ... This should work – put the hair back ... Look into the quantum mirror, Turn once through 360° there ... Superpose with myself ... and, hey presto, ...

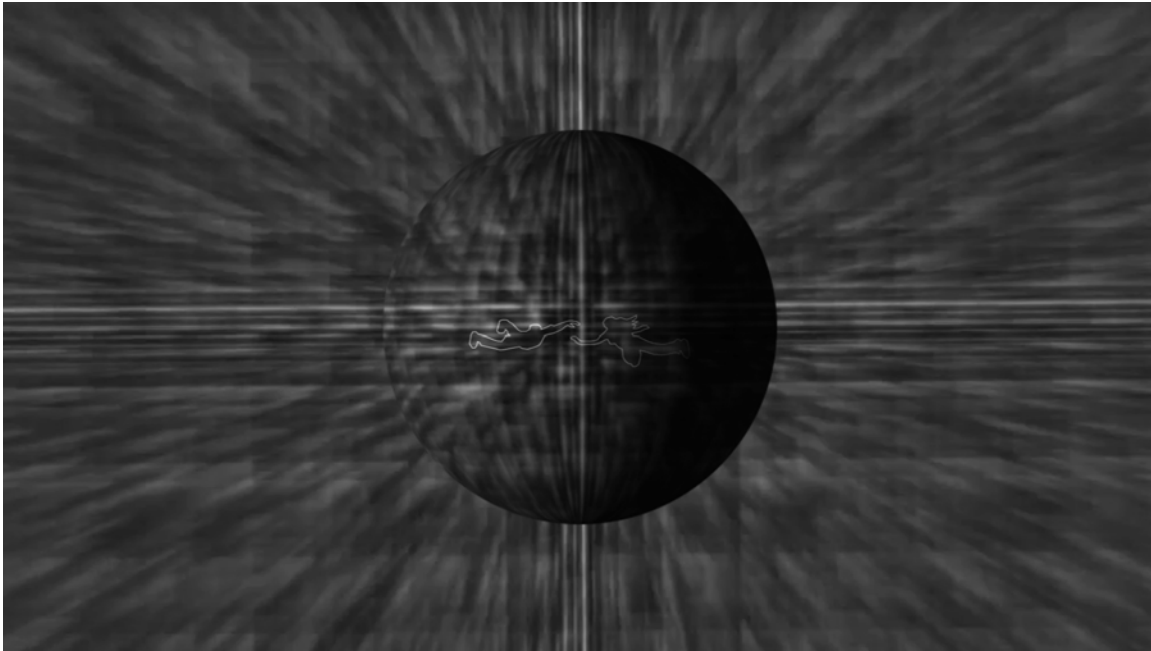


Figure 34. Embarking into the 720° -world: Alice and Bob entering the quantum dimension.

Bob: Alice ...

Alice: Bob, have you made it?

Bob: I believe I am seeing double ...

Alice: No, no - it is all so simple -

Bob: I no longer know where I am ...

Alice: Omega, where has time gone?

4. Mathematical comment

Starting from station U3-4 of the subway line U3, as Alice and Bob have reached the quantum dimension, we will change perspective: our starting point is the quantum dimension beyond space and time, and we come back to the Shadow Worlds only by making distinctions and via Hopf-mapping. The subway stations U3-4, U3-5, U3-6 and U3-7 will explore various aspects of the quantum dimension from a mathematical point of view. Here, we will sketch some of these ideas to be realized as animations movies in future time. In this sense, this mathematical comment can be viewed as the basis for the storyboards for the last stations of the subway line U3: Quantum Symmetries.

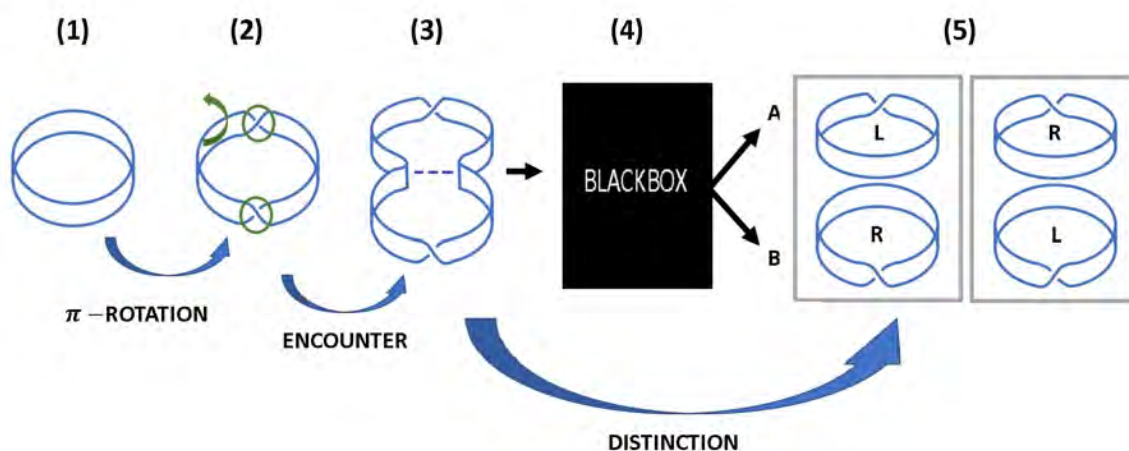


Figure 35. If a closed paper strip without any knots (1) is rotated once around, two loops emerge with opposite twists R and L (2). If both loops are separated (3 and 4), they can be distinguished and labeled as (A, B) (5). The assignment of A and B to the left- and right L, R twist is arbitrary: Before doing so, there is no left or right twist - there is only one closed paper strip without any twists. Starting with many copies of the original paper strip without knots, we will obtain with 50% probability R or L for A in a series of experiments, and anticorrelation for the random results of B . An observer who is only able to see R and L twisted knots would conclude the Black Box produces random results.

First, we introduce our haptic model for entangled state as shown in Fig. 35 without mathematical details: Consider a closed loop (1) and turn it once upside-down (2). As a result, two opposite twists R, L are created, while the global topology of the loop remains unchanged. Next, let two pieces of the loop come close in an encounter (3), where one part of the loop contains the R -twist, the other part the L -twist. Still, the global topology is not changed. Suppose that this configuration is then placed inside a black box (4). Alice and Bob are asked to take one of the two parts of the loop, that is, to separate the two pieces at the position of the encounter. Due to this measurement process, the topology changes. Either Alice receives the R -twist, or Bob. While the assignment of these twists is completely random, correlation is obviously created as the original state contained no twists.

Throughout the project, the same visualization ideas are used. Many of the visualization presented here are based on the seminal work of Majorana, which has been presented by Nicholas Wheeler in a series of lectures, in particular, in [Majorana representation of higher spin states](#) and [Algebraic theory of spherical harmonics](#). Using this mathematical background as inspiration (in particular, the *stellar representation* for spin j -states on the Bloch sphere), we developed the visual language of QuantumVisions. A point of particular importance for all our work is the Hopf-mapping from the unitary group $SU(2)$ to the rotation group $SO(3)$ (and $SL(2, C)$ to the Lorentz group $SO(3, 1)$). It is well-known that this mapping is $2 : 1$, as the 720° -world of $SU(3)$ (the hypersphere S_3) is mapped onto the Bloch-sphere (the usual sphere S_2). Recently, we proposed a generalization of the so-called Dirac-belt trick usually shown just for the spin $j = 1/2$ state to general spin j -states. A more detailed mathematical description can be found in [1], [2]. The key model for QuantumVisions has been published in [3]. Finally, concerning the geometry of $SU(4)$, important for the description of entangled states, we take our inspiration from [4].



Figure 36. Left: Constant amplitude of the entangled state $|\Omega\rangle$, Right: After the measurement, the topology has changed. The node of the remaining photon is either parallel or perpendicular to Alice basis.

4.1. Visualization of the measurement process in U1-12

The topological model shown in Fig, 35 is applied to the Bell state $|\Omega\rangle$. Before the interaction with the detector Alice, the amplitude in any basis rotated by an angle θ is constant and equals $1/\sqrt{2}$. Depending on the choice of basis by Alice, we may express the Bell-state $|\Omega\rangle$ as

$$|\Omega\rangle = \frac{1}{\sqrt{2}}(|0\rangle|0\rangle + |1\rangle|1\rangle) = \frac{1}{\sqrt{2}}(|0_A\rangle|0_A\rangle + |1_A\rangle|1_A\rangle) \quad (1)$$

with $|0_A\rangle = \cos(\theta_A)|0\rangle + \sin(\theta_A)|1\rangle$ and $|1_A\rangle = -\sin(\theta_A)|0\rangle + \cos(\theta_A)|1\rangle$. In Fig. 36, we show a visualization of this constant amplitude in the quantum dimension. Depending on the choice of basis, Alice measurement changes the topology of the remaining state, as the entangled state transforms to the mixed single particle state

$$\text{tr}_A |\Omega\rangle\langle\Omega| = \frac{1}{2}(|0_A\rangle\langle 0_A| + |1_A\rangle\langle 1_A|) \quad (2)$$

Depending on Alice measurement result, Bobs single photon state is either $|0_A\rangle$ (Alice: transmission, \square) or $|1_A\rangle$ (Alice: reflection, \blacksquare). Note that Alice choice of basis is teleported to Bobs side, as Alice choice of basis defines the polarization direction for Bobs. The amplitude of the remaining single photon is then not constant, but $\cos(\theta_A - \theta_B)$ at the angle θ_B chosen by Bob (Alice: transmission, \square) or $\sin(\theta_A - \theta_B)$ (Alice: reflection, \blacksquare).

The conditional probabilities for transmission of the photon at Bobs' side are thus $P_{\square\square} = \frac{1}{2} \cos^2(\theta_A - \theta_B)$ and $P_{\square\blacksquare} = \frac{1}{2} \sin^2(\theta_A - \theta_B)$ (the factor $\frac{1}{2}$ arises as the probability for transmission/reflection at Alice side is 50%). The correlation function is thus determined as

$$\begin{aligned} C(\theta_A, \theta_B) &= (P_{\square\square} + P_{\blacksquare\blacksquare}) - (P_{\blacksquare\square} + P_{\square\blacksquare}) \\ &= \cos^2(\theta_A - \theta_B) - \sin^2(\theta_A - \theta_B) = \cos(2(\theta_A - \theta_B)) \end{aligned} \quad (3)$$

In contrast to the assumption of the existence of the entangled state $|\Omega\rangle$ in the



Figure 37. Alice and Bob will never perceive $|\Omega\rangle$ directly, as a local measurement cannot fully grasp a non-local quantum state.

quantum dimension that causes the non-local correlations between the measurement results, the hidden variable theory originally proposed by Einstein et.al. assumes *independence* between the measurements of Alice and Bob. Mathematically, this is expressed by decomposing the conditional probabilities as simple products. Only under this assumption, the correlation function can be expressed as

$$\begin{aligned} C(\theta_A, \theta_B) &= (P_{\square\square} + P_{\blacksquare\blacksquare}) - (P_{\blacksquare\square} + P_{\square\blacksquare}) \\ &\rightarrow (P_{\square} - P_{\blacksquare})^{\text{Alice}} (P_{\square} - P_{\blacksquare})^{\text{Bob}} \\ &= (P_{\square}^A P_{\square}^B + P_{\blacksquare}^A P_{\blacksquare}^B) - (P_{\blacksquare}^A P_{\square}^B + P_{\square}^A P_{\blacksquare}^B) \end{aligned} \quad (4)$$

As shown in U1-12, this assumption is not consistent with observations.

4.2. The topology of spin- j states

In U3-03-7, we model all spin j states starting from $|\Omega\rangle$ by adding more and more twists: The spin- j state has $2j$ twists in the quantum dimension. Mapped on the Bloch sphere, the spin- j state is characterized by $2j$ nodes in the so-called stellar representation. Note

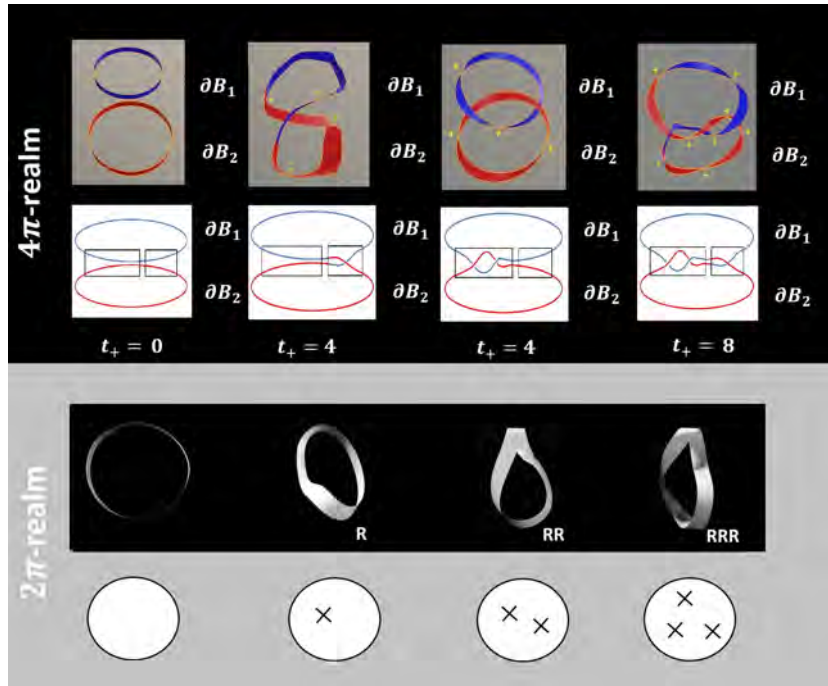


Figure 38. The relation between knots and nodes in the 4π -realm and the 2π -realm.

that care must be taken to distinguish the 720° -topology of the quantum dimension, and the 360° -topology after Hopf mapping. The stellar representations counts nodes on the Bloch sphere, and thus corresponds to the description in 360° -topology as representation of the rotation group $SO(3)$, denoted as 2π -realm. The corresponding $SU(2)$ -representations of spin j states are related to knots the quantum dimension, denoted as 4π -realm. Each *node* in S_2 can be mapped to a knot in the quantum dimension. For bosons, the 4π -geoemtry is essentially equivalent to the 2π -geometry with the only difference that all states identical double-repetitions ($2 \times 2\pi$). Note that for fermions this is not the case: an odd number of twists leads to a Möbius like structure which in Hilbert space is truely 4π without repetition.

Transitions between these states (e.g., spin j to $j \pm 1$ by absorption/emission of a photon) are always related to a change of topology. In Fig. 39, we shown the 720° and the 360° topology of the transition of the spin $j = 0$ to two spin $j = 1/2$ states. The transition shown in Fig. 39 is a straightforward application of the Dirac-belt trick. In Fig. 40, we shown the 720° and the 360° topology of the transition of the spin $j = 0$ to two spin $j = 1$ states. In the 2π -realm, two nodes emerge, which correspond to two twists in the 4π -realm. As the photon has spin $j = 1$, the model shown in Fig. 39 must be applied. Indeed, in the stellar representation, two nodel points (equivalently, one

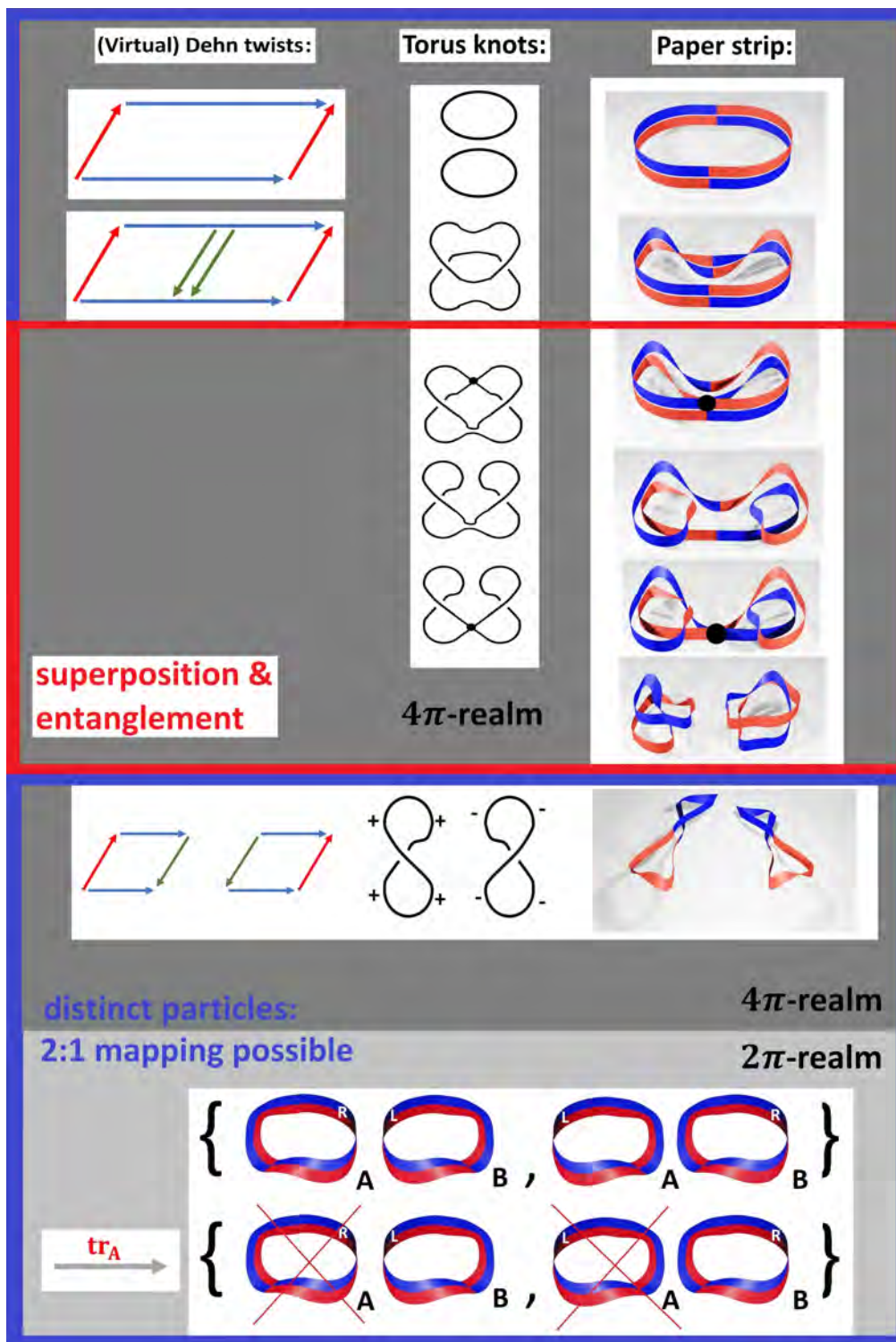


Figure 39. Starting with *nothing* (the unknot), we introduce a virtual Dehn twist by a π -rotation of the torus without cutting it open. After cutting the torus open, two $j = 1/2$ states emerge with $m_j = \pm 1/2$. However, during the topological transition from $j = 0$ (no twists) to $m_j = \pm 1/2$, intermediate states emerge (red box) which cannot be mapped to the 2π -realm.

nodal line) emerges, compare Fig. 36. However, for didactical purposes, it is sufficient just to stick to the simplest model shown in Fig. 35 to grasp the key features of all entangled states.

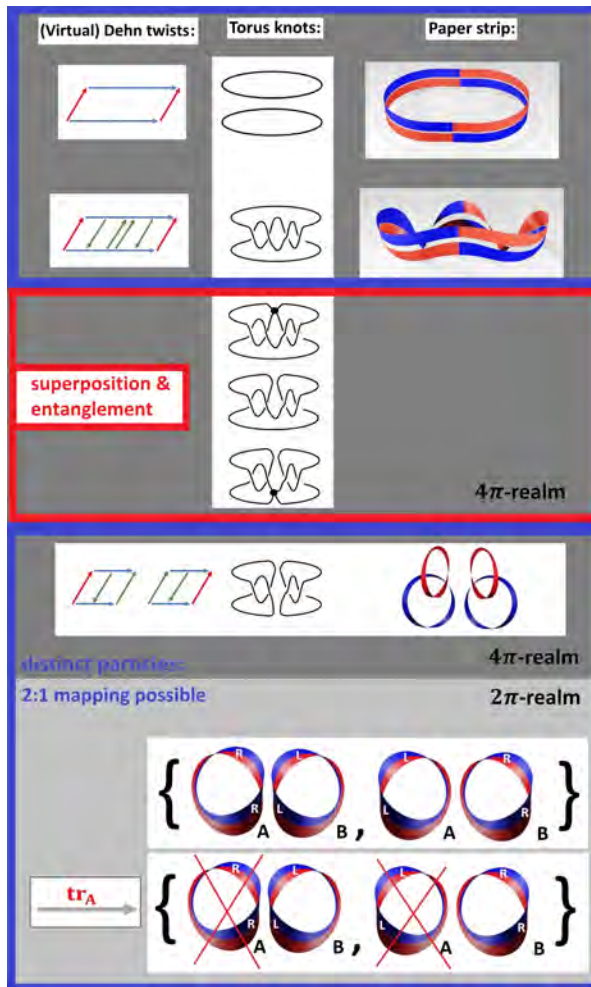


Figure 40. Starting with *nothing* (the unknot), we introduce two virtual Dehn twist by a 2π -rotation of the torus without cutting it open. After cutting the torus open, two $j = 1$ states emerge with $m_j = \pm 1$. However, during the topological transition from $j = 0$ (no twists) to $m_j = \pm 1$, intermediate states emerge (red box) which cannot be mapped to the 2π -realm.

4.3. Making distinctions: From nothing to the speed of light c

Let us conclude this little introduction into the mathematical background of the QuantumVisions project by exploring an idea of Kauffmann [2]: *Everything* can be derived from *nothing*, if we allow for the existence of a *distinction*. We denote the distinction as (A, B) . The only assumption we need is that A , in general, might be different from B in any way.

Once we start to make distinctions, we can operate on them in some very obvious

manner: Let id be the identity operations, then a global reflection is defined as

$$-\text{id}(A, B) \equiv (-A, -B). \quad (5)$$

Distinct objects can be exchanged, which we denote by the operation

$$\phi(A, B) \equiv (B, A). \quad (6)$$

Another very obvious operation is a partial reflection, that is, mapping A to $-A$, or B to $-B$,

$$\begin{aligned} p(A, B) &\equiv (-A, B) \\ q(A, B) &\equiv (A, -B) \end{aligned} \quad (7)$$

Operations can be combined, which leads to the interesting property

$$(\phi q)^2(A, B) = (-A, -B) = (-1)(A, B) \quad (8)$$

It follows $(\phi q)^2 = -1$. Therefore, the combination ϕq can be seen as representation of the complex number i . It seems that the complex nature of the physical world is unavoidable. We may write these operations using 2×2 matrices as follows,

$$\pm \text{id} \simeq \pm \begin{bmatrix} 1 & 0 \\ 0 & 1 \end{bmatrix}, \quad \phi \simeq \begin{bmatrix} 0 & 1 \\ 1 & 0 \end{bmatrix}, \quad q \simeq \begin{bmatrix} 1 & 0 \\ 0 & -1 \end{bmatrix}, \quad \phi q \simeq \begin{bmatrix} 0 & -1 \\ 1 & 0 \end{bmatrix}.$$

These four operations are equivalent to the Pauli matrices and the identity operation,

$$\phi \simeq \sigma_1, \quad \phi q \simeq -i\sigma_2, \quad q \simeq \sigma_3, \quad \pm \text{id}. \quad (9)$$

It is a matter of convention whether we represent i as 2×2 matrix (in this case, the Pauli-matrices would be 4×4 matrices), or to define a new symbol i with $i^2 = -1$. In what follows, we will stick to the latter convention, corresponding to the usual notation. The Pauli-matrices form the algebra

$$[\sigma_i, \sigma_j] = 2i\epsilon_{ijk}\sigma_k \quad (10)$$

Using these basic building blocks, we may introduce coordinates in various interpretations. The most straightforward would be real coordinates, that is, space-time itself, which naturally comes with a hermitian structure

$$h \equiv \text{id } t + \vec{\sigma} \vec{r} = \begin{bmatrix} t + z & x - iy \\ x + iy & t - z \end{bmatrix}, \quad \det h = t^2 - \vec{r}^2 \quad (11)$$

and the Lorentz group $O(3, 1)$ as transformation group leaving $\det h$ invariant. Note that a *distinction* naturally leads to the four operations as defined in equation (9), and in turn to four dimensional space-time. If the time coordinate t is replaced by it , we obtain the imaginary time-formalism. We adopt the situation of $d = 3$ spatial dimensions, and one real time dimension.

4.4. The 4π -realm and the 2π -realm: $SL(2, \mathbb{C})$ as double cover of the Lorentz group $SO(3, 1)$

Next, using the Pauli matrices with *complex* coordinates $\{w_1, w_2, w_3\}$, we can define a six dimensional (tangent) space spanned by

$$u \equiv \vec{\sigma} \vec{w}, \quad \text{tr } u = 0, \quad (12)$$

which is the Lie algebra of the special linear group $SL(2, \mathbb{C})$. The fact that the Pauli matrices are the fundamental building blocks of space-time is reflected in the transformation law

$$h' = e^{+u} h e^{-u}, \quad \det h' = \det h, \quad (13)$$

which indeed is a Lorentz transformation, since $\det h' = \det h$. While the existence of an upper limit for velocities follows from the very nature of Lorentz-transformations, it is impossible to find the value of the speed of light c just from a distinction (as is the case for all other fundamental constants of nature). We set $c = 1$ in what follows.

Now, we derive explicitly the relation between $SL(2, \mathbb{C})$ and $SO(3, 1)$ and propose a simple model for the double cover. We denote by $\Lambda_\mu^\nu \in O(3, 1)$ a Lorentz-transformation, defined as the invariance group for the transformation from reference system $x'_\mu = (t', \vec{x}')$ to $x_\nu = (t, \vec{x})$, with the metric tensor $\text{diag } g_{\mu\nu} = (+1, -1, -1, -1)$. In matrix form, we find $\Lambda^T g \Lambda = g$. It is well known that $O(3, 1)$ can be decomposed into four simply connected parts. Let $O(3, 1)^{\text{id}}$ be the part of the group connected to the identity operation. Then, we can decompose

$$O(3, 1) = O(3, 1)^{\text{id}} \bigoplus O(3, 1)^{\text{id}} \mathbf{P} \bigoplus O(3, 1)^{\text{id}} \mathbf{T} \bigoplus O(3, 1)^{\text{id}} \mathbf{PT}, \quad (14)$$

where \mathbf{P} is the parity operation $\vec{r}' \rightarrow -\vec{r}'$, and \mathbf{T} the time-reversal operation $t \rightarrow -t$. Note, that $\det h = t^2 - \vec{r}^2$ in (11) remains invariant in all four sectors of $SO(3, 1)$. The 2 : 1 mapping with $SL(2, \mathbb{C})$

$$O(3, 1)^{\text{id}} \simeq \frac{SL(2, \mathbb{C})}{\{-1, +1\}} \quad (15)$$

is then explicitly given by

$$\Lambda^\mu{}_\nu \sigma^\nu = h \sigma^\mu h^\dagger, \quad (16)$$

where we introduce the four matrices σ^μ which define the four operations on a distinction (9),

$$\sigma^\mu \equiv (\text{id}, \sigma_1, \sigma_2, \sigma_3). \quad (17)$$

Taking the trace, we find

$$\Lambda^\mu{}_\rho = \frac{1}{2} \text{tr}(h \sigma^\mu h^\dagger \sigma_\rho) \quad (18)$$

with $h \in SL(2, \mathbb{C})$. What is of importance for our reasoning is the fact that $SL(2, \mathbb{C})$ is the two-fold covering group of $SO(3, 1)^{\text{id}}$, meaning that 4π -rotations in $SL(2, \mathbb{C})$ are mapped to two traversals of 2π -rotations in $SO(3, 1)$. Note that this 2 : 1-mapping only emerges for four-dimensional space-time, since $\dim SO(d, 1) = d(d+1)/2$ matches $\dim SL(n, \mathbb{C}) = 2n^2 - 2$ only for the single combination $\{d = 3, n = 2\}$. This is consistent with our observation that space-time is 3 + 1 dimensional.

4.5. Twist-operations in the quantum dimension at the price of Planck's constant \hbar

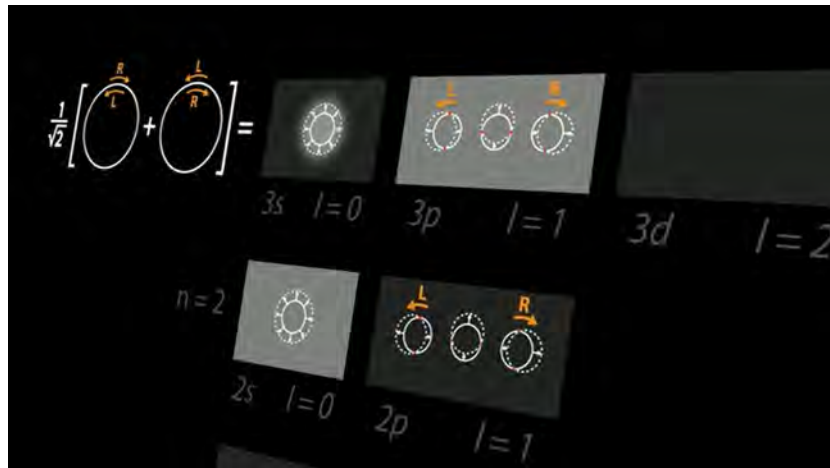


Figure 41. Visualization of selection rules, which in U2-09-2 is applied to the explanation of the HeNe-Laser.

In what follows, we will restrict to $U(1)$ -gauge symmetry. We consider the phase of an spin j -state with $2j$ twists on a given homotopic loop. Gauge invariance just amounts to the fact that an arbitrary number of topologically equivalent quantum phases exist which all map to the same observable state in the (2π) -realm. In particular, we may include additional twists as $2j = 2j + t - t$ without changing any observables, with $t = 0, 1, 2, \dots$. Let $h = e^{i\eta}$ be an additional $h \in U(1)$ -phase factor in the (2π) -realm with t additional twists. The *combined* change of the phase of the wave function and of the gauge field is then trivially

$$\psi = [\psi e^{i\eta}] e^{-i\eta} = [\psi e^{-i\frac{e}{\hbar} \int \vec{A} d\vec{s}}] [e^{+i\frac{e}{\hbar} \int \vec{A} d\vec{s}}] \quad (19)$$

which corresponds to t rotations of the paper strip, leading to a homotopically equivalent quantum phase with $2j = 2j + t - t$ twists. Particle *creation* corresponds topologically to torus splitting, where two cuts separate the quantum phases with the twists $2j+t$ and $-t$. Then, $\psi e^{-i\frac{e}{\hbar} \int \vec{A} d\vec{s}}$ is the phase of the wave function with $2j+t$ twists, and $e^{+i\frac{e}{\hbar} \int \vec{A} d\vec{s}}$ corresponds to the compensating phase of the gauge field with $-t$ twists. Note that the situation for $j = 0$ and $t = 1, 2$ correspond to the quantum phase of two entangled Bell states, with spin $j = 1/2$ (Fig. 39) and $j = 1$ (Fig. 40).

The fact that angular momentum is quantized in units of \hbar thus has a simple topological interpretation: Each twist in the 2π -realm corresponds to the action $\hbar/2$. As only *changes* of the action can be observed, the smallest possible change is $+1 = -1 + 2$ twists, corresponding to the change of angular momentum $\hbar/2 = -\hbar/2 + \hbar$ for the transition of spin up to spin down, thus \hbar is the angular momentum of the emitted (absorbed) photon.

4.6. Selection rules

As an application, we discuss transition amplitudes for bound electrons in atomic physics. Based on topology, we can make predictions on allowed and forbidden transitions, that is, on selection rules in the atom. Consider an electron in the quantum state $2s$ with $j = 0$. As the photon has $l = 1$, we have to deform the quantum phase by rotating ($t = 2$) the closed paper strip twice, see Fig. 42 and Fig. 43 A-B[‡]. After particle creation (corresponding in the paper strip model to the torus splitting, Fig. 43 C-D), the remaining phase of the electron must contain ± 2 twists, which cannot be achieved in the $1s$ state with $l = 0$. For this reason, the fact that the state $2s$ is metastable can be modeled using the paper strip model. On the other hand, the state $3s$ can decay to a $2p$ state with $m = \pm 1$. Due to the minimal interaction, the entangled state

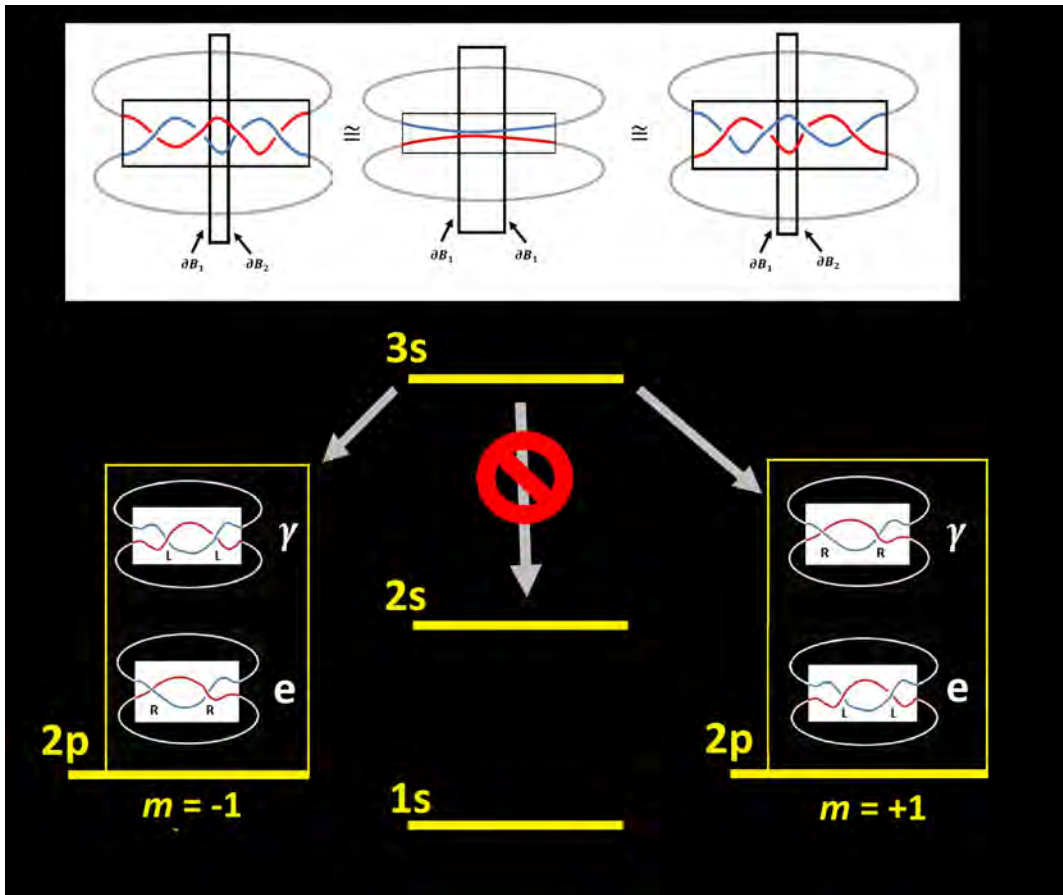


Figure 42. The quantum phase of the state $|3s\rangle$ is homotopically equivalent to $\frac{1}{\sqrt{2}}(|2p, +1\rangle|L\rangle + |2p, -1\rangle|R\rangle)$, see also Fig. ???. The entangled state decays into a mixed state due to interaction of the photon with the environment.

$$|3s\rangle \rightarrow \tag{20}$$

[‡] When orbital angular momentum is included, $l \geq 1$ is also possible

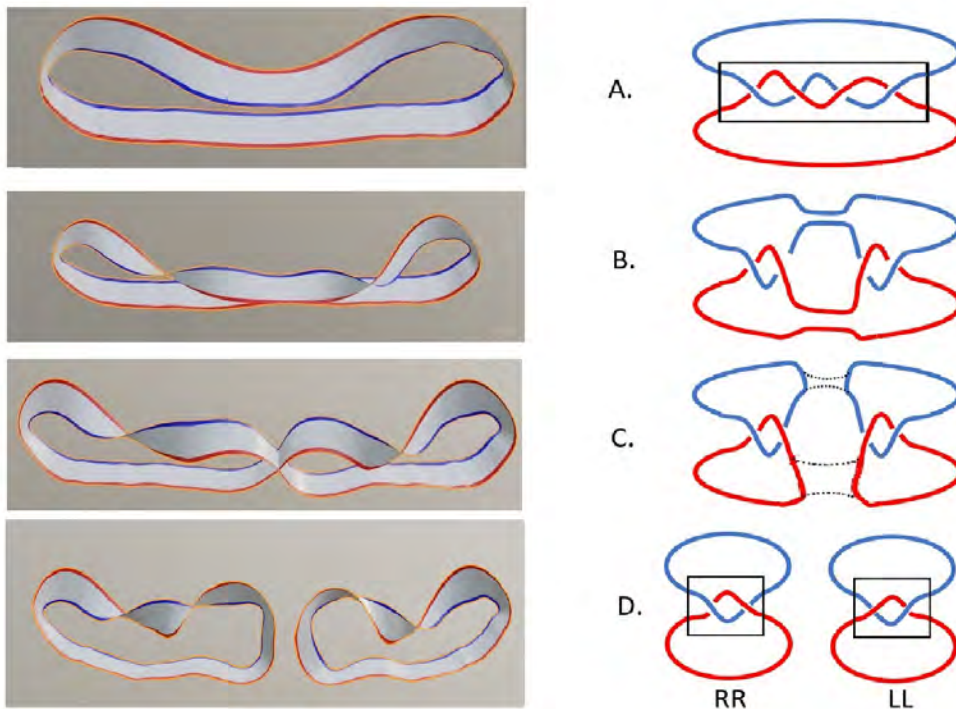


Figure 43. Paper strip model of the quantum phase of the decay $|3s\rangle \rightarrow |2p\rangle$ in the (2π) -realm. If RR is associated with the right-circular polarized photon, the LL described the quantum phase of the electron in the state $|2p, -1\rangle$. With 50% probability, the roles of the pieces RR and LL are interchanged, see Fig. 42. The 4π -realm version of this transition is shown in Fig. 40. Reading the figure in reverse order, starting from D., the transition corresponds to the superposition of two distinguishable states (D) to an indistinguishable entangled state (A).

$$|\psi^+\rangle = \frac{1}{\sqrt{2}}(|2p, +1\rangle|L\rangle + |2p, -1\rangle|R\rangle)$$

will emerge, which due to decoherence will decay to a mixture of left-circular polarized light with an electron in the state $m = +1$, or right-circular polarized light with an electron in the state $m = -1$, see Fig. 42. Note that we come to this prediction without explicit calculation, just by considering the topology of the quantum phase.

It is fascinating to see that the quantum phase does not change due to the interaction - the constant phase of the $|3s\rangle$ state is homotopically equivalent to the quantum phase of the entangled state $\frac{1}{\sqrt{2}}(|2p, +1\rangle|L\rangle + |2p, -1\rangle|R\rangle)$ and remains constant, showing that it is truly a *minimal* interaction. Only after reduction to a mixed state, by ignoring one of the possible realizations $|2p, +1\rangle|L\rangle$ or $|2p, -1\rangle|R\rangle$, the phase is changed. Formally, this is described by taking the partial trace over both possible polarizations of the photon

$$\text{tr}_{R,L}|\psi^+\rangle\langle\psi^+| = \quad (21)$$

$$\frac{1}{2} \left(|2p, +1\rangle \langle 2p, +1| + |2p, -1\rangle \langle 2p, -1| \right).$$

In some sense, interaction can be viewed as ignorance of the remaining part of the entangled state, in other words, by making distinctions.

It is instructive to compare the mathematical formalism necessary for the derivation of transition rules to the ansatz based on the paper strip model. The minimal interaction scheme leads in non-relativistic quantum physics to the Hamiltonian

$$\mathbf{H} = \frac{1}{2m} (\vec{\mathbf{p}} - e\vec{\mathbf{A}})^2 + V(r) = \mathbf{H}_0 + \mathbf{H}_{\text{int}}. \quad (22)$$

Gauge invariance can be proven using

$$e^{i\eta} \vec{\Pi}_\eta^2 e^{-i\eta} = \vec{\Pi}^2. \quad (23)$$

The free Hamiltonian $\mathbf{H}_0 = \mathbf{p}^2/(2m)$ describes the bound electron in the hydrogen atom; and \mathbf{H}_{int} describes the interaction with the gauge field as

$$\mathbf{H}_{\text{int}} = -\frac{e}{2m} [\vec{\mathbf{p}}\vec{\mathbf{A}} + \vec{\mathbf{A}}\vec{\mathbf{p}}] + \frac{e^2}{2m} \vec{\mathbf{A}}^2. \quad (24)$$

For the evaluation of transition amplitudes, we have to consider the matrix elements M_{if} between some initial and final state, defined by

$$M_{if} = \langle f | \mathbf{H}_{\text{int}} | i \rangle. \quad (25)$$

For electromagnetic transitions, the relevant interaction is given by

$$\mathbf{H}_{\text{EM}} = -\frac{e}{m} \vec{\mathbf{p}}\vec{\mathbf{A}} \quad (26)$$

with

$$\vec{\mathbf{A}} = \sqrt{\frac{\hbar}{2\epsilon_0 V}} \sum_{\vec{k}, \lambda} \frac{1}{\sqrt{\omega_k}} \vec{e}_\lambda [\mathbf{a}_\lambda e^{i\vec{k}\vec{r}} + \mathbf{a}_\lambda^\dagger e^{-i\vec{k}\vec{r}}]. \quad (27)$$

The creation and annihilation operator fulfil the commutation relation

$$[\mathbf{a}_\lambda, \mathbf{a}_{\lambda'}^\dagger] = \delta_{\lambda\lambda'}. \quad (28)$$

Here, λ described the polarization of the photon created. In the (2π) -realm, all polarization states can be described on the Bloch sphere §.

In view of Fermi's golden rule, only those modes of the gauge field with $E_{fi} = \hbar\omega_{fi} = \hbar c|\vec{k}_{fi}|$ are relevant for the transition. Thus, we may write to the interaction operator relevant for the creation and emission of a photon as

$$\mathbf{H}_{\text{cr}} = -\frac{e}{m} A_0 (\vec{e}_\lambda \vec{\mathbf{p}}) e^{-i\vec{k}\vec{r}} \mathbf{a}_\lambda^\dagger. \quad (29)$$

§ Here, a subtle remark is in order. Since the photon is massless, no longitudinal modes emerge. For this reason, the degree of freedom of polarization is effectively two dimensional. In contrast to spin, however, no sign change after a 2π -rotation emerges.

The multipole expansion of $e^{i\vec{k}\vec{r}} = 1 + i\vec{k}\vec{r} + \dots$ leads all possible electric and magnetic transitions with creation of a single photon with $l \geq 1$. To leading order, the matrix element M_{if} is given by

$$M_{if} = i\sqrt{\frac{\hbar\omega_{fi}}{2\epsilon_0 V}} \langle f | \vec{e}_\lambda(e\vec{x}) | i \rangle. \quad (30)$$

Here, we used $[x_k, \mathbf{H}_0] = [x, \frac{\mathbf{p}^2}{2m}] = i\hbar\mathbf{p}_k/m$. From this expression, the selection rule ($\Delta l = 1, \Delta m = \pm 1$) can be derived, as anticipated using the paper strip model. Using similar arguments, the higher multipole transitions can also be modeled with the paper strip model.

Finally, we want to comment on the role of the creation and annihilation operators within the paper strip model. Torus splitting and torus merging correspond to the creation and annihilation of particles. Therefore, the expansion of the unitary time development operator $\exp[-(i\mathbf{H}_{\text{EM}}t)/\hbar]$ describes multi-photon processes, where those terms containing \mathbf{H}_{EM}^k involve k torus splittings. Much the same as higher order terms in the multipole expansion for $k = 1$, see equation (29), terms with $k > 1$ are suppressed by higher powers in the fine structure constant $\alpha = e^2/(4\pi\epsilon_0\hbar c) \simeq 1/137$.

To summarize, visualizations and haptic models as proposed in the project QuantumVisions seem to be a powerful tool not only for education, but also for research, as each of the various multiple representations proposed here can provide a different point of view on the problem at hand.

4.7. Quantum dimensions and Shadow World: stroboscopic 2π -realm views in Planck-times τ_{Pl} slices

As shown in Fig. 39 and Fig. 40, some intermediate states in the 4π -realm cannot be mapped to the 2π -realm. Therefore, we "lose track" of the intermediate states, as indicated by the Black Box in the simple model Fig. 35. If the topological model in the 4π -realm is considered as *ontic* description of quantum states, randomness hence emerges due to the fact that some features of these states are structurally inaccessible from an *epistemic* point of view, since human perception is restricted to the realm of observables, i. e., the 2π -realm.

As shown in Fig. 44, the combination of Dehn twists with angles $j_1\pi$ and $j_2\pi$ leads in the intermediate state to $|j_1 - j_2| \leq j_{\text{sum}} \leq |j_1 + j_2|$ Dehn twists, in accordance with the addition rules of angular momentum: In the extreme cases $j_1 \pm j_2$, all twists are either added or subtracted from each other, depending on the orientation in which the tori are glued together. A full (2π) -Dehn twist corresponds to the action \hbar . All transitions are smooth in the quantum dimension.

A collapse of the wave function seems to exist only from an epistemic perspective on quantum objects rooted in the 2π -realm, since only a limited amount of the knot structures can be mapped here, in particular, all spin j -state. The change of a full (2π) -Dehn twist is the minimal observable change, thus, \hbar is the smallest change in angular momentum that can be observed in the 2π -realm. As interactions are unobservable, Fig.

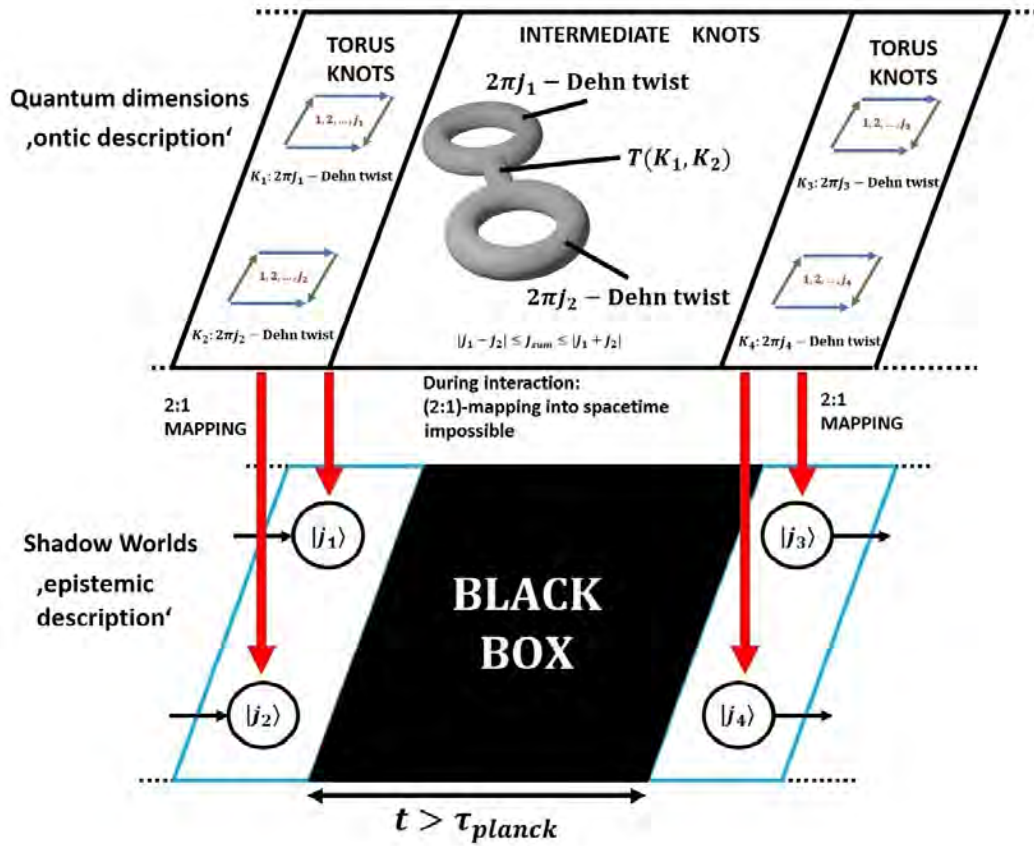


Figure 44. While unitary (time) development in Hilbert space (the 4π -realm) is smooth and corresponds to various topological changes of the knot structures, in space-time (the 2π -realm), only $(2j, 2)$ -torus knots can be observed, see Fig. 39 and Fig.40 for explicit examples. Therefore, (ontic) transitions during interactions between quantum states are (epistemically) unobservable in space-time. Here, we display interactions as tube $T(K_1, K_2)$ connecting the two tori with knot structures K_1, K_2 . Topological changes are mediated via this tube. Equivalently, we may think of virtual Dehn twist and torus splitting as interaction between the particles.

44 suggests the existence of a minimal time step between successive observable states, as the process of changing topology, e.g. from the unknot to a pair of complementary $(2j, 2)$ -torus knots, remains unobservable. In our universe, the explicit value for this minimal time step is the Planck time $\tau_{Pl} = \sqrt{(\hbar G)/(c^3)} \simeq 5.39 \times 10^{-44} s$. While the *existence* of t_{Pl} follows from our argument, the explicit value cannot be derived.

To summarize, by introducing a distinction, we naturally come to a $(3 + 1)$ -dimensional universe with maximal velocity c , minimal observable topological change \hbar (corresponding to a 2π -twist), and a minimal time τ_{Pl} for smooth transitions in the 4π -realm to be mapped to observable spin j -states in the 2π -realm. It would be desirable to include the role of Gravity in this model along the lines of Twistor theory [6].

For more details, we refer to our publications and on the project homepage [QuantumVisions](#).

5. Acknowledgements

Financial support of Joachim Herz Foundation (Remake U1: quantum dimensions, 2023) is acknowledged.

References

- [1] Kauffman, L. H., The mathematics and physics of knots, Rep. Prog. Phys., Vol. 68, No. 12 (2005)
- [2] Kauffman, L. H., Knoten: Diagramme, Zustandsmodelle, Polynom invarianten, Spektrum (1995)
- [3] Heusler, S.; Schlummer, P; Ubben, M [The Topological Origin of Quantum Randomness](#), Symmetry 2021, 13(4), 581
- [4] Kuś, M.; Życzkowski, K., Geometry of entangled states, Phys. Rev. A, Vol. 63, No. 3 (2001)
- [5] Wheeler, N. lecture notes on [Algebraic theory of spherical harmonics](#) (1996) and [Majorana representation of higher spin states](#) (2000)
- [6] Penrose, R.; MacCallum, M.A.H. (1973). Twistor theory: An approach to the quantisation of fields and space-time. Physics Reports. 6 (4): 241–315, doi:10.1016/0370-1573(73)90008-2